

## CHAPTER 35

### CONTAINMENT EVENT TREE ANALYSIS

#### 35.1 Introduction

A containment event tree (CET) displays the characteristics of the severe accident progression that impact the fission-product source term to the environment. It is used to provide the likelihood, magnitude, and timing of the possible accident progressions and the fission-product releases to the environment for each of the AP1000 accident classes.

A containment event tree has been developed for the AP1000 Probabilistic Risk Assessment (PRA) at-power events and is shown in Figure 35-1. The purpose of this chapter is to present a detailed description of the containment event tree structure, top events, and end-states.

#### 35.2 Containment Event Tree – General Discussion

The containment event tree is a tool that provides a logical and practical structure for uniting the complex phenomenology of postulated severe accident event sequences. The event tree approach allows the analyst to determine the likelihood of a particular event sequence progression. This approach also permits evaluation of the impact of uncertainty of the event progression on the overall results and conclusions of the study. The treatment of severe accidents provided by the containment event tree provides assurance that important contributors to fission-product release are identified and evaluated in a structured and disciplined approach. The bases for the top events (or nodes) on the tree are supported by analyses, evaluations and testing, empirical data from past studies, and by the AP1000 design.

This section details the preparation of the containment event tree for the AP1000 PRA. The following sections outline the thought process involved in creating the tree structure and present the containment event tree questions.

A containment event tree serves a number of purposes, including the following:

- It provides a logical, systematic approach to map the severe accident sequence progressions that may occur. Each path on the tree represents a possible accident sequence progression resulting in some final containment state.
- It provides a convenient method of identifying the fission-product release timing and magnitude. The end-state of each path on the event tree represents a fission-product release.
- It provides a means of quantifying the likelihood of each of the proposed accident sequences. Each node on the tree is assigned a probability of success or failure conditional on upstream event outcomes. The product of all the nodal probabilities on a path is the overall probability of the sequence.

- It provides a means of quantifying the likelihood of fission-product release magnitude and timing. The sum of the probabilities of similar fission-product release “end-states” provides the overall probability of these “release categories.”

For example, the containment event tree could simply ask, “Does the containment fail?” The outcome results in two end-states via failure or success. A tree this simple is impractical since the final end-states are too coarse to reasonably identify all the possible release states. Additionally, the number of different possible sequences and resulting phenomena make the question impossible to quantify. On the other hand, it is possible to ask many questions of phenomena that will affect the containment and release state, resulting in many hundreds of thousands of end-states. This also is impractical, as it becomes unmanageable to quantify or comprehend such a large tree. A balance must be found between a sufficient number of top nodes to adequately describe the accident progression and a tree that is practically sized for easy understanding.

A practically sized containment event tree still results in many end-states. It is possible, to a first order, to group a number of different sequences into the same release category. Similarities in accident progression, containment failure time, and the containment fission-product source term make it reasonable to do this. In this way, the number of end-states that must be tracked is reduced.

### 35.3 Event Tree Construction

The end-states of the Level 1 PRA system event tree paths are the input-states to the containment event tree. Their frequencies are propagated through the tree to evaluate the potential for operator actions and the containment structure to mitigate the release of radiation to the offsite environment and to calculate a large release frequency. The containment structural integrity is evaluated with respect to severe accident phenomenological uncertainties and timing of potential containment failure. The accident sequence itself can affect the likelihood of successful mitigation. For example, one sequence may submerge the reactor vessel through the progression of the accident, while another may require operator action for successful cavity flooding. The end-states of the containment event tree describe the timing and magnitude of the offsite fission-product releases to the environment. Therefore, to construct a containment event tree for the AP1000, several topics are considered. Each of these topics is discussed in sections of this chapter:

- Level 1/Level 2 Interface (Tables 35-1 and 35-2)
  - Accident class definitions
- Containment Event Tree Top Events (Table 35-3)
  - Severe accident phenomena
  - Mitigative operator actions and systems
- Release Category Definitions (Table 35-4)
  - Timing of containment failure
  - End-states for the event tree paths

Based on this information, the containment event tree structure, as presented in Figure 35-1, is constructed for the AP1000 PRA.

#### 35.4 Level 1/Level 2 Interface

The core damage end-states of the Level 1 PRA event trees describe the accident sequences that are considered for the Level 2 containment analysis. Therefore, all sequences considered in Level 2 containment analysis have some degree of damage to the core and fission-product release. There are 190 non-zero-frequency core damage end-state sequences in the Level 1 PRA event trees. To analyze each sequence individually for the containment analysis would be unduly cumbersome. Since many of the sequences have similar accident progressions, sequences that present similar initial conditions to the containment analysis are binned into an "accident class," which defines these initial conditions. The dominant sequences in each accident class, by frequency, can be examined to determine the uncertainties in the boundary conditions. The Level 1 sequences are grouped based on the following characteristics:

- The initiating event type, such as loss-of-coolant accident (LOCA), transient, and anticipated transient without scram (ATWS) leading to core damage
- Containment integrity at the time of core damage (intact, not isolated, or bypassed)
- Timing of core damage (early or late)
- The primary system pressure at the time of initial core uncover (high or low)
- Disposition of water in the containment at the time of core damage

The functional definitions of the AP1000 accident classes are presented in Table 35-1. Table 35-2 presents the initial conditions for the Level 2 analysis for each accident class.

#### 35.5 Containment Event Tree Top Events

The top events on the containment event tree describe the points in the accident progression that may affect the containment integrity. Typical top events are related to: 1) containment systems that are not evaluated in the Level 1 analysis, which can mitigate large releases, 2) operator actions to mitigate large releases, or 3) severe accident phenomena that may challenge the containment integrity. A question is posed at each top event with respect to the actuation of a system, performance of an operator action, or occurrence of a phenomenon. The outcome (success or failure) determines the path that the sequence follows. Success follows the top path and failure follows the bottom path. Table 35-3 presents a summary of the top-event questions for the AP1000 containment event tree. These questions are discussed in detail in Section 35.7.

##### 35.5.1 Severe Accident Phenomena Considerations

Consideration of severe accident phenomena that may challenge containment integrity forms the basis for the nodes on the containment event tree. Operator actions or systems top events are generally considered with respect to preventing or mitigating severe phenomena. The

containment event tree considers the following phenomena that represent the severe accident issues relevant to the AP1000 containment integrity:

- In-vessel fuel-coolant interactions
- In-vessel hydrogen generation
- Creep rupture failure of steam generator tubes
- High-pressure melt ejection
- Melt attack on the containment pressure boundary
- Containment overpressurization from decay heat
- Reactor vessel integrity
- Ex-vessel fuel-coolant interactions
- Core-concrete interaction and hydrogen generation
- Hydrogen deflagration and detonation
- Elevated temperatures of the containment shell (diffusion flame heating)
- Elevated gas temperatures (equipment survivability)

Each of the severe accident phenomena presented above is addressed on the AP1000 containment event tree. The containment event tree was constructed under a set of conservative assumptions made to simplify the quantification of the tree and resolve uncertainties related to the severe accident phenomena presented above. These assumptions are as follows:

- High-pressure sequences with reactor coolant system (RCS) pressure above the secondary safety valve setpoint from the time of core uncover until the time of significant cladding oxidation severely challenge steam generator tubes, causing creep rupture failure of the tubes. This allows any reactor coolant system leakage to bypass the containment through the secondary system safety valves.

This assumption resolves the significant uncertainties in severe accident phenomena related to high-pressure core melt progression, especially creep failure of the reactor coolant system pressure boundary and high-pressure melt ejection. The AP1000 reactor coolant system has no pump-bowl loop seals. This design promotes large post-core-uncovery natural circulation of superheated steam and hydrogen and heat transfer from the core to the reactor coolant system metal, including steam generator tubes. The heat transfer prolongs the time from core uncover to rapid oxidation of the cladding, but subjects the steam generator tubes and other reactor coolant system components to significant creep. The AP1000 addresses these uncertainties by providing a reliable, diverse, and redundant automatic depressurization system (ADS) to mitigate the challenging conditions.

With a postulated failure of automatic depressurization system operation and the assumptions in binning the accident classes, only accident classes 1A and 1AP may include sufficient pressurization to challenge steam generator tubes or eject debris from the reactor coolant system at high pressure. All of the accident classes considered for containment integrity success on the containment event tree are marked by depressurization below 150 psi.

- Large-scale relocation of core debris to the containment cavity is assumed to result in early containment failure.

Debris coolability and cavity wall integrity cannot be assured if debris relocates to the containment despite the large spreading area provided in the AP1000 reactor cavity. Given the large uncertainties and conflicting success configurations associated with ex-vessel debris spreading and fuel-coolant interactions, containment integrity is uncertain if debris relocates to the containment. A vessel failure that results in a slow pour of core debris from the vessel to the cavity has little chance of large-scale fuel-coolant interaction, but will not allow the debris to spread into a coolable configuration. Substantial core-concrete interaction will occur. A vessel failure that results in a fast debris pour will spread the debris but has the potential to produce an ex-vessel steam explosion, which can challenge load-bearing cavity walls supporting the reactor vessel. Shifting of the reactor vessel is a potential containment failure mode. Therefore, in the event of the relocation of a large debris mass to the containment, early containment failure is assumed from ex-vessel phenomena. Although there is no pathway for debris impingement on the containment shell, this assumption also resolves any issues in the PRA associated with melt attack on the containment pressure boundary.

### 35.5.2 Operator Action and Systems Top-Event Considerations

Operator actions and containment systems that address, prevent, or mitigate the severe accident phenomena are considered on the containment event tree. The operator actions and systems that are explicitly modeled on the containment event tree are:

- Depressurization of anticipated transient without scram or high-pressure sequences after core uncover
- Containment isolation
- Passive containment cooling
- Containment Venting
- Reactor cavity flooding to submerge the vessel
- Hydrogen control (glow-plug igniters)

The conservative, simplifying assumptions in the containment event tree made with respect to systems are:

- Failure to recover from anticipated transient without scram (accident class 3A) is assumed to overpressurize the reactor coolant system and result in containment bypass due to induced steam generator tube failure.

Failure to recover from anticipated transient without scram would cause the system to pressurize until the reactor coolant system piping fails. The failure location is uncertain,

so the worst location, an induced steam generator tube failure that results in containment bypass, is assumed.

- Failure of in-containment refueling water storage tank (IRWST) reactor cavity flooding is assumed to result in vessel failure.

The analysis, which supports the AP1000 position on in-vessel retention of core debris through external cooling of the reactor vessel (Reference 39-1 and Chapter 39), concludes that a substantial molten metal mass will accumulate in the lower part of the reactor vessel along with the oxide fuel mass. The decay heat in the debris will produce a challenging heat flux to the lower head of the reactor vessel. ULPU tests performed for AP1000 (Reference 35-2) demonstrate the water level in the cavity must be high enough to produce two-phase natural circulation of water through the cavity, past the vessel to cool the lower head sufficiently. Without in-containment refueling water storage tank water flooding the reactor cavity, the required cavity water level cannot be achieved.

Therefore, reactor vessel failure is expected if in-containment refueling water storage tank cavity flooding is not successful. The AP1000 design addresses vessel failure by making the cavity flooding system reliable.

- Success of the hydrogen control system (glow-plug igniters) limits the well-mixed hydrogen concentration in the containment below the lower limits of global combustion and ignites hydrogen plumes.

Analyses presented in Chapter 41 demonstrate that, for in-vessel releases, the hydrogen igniter operation prevents mixture concentrations that produce global deflagration and detonation in the AP1000 containment assuming oxygen can be provided to support the burning. If oxygen cannot be provided, the concentration will increase, but the mixture will not be flammable until it reaches atmospheric conditions that can support burning. The plume will form a diffusion flame when it is ignited. Therefore, operation of the igniters, while mitigating deflagration and detonation, does not prevent the formation of diffusion flames in the core makeup tank (CMT) room or at the in-containment refueling water storage tank vent. The threat to containment integrity from diffusion flame formation is evaluated in locations where hydrogen plumes are postulated to burn and threaten containment integrity.

- If the hydrogen glow-plug igniters fail, random hydrogen ignition is assumed to occur within 24 hours after initial core damage.

The threat to the containment integrity from hydrogen combustion is evaluated at the mixture concentration corresponding to the full extent of zirconium oxidation for the sequence. This treatment maximizes the threat from deflagration and detonation for a given sequence. Since ex-vessel debris relocation is assumed to fail the containment, this assumption applies to in-vessel hydrogen releases only. The containment conditions prior to the burn are based on those that result when the debris is retained in the reactor vessel.

- Passive autocatalytic recombiners (PARs) are not credited with reducing hydrogen concentration.

PARs are in place in the AP1000 containment to control the hydrogen released by the radiolysis of water in design-basis accidents. The hydrogen recombination capacity of the AP1000 PARs for a severe accident is not sufficient to prevent a buildup of hydrogen in the containment. Therefore, the analysis conservatively ignores the presence of the PARs in the AP1000 containment.

### 35.6 Release Category Definitions

The end-state of each path on the containment event tree describes the effectiveness of the containment to mitigate offsite doses for that accident sequence. The radiological consequences of the core-melt accident are largely determined by three major considerations:

- The mode of the postulated containment failure (bypass, isolation failure, gross failure, or intact containment)
- The time of postulated containment failure relative to the time of major fission-product release from the core or core debris
- Fission-product removal mechanisms in the containment

Natural deposition processes, gravitational settling, thermophoresis, and diffusiophoresis are the primary removal mechanisms that scrub aerosols from the containment atmosphere. These natural processes are time-dependent, thus the mode of containment failure, timing of the containment failure, and magnitude of the offsite release are directly related and treated together for the AP1000 containment event tree development.

For the purposes of the offsite doses, time zero occurs after core uncover when significant fission-product masses are released from the fuel. During the initial stages of the severe accident, the core uncovers and the fuel temperature rapidly increases because of decay heat and heat of zirconium oxidation. The core heatup leads to failure of the fuel rod cladding. As the cladding fails, a fraction of the noble gases and volatile fission products, normally present in the fuel-clad gap, is released into the reactor coolant system. This is the "gap release." As the fuel pellet temperature rises toward the melting point, the release of volatile fission products from the fuel is enhanced. This is "temperature-enhanced release." During the melting of the fuel matrix, a large proportion of the total core inventory of volatile fission products is released from the fuel. This is the "melt release."

The gap release, temperature-enhanced release, and initiation of melt release occur sufficiently close together that they are considered to occur coincidentally and termed the onset of core damage. Indications of the onset of core damage are in-vessel hydrogen generation and noble gas and volatile fission products in the reactor coolant system and containment.

The AP1000 release category definitions consider four time frames for the definition of release categories:

- Time Frame 1: accident initiation until onset of core damage – If the containment fails in time frame 1, the containment function is impaired before fission-product release from the core begins, reducing the capacity for fission-product release attenuation. Containment failure in time frame 1 is typically a system failure, such as containment isolation.
- Time Frame 2: onset of core damage until end of core relocation – If the containment fails in time frame 2, the initially intact containment function is impaired during fission-product release before significant fission-product deposition can occur, reducing the capacity for fission-product attenuation. Containment failure in time frame 2 is typically caused by a high-energy severe accident phenomenon associated with core degradation, such as hydrogen combustion or vessel failure.
- Time Frame 3: after the end of core relocation until 24 hours after core damage – If the containment fails in time frame 3, the containment function is impaired after the release of fission products has ceased. Time is available for deposition of aerosol fission products to attenuate the source term. Containment failure in time frame 3 is typically due to hydrogen combustion.
- Time Frame 4: greater than 24 hours after core damage – If the containment fails in time frame 4, the containment function is impaired long after the release of fission products has ceased. Most of the aerosol fission products have deposited out of the containment atmosphere. Containment failure in time frame 4 is typically due to the long-term overpressurization of the containment from decay heat.

Each release category is represented by a fission-product source term that is used to evaluate the offsite consequences in the Level 3 analysis. The source term is an offsite release specified in terms of the timing, magnitude, and energy. The release categories define the timing and the magnitude of the releases, and energy is conservatively assumed to be very low to maximize the site boundary doses. The release categories are summarized in Table 35-4.

#### 35.6.1 Release Category BP – Containment Bypass

Accident sequences in which fission products are released directly from the reactor coolant system to the environment via the secondary system or other interfacing system bypass the containment. The containment failure occurs in time frame 1 and is a result of the initiating event or adverse conditions occurring at core uncover. The fission-product release to the environment begins approximately at the onset of fuel damage, and there is no attenuation of the magnitude of the source term from natural deposition processes beyond that which occurs in the reactor coolant system, in the secondary system, or in the interfacing system. Accident sequences that bypass the containment are binned into release category BP.

### 35.6.2 Release Category CI – Containment Isolation Failure

A containment isolation failure occurs because of the postulated failure of the system or valves that close the penetrations between the containment and the environment. Containment isolation failure occurs during time frame 1. For such a failure, fission-product releases from the reactor coolant system can leak directly from the containment to the environment with diminished potential for attenuation. Most isolation failures occur at a penetration that connects the containment with the auxiliary building. The auxiliary building may provide additional attenuation of aerosol fission-product releases. However, this decontamination is not credited in the containment isolation failure cases. Accident sequences in which the containment does not isolate prior to core damage are binned into release category CI.

### 35.6.3 Release Category CFE – Early Containment Failure

Early containment failure is defined as failure that occurs during time frame 2. During the core melt and relocation process, several dynamic phenomena can be postulated to result in rapid pressurization of the containment to the point of failure. The combustion of hydrogen generated in-vessel, steam explosions, and reactor vessel failure from high pressure are major phenomena postulated to have the potential to fail the containment. If the containment fails during or soon after the time when the fuel is overheating and starting to melt, the potential for attenuation of the fission-product release diminishes because of short fission-product residence time in the containment. The fission products released to the containment prior to the containment failure are discharged at high pressure to the environment as the containment blows down. Subsequent release of fission products can then pass directly to the environment. Containment failures postulated within the time of core relocation are binned into release category CFE.

### 35.6.4 Release Category CFI – Intermediate Containment Failure

Intermediate containment failure is defined as failure that occurs during time frame 3. After the end of the in-vessel fission-product release, the airborne aerosol fission products in the containment have several hours for deposition to attenuate the source term. The global combustion of hydrogen generated in-vessel from a random ignition prior to 24 hours can be postulated to fail the containment. The fission products in the containment atmosphere are discharged at high pressure to the environment as the containment blows down. Containment failures postulated within 24 hours of the onset of core damage are binned into release category CFI.

### 35.6.5 Release Category CFL – Late Containment Failure

Late containment failure is defined as containment failure postulated to occur later than 24 hours after the onset of core damage. Since the PRA assumes the dynamic phenomena, such as hydrogen combustion, to occur before 24 hours, this failure mode occurs only from the loss of containment heat removal as a result of passive containment cooling system annulus blockage. The fission products that are airborne at the time of containment failure will be discharged at high pressure to the environment, as the containment blows down. Subsequent release of fission products can then pass directly to the environment. Accident sequences with failure of containment heat removal are binned in release category CFL.

### 35.6.6 Release Category CFV – Containment Venting

If the containment is pressurizing in an uncontrolled manner by either decay heat steaming or non-condensable gas generation from core-concrete interaction, the operator can vent the containment. Venting is performed to prevent the containment from failing catastrophically, and so that release of fission products to the environment can be controlled. Venting is not expected to occur until at least 24 hours after the onset of core damage. A venting release is limited in magnitude and duration.

### 35.6.7 Release Category IC – Intact Containment

If the containment integrity is maintained throughout the accident, then the release of radiation from the containment is due to nominal leakage and is expected to be within the design basis of the containment. This is the “no failure” containment failure mode and is termed intact containment. The main location for fission-product leakage from the containment is penetration leakage into the auxiliary building where significant deposition of aerosol fission products may occur.

## 35.7 Top-Event Nodal Questions and Success Criteria

After the application of the assumptions listed in Section 35.5, the following severe accident issues are included as top events on the containment event tree to quantify the frequencies of the release categories for the Level 1 accident classes:

- Reactor coolant system pressure
- Containment isolation
- Reactor cavity flooding
- Damaged core reflooding
- Reactor vessel integrity
- Passive containment cooling
- Containment venting
- Hydrogen control
- Hydrogen deflagration
- Hydrogen detonation
- Elevated temperatures of the containment shell (from burning)
- Containment integrity

Each of these issues is presented as a question. The outcome (success or failure) determines the path on the containment tree that the sequence follows at that node. Success proceeds onto the top branch, failure onto the bottom branch. If the outcome determines a release or containment failure, no more questions are asked on that path and the path goes to an end-state release category. If no containment failure is predicted (success at each containment failure node) then the containment is intact. Figure 35-1 presents the containment event tree structure. The following sections present questions, success criteria, and severe accident phenomena that are addressed for each top event. Table 35-3 summarizes the top-event nodal questions. The success criteria are summarized in Table 35-5. Operator actions credited on the containment event tree are summarized in Table 35-6.

**35.7.1 Top Event DP – RCS Depressurization After Core Uncovery**

Nodal Question: Is the reactor coolant system sufficiently depressurized prior to steam generator tube failure or core relocation?

Success Criteria:

- Accident classes 1A, 1AP: 2 of 4 stage 4 automatic depressurization system lines open prior to steam generator tube creep rupture failure or fuel relocation to lower head. RCS pressure less than 150 psia.
- Accident class 3A: 4 of 4 reactor coolant pumps trip, 1 of 2 core makeup tanks actuated, and steam generator tubes intact through pressure transient, passive residual heat removal (PRHR) actuated. RCS pressure peak less than 3200 psia to preserve RCS integrity and RCS long-term pressure less than 2500 psia to retain cooling water in system.
- Accident class 6: 2 of 4 stage 4 automatic depressurization system lines open prior to the onset of core damage.
- Other accident classes: Success defined by the definition of the accident class.

Severe Accident Phenomena Addressed:

- Creep rupture failure of steam generator tubes
- High-pressure melt ejection
- Melt attack on the containment pressure boundary
- Reactor vessel integrity

Actuation:

- Accident classes 1A, 1AP – manual only
- Accident class 3A – automatic reactor coolant pump trip, core makeup tank, and PRHR actuation
- Accident class 6 – automatic or manual

Post-Core-Uncovery Cue for Operator Action: Emergency Response Guideline (ERG) AFR.C-1 entered at 1200°F (920K).

For high-pressure sequences (accident classes 1A, 1AP), the Level 1 PRA credits the operator with a maximum of 30 minutes to depressurize the reactor coolant system prior to core uncovery to prevent core damage. In core damage sequences, additional time may be available to credit operator action to depressurize the reactor coolant system after core uncovery to mitigate the consequences of a high-pressure core melt. After core uncovery, the operator enters the AFR.C-1 ERG. The operator is instructed to manually depressurize the reactor coolant system through the automatic depressurization system in this procedure.

The time available for the operator to mitigate the accident progression to prevent tube creep rupture failure or high-pressure melt ejection is needed to evaluate success. The creep rupture failure is predicted by MAAP4, using the Larson-Miller Parameter (Reference 35-3) to estimate the creep damage in the tube. The use of Larson-Miller is conservative as it underestimates the time to creep rupture (Reference 35-4). Low-pressure sequences with no natural circulation are used to evaluate minimum time to core melting to bound the reactor coolant system natural circulation. Fault trees evaluating hardware and operator success are linked to top event DP to quantify success for accident classes 1A and 1AP.

In anticipated transients without scram sequences (accident class 3A), core damage may be postulated in Level 1 PRA due to departure from nucleate boiling (DNB) while system successes prevent RCS overpressure failure. Automatic protection systems trip the pumps and actuate the core makeup tanks to prevent reactor coolant system overpressure (less than 3200 psi) and potential breaching of the reactor coolant system. Success at node DP allows these automatic actions to be credited for mitigating the consequences of core damage due to anticipated transients without scram. The Level 1 consequential tube rupture probability is used to assess the capability of the steam generator tubes to survive the anticipated transients without scram pressure transient. Passive residual heat removal is credited to bring the plant to a safe, stable condition. Fault trees evaluating the systems successes are linked to top event DP to quantify success for accident class 3A.

Steam generator tube rupture sequences (accident class 6E and 6L) are evaluated based on whether or not the full reactor coolant system depressurization is actuated. The RCS may be depressurized either by the accident progression or by manual operator action in AFR.C-1 prior to core damage. Success at node DP will isolate the break and prevent containment bypass through the failed steam generator tubes.

Other accident classes are marked by depressurization below 150 psi by virtue of the accident progression and are guaranteed success at this top event.

The equipment used to diagnose the high-pressure condition and depressurize the reactor coolant system for success at node DP is safety-related and covered under the design-basis equipment qualification program. The operator action is credited within the conditions of ERG AFR.C-1.

### 35.7.2 Top Event IS – Containment Isolation

Nodal Question: Is the containment isolated prior to core damage?

Success Criterion: One isolation valve closed in each penetration line prior to core damage subject to the screening action discussed in Chapter 24.

Severe Accident Phenomenon Addressed: Initial containment integrity.

Actuation: Automatic via protection and safety monitoring system (PMS) or manual.

Post-Core-Uncovery Cue for Operator Action: ERG E-0 entered at reactor trip or safety injection signal.

Successful containment isolation determines initial containment integrity. If the containment is not isolated, the result is a fission-product release to the environment from the initial stages of core damage. The containment is isolated by the protection and safety monitoring system or by the operator at step 5 in the E-0 ERG. Containment isolation is required before the accident conditions progress to the onset of core damage. The time available prior to significant fission-product release for the operator to isolate the containment is at least 30 minutes (Chapter 37), except in the 3A, 3BR, and 3C accident classes, in which core damage occurs relatively quickly due to inability to reflood the vessel. In accident classes 3A, 3BR, and 3C, only automatic containment isolation is credited.

Equipment survivability of the containment isolation system is covered under the design-basis equipment qualification program. A fault tree evaluating hardware and operator success is linked to top event IS to quantify success of containment isolation.

### 35.7.3 Top Event IR – Reactor Cavity Flooding

**Nodal Question:** Is the water level in the reactor cavity sufficient to submerge the reactor vessel above the 98-ft elevation in the containment?

**Success Criteria:** 2 of 2 valves open in 1 of 2 recirculation lines from the in-containment refueling water storage tank to the containment recirculation screens or in-containment refueling water storage tank injection through the progression of the accident.

**Severe Accident Phenomena Addressed:**

- Reactor vessel integrity
- Melt attack on the containment pressure boundary
- Ex-vessel fuel-coolant interactions
- Core-concrete interaction and hydrogen generation

**Actuation:** Automatic or manual.

**Post-Core-Uncovery Cue for Operator Action:** Entry into ERG AFR.C-1 when core-exit thermocouple temperature exceeds 1200°F. The success criteria require it to be performed within 5 minutes of entry into AFR.C-1.

The basis for in-vessel retention (IVR) of molten core debris in the AP1000 is the DOE/ARSAP report (Reference 35-1) on IVR and Chapter 39. The success of IVR is demonstrated if the reactor coolant system is depressurized and the reactor vessel is adequately submerged. The ULPU Configuration IV test provides the basis for the critical heat flux limits for these conditions (Reference 35-2). The operator determines the need for cavity flooding upon entry into ERG AFR.C-1 based on core-exit thermocouple temperature. For successful IVR, the cavity water level must be at least to the 98' elevation within 70 minutes after the core-exit thermocouple temperature reaches 1200°F. The required elevation for successful flooding is based on producing high velocity two-phase natural circulation flow through the insulation/reactor vessel flow path to enhance the critical heat flux on the outer surface of the vessel as required for the AP1000. Failure at node IR is conservatively assumed to result in vessel failure and subsequent early containment failure by

ex-vessel steam explosion. A fault tree evaluating hardware and operator success is linked to top event IR to quantify the success of cavity flooding.

The equipment used to diagnose and perform the cavity flooding action is safety-related and covered under the design-basis equipment qualification program. The action to flood the cavity is credited within ERG AFR.C-1.

#### 35.7.4 Top Event RFL – Reflooding of a Degraded Core

Nodal Question: Is the in-vessel damaged core reflooded?

Success Criterion: Reactor coolant system is fully depressurized and the break is sufficiently covered or in-containment refueling water storage tank injection is available to allow water to reflood the reactor vessel after core damage.

Severe Accident Phenomena Addressed:

- In-vessel fuel-coolant interactions
- In-vessel hydrogen generation
- Reactor vessel integrity

Actuation: None.

If the reactor coolant system is sufficiently depressurized and water is available to the core, then the vessel can reflood. Reflooding provides additional water to cool the debris and reactor vessel wall, as well as to react with unoxidized zirconium and molten core debris. Downstream on the containment event tree paths, reflooding or failure of reflooding in accident sequences is considered in the degree of hydrogen production and is addressed for vessel lower head integrity both as a cooling mechanism and as a potential lower head failure mode due to in-vessel steam explosion.

The water level in the containment with the in-containment refueling water storage tank injected is sufficient to reflood the reactor vessel if the break is in the floodable compartments. If the break is in a valve vault (direct vessel injection (DVI) line break), it can only be reflooded if the in-containment refueling water storage tank injects through the broken injection side of the DVI line. Otherwise the water cannot reflood into the valve vault. The failure probability of node RFL is based on the accident class, the location of the reactor coolant system break, and conditional probability of in-containment refueling water storage tank injection into the valve vault (for DVI line breaks only).

#### 35.7.5 Top Event VF – Debris Relocation to the Reactor Cavity

Nodal Question: Is the core debris maintained inside the reactor vessel?

Success Criteria: No large-scale relocation of core debris from the reactor vessel to the cavity.

**Severe Accident Phenomena Addressed:**

- Reactor vessel integrity
- Melt attack on the containment pressure boundary
- Ex-vessel fuel-coolant interactions
- Core-concrete interaction and hydrogen generation

Maintaining the core debris in the reactor vessel eliminates the large uncertainties associated with ex-vessel severe accident phenomena related to the relocation of molten debris to the containment. Chapter 39 concludes that vessel failure will not occur if the reactor coolant system is adequately depressurized and the vessel is adequately submerged to produce two-phase natural circulation through the reactor cavity. The analysis considers the challenge to vessel integrity from molten debris impingement and in-vessel steam explosion (Reference 35-5) as well as from heat loads produced by molten debris resident in the lower plenum.

Relocation of a significant fraction of the core debris to the reactor cavity is conservatively assumed to result in early containment failure (release category CFE) from a postulated ex-vessel steam explosion.

For all accident classes except 3C (vessel rupture initiating event), maintaining the debris in the vessel is assured by vessel integrity (success at nodes IR and DP). In accident class 3C, the vessel is failed below the intact core as a result of the initiating event. Core damage is caused by the inability to reflood the core until the reactor cavity is filled, regardless of the availability of the injection systems. The AP1000 has cavity flooding capability such that, once the cavity is filled up to the break, water can reflood into the vessel as the containment compartments fill, to arrest core damage before full core relocation. Only a limited amount of debris is likely to relocate to the lower head. The likely failure for the reactor vessel initiating event is a local failure above the top of the lower-head hemisphere at the beltline of the vessel. This location has the highest fluence and brittleness from exposure. Debris relocated into the lower head is guaranteed to be water cooled in the vessel. Therefore, for accident class 3C, a scalar failure probability value for debris relocation is assigned to node VF and the sensitivity to this value is investigated.

**35.7.6 Top Event PC – Passive Containment Cooling**

**Nodal Question:** Is the passive containment cooling system (PCS) containment shell adequately cooled with water?

**Success Criterion:** Success of 1 of 3 passive containment cooling system water lines opened or operator action to provide alternate source of water to the containment shell.

**Actuation:** Automatic or manual.

**Post-Accident Cue for Operator Action:** Increasing containment pressure above 3 bars. Operator has a long time for actuation before threat to containment integrity.

Severe Accident Phenomena Addressed:

- Containment pressurization by decay heat
- Containment integrity

Water cooling of the PCS shell provides sufficient heat removal capacity to maintain the containment pressure well below ASME Service Level C and assures that there is no likely failure mechanism from the long-term generation of steam.

Rapid pressurization and dynamic loading of the containment shell are addressed on other nodes of the containment event tree. If the containment is not being cooled by water on the shell, the containment atmosphere is sufficiently steam inerted such that hydrogen combustion cannot occur. Therefore, paths downstream from failure at node PC do not address hydrogen combustion.

### 35.7.7 Top Event VNT – Containment Venting

Nodal Question: Is the overpressurized containment vented?

Success Criterion: Success of 1 of 1 containment vent pathways.

Actuation: Manual.

Post-Accident Cue for Operator Action: Containment pressure above design pressure.

Severe Accident Phenomena Addressed:

- Containment pressurization by decay heat
- Uncontrolled fission product releases to the environment

In the event that PCS water is not available to cool the containment, the containment will pressurize above the design pressure and potentially above service level C. Based on actions defined in the severe accident management guidelines (SAMG), the operator will attempt to vent the containment to reduce the pressure and prevent an uncontrollable release to the environment (containment failure). Successful venting will reduce the containment pressure and increase the concentration of steam such that passive heat removal becomes more efficient, the containment pressure will reach equilibrium below service level C, and no more venting is needed. The release to the environment is limited in magnitude and duration. Venting success sequences are grouped into release category CFV. Failure of venting is evaluated for timing of containment failure at node IF.

### 35.7.8 Top Event IF – Intermediate Containment Failure

Nodal Question: Does the overpressurized containment not fail before 24 hours?

Success Criterion: Containment pressure below the ultimate pressure as defined in the containment fragility curve.

**Severe Accident Phenomena Addressed:**

- Containment pressurization by decay heat
- Uncontrolled fission product releases to the environment

In the event that the containment is pressurized by decay heat steaming and the operator does not vent the containment to reduce the pressure, the potential for containment failure within 24 hours is addressed. Failure at node IF results in intermediate containment failure (release category CFI). The success path at node IF is conservatively assigned to release category CFL (late containment failure), despite the fact that there is a strong probability that the passively air-cooled containment will not fail.

**35.7.9 Top Event IG – Hydrogen Control System**

Nodal Question: Are the hydrogen igniters operating?

Success Criteria: Success of 1 of 3 igniter power sources and operator action to actuate the system. Success criteria for the operator action require it to be performed within 15 minutes.

Severe Accident Phenomenon Addressed: Hydrogen deflagration and detonation.

Actuation: Manual only.

Post-Accident Cue for Actuation: Entry into AFR.C-1.

Operation of the hydrogen igniter system prevents the concentration of hydrogen to reach globally flammable limits in the containment (see Chapter 41). The igniters are powered from ac power or from either of the two nonsafety-related diesel generators. The igniters are actuated early in emergency response guideline AFR.C-1 when the core-exit temperature exceeds 1200°F (920K). Failure of the igniters allows the containment to be challenged by hydrogen deflagration and detonation. Igniters do not provide protection from diffusion flames heating the containment shell in the core makeup tank room and near the in-containment refueling water storage tank vents. A fault tree evaluating hardware and operator success is linked to top event IG to quantify the failure probability.

**35.7.10 Top Event DF – Diffusion Flame**

Nodal Question: Does the containment not fail from elevated temperature due to diffusion flame near the containment shell?

Success Criteria: Successful closure of the louvered vents on the IRWST or at least two stage-4 ADS lines open to vent hydrogen from the RCS away from the IRWST.

Severe Accident Phenomenon Addressed:

- Elevated temperatures of the containment shell

The release of hydrogen plumes near the containment shell has been postulated from the IRWST and Passive Core Cooling System (PXS) compartment vents. The threat to the containment integrity from a diffusion flame near the containment shell at these locations has been addressed in the design of the vents from the IRWST and PXS. The IRWST vents along the containment wall have been louvered and turned inboard, pointing away from the wall. The louvers are designed to close when they are not venting. The vents along the steam generator doghouse wall have covers that open, and remain open, at a lower pressure than the louvers. These vents remain open to vent hydrogen from the IRWST to the middle of the containment, where they will not present a challenging heat load to the containment shell.

Venting from PXS compartments is situated away from the containment shell and penetrations. Access portals to the PXS compartments that may be near the containment wall are covered and locked closed.

For defense in depth, open stage-4 ADS valves provide a path of least resistance to vent hydrogen from the core to the steam generator compartments, which are shielded from the containment shell.

#### 35.7.11 Top Event DTE – Early Hydrogen Detonation

Nodal Question: Does the containment not fail from detonation during in-vessel hydrogen release to containment?

Success Criteria: No hydrogen detonation.

Severe Accident Phenomena Addressed:

- Hydrogen detonation
- Containment integrity

Hydrogen released to the steam generator rooms and relatively confined compartments below the operating deck can accumulate to high concentrations during the release. The deflagration of high concentration mixtures within such confined geometries can be postulated to accelerate to detonation.

A detonation in any compartment is assumed to fail the containment. Hydrogen detonation in the AP1000 is limited to deflagration-to-detonation transition (DDT). There are no ignition sources in containment strong enough to directly initiate detonation for the dry-air/hydrogen mixture generated by 100-percent cladding oxidation. Hot jets are also not considered to be a credible detonation source since the cases that are evaluated at this top event have accomplished successful depressurization at node DP.

The detonation-to-deflagration transition potential in the containment is evaluated using the Sherman-Berman methodology outlined for the Bellefonte nuclear power plant in Reference 35-7 and applied to the AP1000 in Chapter 41. The potential for DDT is a function of the mixture composition and the compartment geometry. If the igniters are available, the gas composition will not reach detonable mixtures. If the igniters are not available, the probability of an ignition source is assumed to be 0.5 in the in-containment refueling water

storage tank, in the valve vault, or in the chemical and volume control system rooms. Failure at top event DTE results in early containment failure.

### 35.7.12 Top Event DFG – Hydrogen Deflagration

Nodal Question: Does the containment not fail from hydrogen deflagration?

Success Criteria: Peak pressure from adiabatic, isochoric, complete combustion (AICC) deflagration of all hydrogen generated in a sequence less than containment ultimate pressure.

Severe Accident Phenomena Addressed:

- Hydrogen deflagration
- Elevated temperature of the containment shell
- Containment integrity

The loading on the containment from a relatively slow burn or deflagration is spatially uniform and quasi-static. AICC bounds the peak gas temperature and pressure that can be generated from the deflagration of hydrogen. The AICC pressure is a function of the mass of hydrogen burned and the composition of the gas mixture that is heated. The loading on the containment is quasi-static.

The containment ultimate pressure is given by a probability distribution presented in Chapter 42. The containment ultimate pressure probability distribution is calculated assuming that the containment shell temperature is 400°F (480K). Therefore, the peak temperature of the shell following such a burn must remain below 400°F to demonstrate applicability of the ultimate pressure probability distribution. All of the hydrogen generated in-vessel is assumed to be ignited by a random source prior to 24 hours. Failure at top event DFG results in intermediate containment failure.

### 35.7.13 Top Event DTI – Intermediate Hydrogen Detonation

Nodal Question: Does the containment not fail from hydrogen deflagration-to-detonation transition (DDT) before 24 hours?

Success Criteria: No detonation.

Severe Accident Phenomena Addressed:

- Hydrogen detonation
- Containment integrity

This node addresses DDT prior to 24 hours and conservatively assumes stratification in containment. As in the analysis for early detonation, hydrogen detonation in the intermediate time frame is limited to deflagration-to-detonation transition. Based on insights from the passive containment cooling large-scale test (Reference 35-7) on the steady-state natural circulation of the containment atmosphere, on a dry basis, hydrogen and air are well mixed in the containment within several percent above and below the operating deck. However,

because of the buoyancy of the steam in the containment, condensation on the passive containment cooling shell and the downdraft of cool, dry air along the wall, the steam concentration in the core makeup tank room can be postulated to be much lower than that predicted by MAAP4 or other lumped-parameter models that tend to overmix the atmosphere. Therefore, the mixture in the core makeup tank room is conservatively bounded as a dry-air mixture to evaluate the DDT potential prior to 24 hours.

### 35.8 Summary

The containment event tree is a tool that allows the quantification of the likelihood, timing, and magnitude of large releases from the containment. The containment event tree addresses the containment systems, operator actions, and severe accident phenomena that prevent, mitigate, or cause large releases of fission products to the environment. The interface between the Level 1 core damage frequency analysis and the Level 2 large release frequency analysis is developed and summarized in Table 35-1. The event tree structure is presented in Figure 35-1, and the top events are summarized in Table 35-3. The containment event tree end-states or release categories represent the timing and magnitude of the release to the environment. The release categories are summarized in Table 35-4.

### 35.9 References

- 35-1 Theofanous, T. G., et al., "In-Vessel Coolability and Retention of a Core Melt," DOE/ID-10460, July 1995.
- 35-2 Theofanous, T. G., et al., "Quantification of Limits to Coolability in ULPU-2000 Configuration IV," CRSS-01/11, November 28, 2001.
- 35-3 Larson, F. R., Miller, J., "A Time-Temperature Relationship for Rupture and Creep Stress," Transactions of the American Society of Mechanical Engineers, pp. 765-775, July 1952.
- 35-4 Stickler, L. A., Rempe, J. L., et al., "Calculations to Estimate the Margin to Failure in the TMI-2 Vessel," TMI V(93)EG01, October 1993.
- 35-5 Theofanous, T. G., et al., "Lower Head Integrity Under In-Vessel Steam Explosion Loads," DOE/ID-10541, July 1996.
- 35-6 Sherman, M. P., Berman, M., "The Possibility of Local Detonations During the Degraded-Core Accidents in the Bellefonte Nuclear Power Plant," NUREG/CR-4803, SAND86-1180, January 1987.
- 35-7 Final Data Report for PCS Large-Scale Tests, Phases 2 and 3, WCAP-14135 (Proprietary), July 1994.

Table 35-1

**FUNCTIONAL DEFINITIONS OF LEVEL 1 ACCIDENT CLASSES**

<b>Accident Class</b>	<b>Subclass</b>	<b>Definition</b>
1	A	Core damage with RCS at high pressure following transient or RCS leak
	AP	Core damage with no depressurization following small LOCA and RCS leak with passive residual heat removal operating or intermediate LOCA
	D	Core damage with partial depressurization of RCS following transient
3	A	Core damage with RCS at high pressure following anticipated transient without scram or main steam line break inside containment
	BR	Core damage following large LOCA with full RCS depressurization, but accumulator failed
	BE	Core damage following large LOCAs or other event with full depressurization
	BL	Core damage at long term following failure of water recirculation to reactor vessel after successful gravity injection
	C	Core damage following vessel rupture
	D	Core damage following LOCA (except large) with partial depressurization
6	E	Core damage following steam generator tube rupture or interfacing system LOCA. Early core damage (loss of injection)
	L	Core damage following steam generator tube rupture. Late core damage (loss of recirculation)

Table 35-2

**CET INITIAL CONDITIONS FOR LEVEL 1 ACCIDENT CLASSES**

Accident Class	Subclass	RCS Pressure during Core Uncovery (psig)
1	A	>1100
	AP	~1100
	D	<150
3	A	>1100
	BR	0
	BE	0
	BL	0
	C	0
	D	<150
6	E	Sequence specific
	L	0

Table 35-3

**CONTAINMENT EVENT TREE NODAL QUESTIONS**

<b>Node</b>	<b>Question</b>
Node DP	Is the reactor coolant system sufficiently depressurized prior to steam generator tube failure or core relocation?
Node IS	Is the containment isolated prior to core damage?
Node IR	Is the water level in the reactor cavity sufficient to submerge the reactor vessel above the 98-ft elevation in the containment?
Node RFL	Is the in-vessel damaged core reflooded?
Node VF	Is the core debris maintained inside the reactor vessel?
Node PC	Is the passive containment cooling system containment shell adequately cooled with water?
Node VNT	Is the overpressurized containment vented?
Node IF	Does the overpressurized containment not fail before 24 hours?
Node IG	Are the hydrogen igniters operating?
Node DF	Does the containment not fail from elevated temperature due to diffusion flame in the CMT room and at the IRWST vent?
Node DTE	Does the containment not fail from detonation during in-vessel hydrogen release to containment?
Node DFG	Does the containment not fail from hydrogen deflagration?
Node DTI	Does the containment not fail from hydrogen deflagration-to-detonation transition (DDT) before 24 hours?

Table 35-4				
SUMMARY OF RELEASE CATEGORY DEFINITIONS				
Release Category	Definition	Release Category Description	Release Magnitude	Release Timing
IC	Intact Containment	Containment integrity is maintained throughout the accident, and the release of radiation to the environment is due to nominal leakage.	Normal Leakage	-
BP	Containment Bypass	Fission products are released directly from the RCS to the environment via the secondary system or other interfacing system bypass. Containment failure occurs prior to onset of core damage	Large Release	Time Frame 1
CI	Containment Isolation Failure	Fission-product release through a failure of the system or valves that close the penetrations between the containment and the environment. Containment failure occurs prior to onset of core damage.	Large Release	Time Frame 1
CFE	Early Containment Failure	Fission-product release through a containment failure caused by severe accident phenomenon occurring after the onset of core damage but prior to core relocation. Such phenomena include hydrogen combustion phenomena, steam explosions, and vessel failure.	Large Release	Time Frame 2
CFV	Containment Venting	Fission-product release through a containment vent line during intentional depressurization of the containment	Controlled Release	Time Frame 3
CFI	Intermediate Containment Failure	Fission-product release through a containment failure caused by severe accident phenomenon, such as hydrogen combustion, occurring after core relocation but before 24 hours.	Large Release	Time Frame 3
CFL	Late Containment Failure	Fission-product release through a containment failure caused by severe accident phenomenon, such as a failure of passive containment cooling, occurring after 24 hours.	Large Release	Time Frame 4

Table 35-5 (Sheet 1 of 3)

**SUMMARY OF CONTAINMENT EVENT TREE SUCCESS CRITERIA**

Top Event Name	Event Case Name	Success Criteria	Manual Actions	Dependencies and Modeled Actuation	Mission Time	Basis
DP	ADTLT – post-core-damage RCS depressurization following failure to depressurize prior to core damage	2 of 4 ADS-4 valves and isolation valves open	Credit for manual actuation only [operator actions: LPM-REC01 ADN-REC01]	None	Demand to open, 24 hours to remain open	Ch. 11
	ADALT – post-core-damage RCS depressurization following system recovery of ATWS	4 of 4 RCPs trip and 1 of 2 CMTs actuates, SG tubes intact through pressure transient	Credit for auto actuation of RCPs trip and CMTs	Automatic RCP trip and CMT actuation via PMS on high hot leg temperature coincident with low wide-range SG level	Demand to open, 24 hours to remain open	Ch. 43
IS	CIC – containment isolation	1 isolation valve closed in each penetration line (subject to PRA screening criteria)	Credit for manual actuation if automatic fails [operator action: CIC-MAN01]	Automatic signal via PMS SI-signal or high containment pressure	Demand for actuation and 72 hours to remain closed	Ch. 24
	CID – containment isolation	1 isolation valve closed in each penetration line (subject to PRA screening criteria)	None	Automatic signal via PMS SI-signal or high containment pressure	Demand for actuation and 72 hours to remain closed	Ch. 43
	OTH-CNB – containment isolation	No containment failure as a result of vessel rupture	None	None	Demand	Ch. 31

Table 35-5 (Sheet 2 of 3)

**SUMMARY OF CONTAINMENT EVENT TREE SUCCESS CRITERIA**

Top Event Name	Event Case Name	Success Criteria	Manual Actions	Dependencies and Modeled Actuation	Mission Time	Basis
IR	IWF – reactor cavity flooding from IRWST via recirculation path following core damage	2 of 2 valves open in 1 of 2 recirculation lines from IRWST to containment sump	Credit manual actuation only [operator action: REN-MAN03]	None	Demand for valves to open, 24 hours to remain open	Ch. 12
RFL	Phenomenological event – accident class-dependent scalar value	Full RCS depressurization and break submerged	none	None	24 hours	Ch. 38
VF	Phenomenological event – scalar value	No vessel failure, or vessel failure does not release debris to cavity (Accident Class 3C)	none	None	72 hours	Ch. 39
PC	PCT – passive containment cooling water valves open	1 of 3 PCS lines opens to drain water from PCS water tank to containment shell	Credit is given for manual actuation if automatic fails [operator action: PCN-MAN01]	Automatic signal via PMS high containment pressure	24 hours	Ch. 13
VT	VNT – operator opens containment vent line	1 of 1 containment vent lines opens to depressurize containment.	Credit for manual action only [operator action: VNT-MAN01]	None	Demand	Ch. 40
IF	Phenomenological event – scalar value	Containment maintains barrier to fission product release	None	None	24 hours	Ch. 40

Table 35-5 (Sheet 3 of 3)

**SUMMARY OF CONTAINMENT EVENT TREE SUCCESS CRITERIA**

Top Event Name	Event Case Name	Success Criteria	Manual Actions	Dependencies and Modeled Actuation	Mission Time	Basis
IG	VLH – containment hydrogen control	Sufficient number of igniters operate to limit hydrogen concentration in containment	Credit for manual actuation only [operator action: VLN-MAN01]	None	24 hours	Ch. 16
DF	Louvered IRWST vents closed or ADS-4 open to vent hydrogen away from shell	2 of 4 ADS-4 lines open to vent H <sub>2</sub> away from shell	None	None	Release duration	Ch. 41
DTE	Phenomenological event – accident class-dependent scalar value	DDT does not occur during hydrogen release to containment	None	None	Release duration	Ch. 41
DFG	Phenomenological event – accident class-dependent scalar value	Containment not failed by overpressure, shell not failed by overtemperature	None	None	24 hours	Ch. 41
DTI	Phenomenological event – accident class-dependent scalar value	DDT does not occur during burn	None	None	24 hours	Ch. 41

Table 35-6

## SUMMARY OF OPERATOR ACTIONS CREDITED ON CONTAINMENT EVENT TREE

Top Event	Description of Operator Error	Event ID	Cue(s)	Time Window
DP	Failure to recognize need for post-core-uncovery RCS depress during small LOCA or transient with loss of PRHR	LPM-REC01	core-exit T/C > 1200°F (ERG AFR.C-1)	30 minutes
	Failure to complete ADS as recovery from failure of automatic actuation or manual actuation after core damage	ADN-REC01	core-exit T/C > 1200°F (ERG AFR.C-1)	30 minutes
IS	Failure to recognize need and failure to isolate the containment, given core damage following an accident	CIC-MAN01	high containment pressure, high containment temperature, high containment radiation (ERG E-0)	30 minutes
IR	Failure to recognize need and failure to open recirculation valves to flood reactor cavity after core damage	REN-MAN03	core-exit temperature > 1200°F (ERG AFR C-1)	5 minutes
PC	Failure to recognize need and failure to open PCS water valves to drain cooling water on containment shell	PCN-MAN01	high containment pressure (ERG E-0)	60 minutes
VNT	Failure to recognize need and failure to open containment vent to reduce containment pressure	VNT-MAN01	high containment pressure (SAMG)	60 minutes
IG	Failure to recognize need and failure to actuate hydrogen control system, given core damage following an accident	VLN-MAN01	core-exit T/C > 1200°F (ERG AFR.C-1)	10 minutes

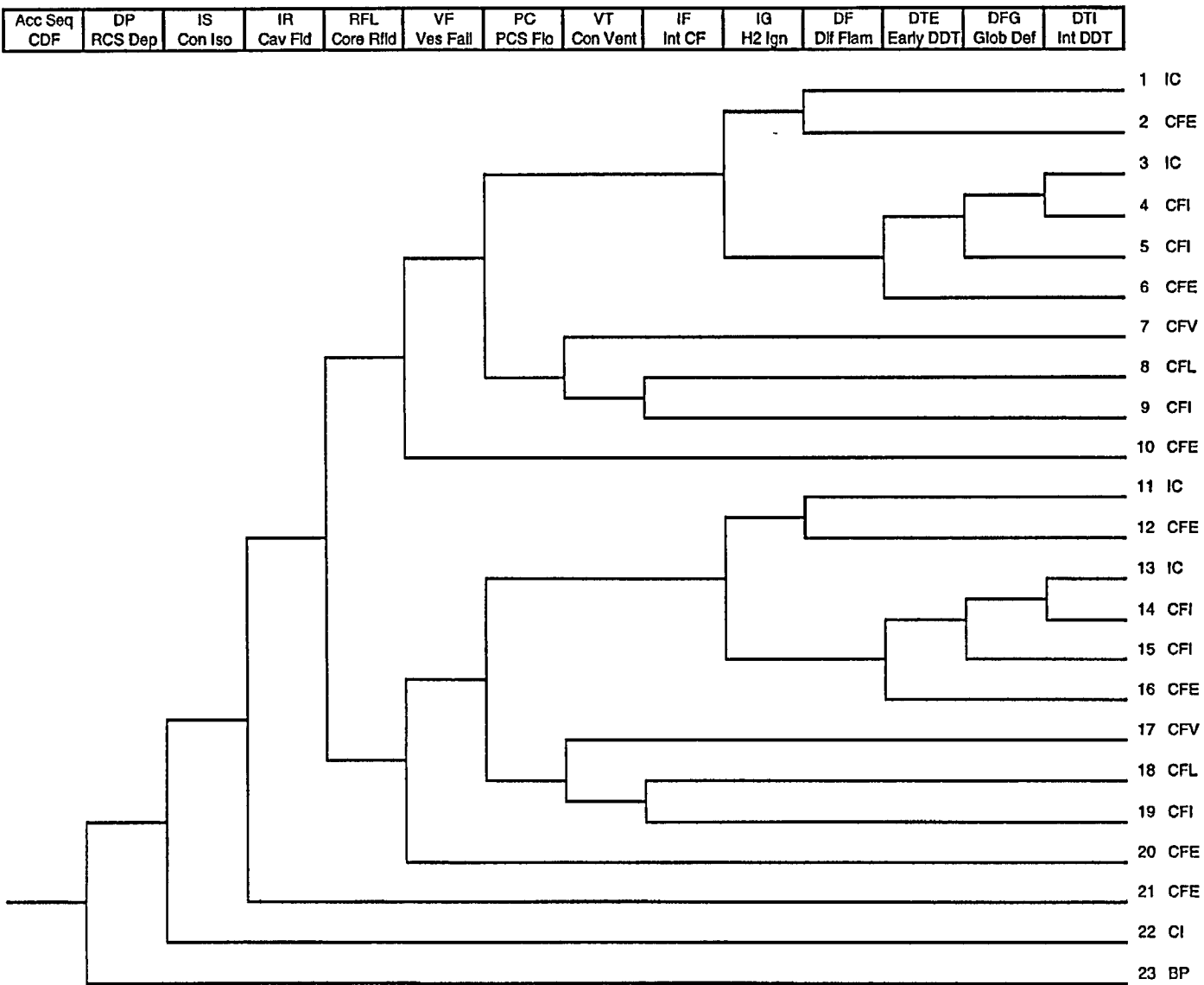


Figure 35-1

Containment Event Tree

## CHAPTER 39

### IN-VESSEL RETENTION OF MOLTEN CORE DEBRIS

#### 39.1 Introduction

In-vessel retention (IVR) of molten core debris via water cooling of the external surface of the reactor vessel is an inherent severe accident management feature of the AP1000 passive plant. During postulated severe accidents, the accident management strategy to flood the reactor cavity with in-containment refueling water storage tank (IRWST) water and submerge the reactor vessel is credited with preventing vessel failure in the AP1000 probabilistic risk assessment (PRA). The water cools the external surface of the vessel and prevents molten debris in the lower head from failing the vessel wall and relocating into the containment. Retaining the debris in the reactor vessel protects the containment integrity by preventing ex-vessel severe accident phenomena, such as ex-vessel steam explosion and core-concrete interaction, which have large uncertainties with respect to containment integrity.

The passive plant is uniquely suited to in-vessel retention because it contains features that promote external cooling of the reactor vessel:

- The reliable multi-stage reactor coolant system (RCS) depressurization system results in low stresses on the vessel wall after the pressure is reduced.
- The vessel lower head has no vessel penetrations to provide a failure mode for the vessel other than creep failure of the wall itself.
- The reactor cavity can be flooded to submerge the vessel above the coolant loop elevation with water intentionally drained from the in-containment refueling water storage tank.
- The reactor vessel insulation design concept provides an engineered pathway for water-cooling the vessel and for venting steam from the reactor cavity.

The purpose of the analysis provided in this chapter is to demonstrate that, given adequate cavity flooding to promote natural circulation flow through the reactor cavity, there is significant margin to vessel failure for the AP1000.

#### 39.2 Background on the Application of IVR to the Passive Plant

The analysis of the in-vessel retention phenomena using the Risk-Oriented Accident Analysis Methodology (ROAAM) (References 39-1 and 39-2) provided the basis for the application of the IVR accident management strategy to the AP600 passive plant and quantification of vessel failure in the AP600 PRA (Reference 39-3). The ROAAMs included an analysis of the in-vessel melt progression and evaluation of the structural and thermal challenges to the vessel during the relocation to the lower head, including in-vessel steam explosion. Testing and evaluation of the uncertainties associated with the thermal loading produced by the molten debris pool and heat removal limitations due to boiling crisis on the exterior vessel surface were performed in the ACOPO (Reference 39-4) and ULPU programs

(References 39-1 and 39-5). The conclusions from the ROAAMs showed that the limiting challenge to the vessel integrity is the thermal loading produced during the steady-state heat transfer to the lower head wall after complete debris relocation to the lower plenum. The IVR ROAAM analyses and testing showed that the water in the AP600 cavity removes the heat produced by the molten debris bed in the lower head with significant margin while the structural integrity of the lower head was maintained.

Based on the ROAAM results, reactor vessel failure in the AP600 was considered to be physically unreasonable, and a probability of zero was applied to vessel failure in the AP600 PRA if the following conditions of the ROAAM analysis were met (Reference 39-3):

- The reactor coolant system was depressurized.
- The reactor vessel was submerged adequately to wet the heated surface.
- Reactor vessel reflective insulation and containment water recirculation flow paths allowed sufficient ingress of water and venting of steam from the cavity.
- The treatment of the lower head outside surface (painting, coatings, etc.) did not interfere with water cooling of the vessel.

### 39.3 Application of IVR to the AP1000 Passive Plant

Much of the passive plant design has not changed in the power uprating from the AP600 to the AP1000. The overall containment design below the operating deck remains essentially the same. The volume of the containment that floods to submerge the reactor vessel and the valves and piping used to drain the water from the IRWST are essentially the same. A check valve has been added to the refueling canal drain, which permits the containment to flood more rapidly by reducing the volume that fills with water. The reactor vessel diameter and lower head geometry has been retained from the AP600 design.

Increasing the power output of the passive plant has resulted in several changes to the reactor core, and reactor pressure vessel and internals, and all must be carefully considered in assessing the plant's capability for successful IVR:

- The reactor power is increased from 1933 MWt to 3400 MWt.
- The reactor core size is increased from 145 12-ft fuel assemblies to 157 14-ft fuel assemblies.
- The length of the reactor vessel was extended 19.5 inches through the core region to accommodate the longer fuel.
- The core reflector is modified to be a thick core shroud to accommodate the additional fuel assemblies within the core barrel.
- The lower core support plate is 1" thicker to accommodate the weight of the larger core.

These changes have an impact on the direct application of the methodology as performed in IVR ROAAM to the AP1000. Specifically, the large margin to vessel failure with respect to the critical heat flux (CHF) limits as defined in Reference 39-1 that was demonstrated in the AP600 ROAAM has been reduced by the increase in reactor power in the AP1000. Figure 39-1 presents a conservative heat flux calculation for the AP1000 compared to the critical heat flux success criterion used in the AP600 IVR ROAAM. The increased heat load in the AP1000 is offset somewhat by the increased mass of the core, but the margin to the AP600 critical heat flux limit is small.

To establish a strong basis for crediting in-vessel retention in the AP1000, the heat removal capacity of the water cooling the vessel wall needs to be increased to reclaim margin.

To extend the IVR accident management strategy and the conclusion from the AP600 IVR ROAAM that vessel failure is physically unreasonable as applied to the AP1000, the following steps are taken:

- Increase the capability of the water in the reactor cavity to remove heat from the external surface of the reactor vessel (e.g. increase CHF).
- Demonstrate that for the increased critical heat flux, thermal failure remains as the limiting failure over structural failure for the AP1000.
- Demonstrate that the AP1000 in-vessel melt progression does not change significantly from the AP600 melt progression in such a way as to challenge the vessel integrity during relocation.
- Demonstrate that the correlations used to calculate heat loads scale appropriately to the AP1000.
- Quantify the thermal loads using the methodology from the IVR ROAAM (Reference 39-1) using AP1000 specific input probability distributions.

Each of these subjects is addressed in the following sections.

#### 39.4 Reactor Vessel Failure Criteria

A significant effort was expended in Chapter 4 of Reference 39-1 to demonstrate that no structural challenge was presented to the vessel as long as the thermal success criterion was met (e.g., heat load on the vessel wall less than critical heat flux at all points on the lower head). Bounding analyses for dead weight loading, thermal stresses, ductile tearing and creep rupture were performed. These arguments and analyses can be extended to the AP1000 as long as it is demonstrated that the structural margins for the AP1000 vessel are on the same order of magnitude as the margins in the AP600 analyses.

The analysis assumes that the RCS has been depressurized. For the AP1000, the dead weight including the lower head and the debris is approximately  $1.9 \times 10^6$  N. The buoyancy force for the vessel lower head displacing water up to the elevation of the nozzle gallery (~98') is approximately  $8 \times 10^5$  N. Therefore, the dead loading is  $1.1 \times 10^6$  N.

The yield strength of carbon steel at temperatures of 900 K is 350 MPa (Reference 39-1). At the loading of  $1 \times 10^6$  N, the minimum area that would be required to carry this load would be:

$$\text{minimum required area} = \frac{\text{load}}{\text{yield strength}} = \frac{1.1 \times 10^6 \text{ N}}{350 \times 10^6 \frac{\text{N}}{\text{m}^2}} = 3 \times 10^{-3} \text{ m}^2 \quad (39-1)$$

The minimum area required to carry the dead load corresponds to a thickness of 0.022 cm of the AP1000 vessel wall at the outer radius of 2.1524 m.

The wall thickness that carries the loading is the portion of the wall with a temperature from the yield strength temperature (900 K) to the saturation temperature (373 K) at the peak critical heat flux obtainable by the AP1000 configuration. The peak critical heat flux is conservatively estimated to be 2000 kW/m<sup>2</sup> for this calculation. The thickness can be calculated from the thermal conductivity (32 W/m-K) through the vessel wall using the standard conduction rate equation and solving for the thickness:

$$x_v = \frac{K_v (T_{\text{yield}} - T_{\text{sat}})}{q_w} = \frac{32 * (900 - 373)}{2000 \times 10^3} = 0.8 \text{ cm} \quad (39-2)$$

The AP1000 vessel wall, conducting heat at the peak critical heat flux, is 36 times thicker than the minimum thickness required to carry the dead load. The AP600 vessel is 73 times thicker than the minimum thickness required to carry the dead load (Reference 39-1). Therefore, the margin to structural failure is the same order of magnitude as the AP600.

It should be noted that the actual peak heat fluxes in the AP1000 are expected to be significantly lower than the critical heat flux limit of 2000 kW/m<sup>2</sup>. Based on the calculation presented in Figure 39-1, the peak heat flux to the vessel wall is on the order of 1400 kW/m<sup>2</sup>, which increases this margin to 50 times the thickness required to carry the load.

The conclusions of the structural analyses performed for the AP600 in Reference 39-1 can be comfortably extrapolated to the AP1000. Thus, for the AP1000, success of IVR can be based solely on the thermal success criterion.

### 39.5 In-Vessel Melt Progression and Relocation

In the AP600 ROAAM analysis of in-vessel retention (Reference 39-1) and in-vessel steam explosion (References 39-2, 39-10, 39-11, and 39-12), the melt progression and relocation to the lower plenum was analyzed. One of the conclusions from the AP600 analysis was that the reactor vessel lower internals, particularly the reflector situated inside the core barrel, significantly impacted the relocation such that:

- The debris relocation to the lower plenum occurs due to melt-through of the core barrel. The quantity of the initial mass of the molten debris that mixes with the lower plenum water is dictated by the failure size and includes only a small fraction of the debris.

- The relocation pathway to the lower plenum from the fuel region downward through the support plate is blocked by metal, which melts and re-freezes around the zirc plugs, lower fuel assembly nozzles and support plate.
- The relocation pathway to the lower plenum from the region between the reflector and the core barrel downward through the support plate is blocked by metal relocated from the failure of the core reflector.
- A fraction of the total molten  $\text{UO}_2$  is needed to fill the lower plenum to contact the lower support plate, allowing the lower support plate and reflector to melt into the debris mass.
- The large metal mass from the melting of the reflector and support plate in the lower plenum produces a thick metal layer that mitigates any focusing effect of the metal layer and prevents a large heat flux from occurring at the top of the debris pool.

The AP1000 core and lower internals geometry has been changed from the AP600 geometry as a result of the higher power output. The core is made up of 157 fuel assemblies with a 14-foot active fuel length. To accommodate the larger reactor core, the thick stainless steel reflector has been replaced by a 7/8" thick core stainless steel shroud (Figure 39-2). The thick bottom plate of the shroud is mounted flush on the support plate. There are no former plates in the annulus between the shroud and the core barrel. The core barrel is 2" thick and hangs from the upper head flange. Cooling holes through the core shroud provide cooling flow to the shroud from the core flow.

The phenomena associated with melting the core and the relocation of the molten debris to the lower plenum play an important role in the composition and configuration of the debris pool (Reference 39-2). In turn, the characteristics of the debris pool significantly impact the heat loading to the lower head wall and the challenge to lower head integrity (Reference 39-1). Therefore, understanding the melting and relocation scenarios plays an important role in the assessment of in-vessel retention of molten core debris in the lower plenum. Attachment 39A provides analysis of the core melting and relocation, considering the impact of the AP1000 specific geometry, and addresses the timing and interactions of the various debris materials in the formation of a lower plenum debris bed.

The important conclusions from the Attachment 39A analysis of the lower plenum debris pool formation are:

- The lower plenum debris bed is cooled with water during the entire relocation process prior to contact with the support plate. Transient debris configurations are not predicted to threaten vessel integrity.
- The lower plenum oxide debris subsumes the lower core support plate before dry out in the lower plenum occurs. If the relocated debris is assumed to be instantaneously quenched in the lower plenum water, the oxide debris contacts the lower support plate before the debris can return to a superheated condition. Therefore, the lower core support plate, the core shroud, and a sizeable fraction of the core barrel are subsumed in the debris bed. The focusing effect is mitigated.

- The lower plenum debris bed is predicted to form a metal layer over oxide pool configuration.
- The potential for debris interaction creating a bottom metal pool of uranium dissolved in zirconium is expected to be small.
- The earliest time to achieve the fully molten, circulating debris bed in the lower plenum is 2.7 hours after event initiation.

### 39.6 Application of Heat Transfer Correlations to the AP1000

#### 39.6.1 Debris Pool to Vessel Wall Heat Transfer

The heat transfer from the oxide pool containing the decay heat to the lower head wall of the reactor vessel is described using the Angelini-Theofanous correlations (Reference 39-4) that were developed based on the results of the ACOPO experiments.

$$Nu_{up} = 1.95 Ra'^{0.18} \quad (39-3)$$

$$Nu_{dn} = 0.30 Ra'^{0.22} \quad (39-4)$$

The local heat flux from the oxide pool to the lower head at angle  $\theta$  is found from Equation 39-5, where  $\theta_p$  is the angular position at the top of the oxide pool (Reference 39-1):

$$\frac{Nu_{dn}(\theta)}{Nu_{dn}} = 0.1 + 1.08 \left( \frac{\theta}{\theta_p} \right) - 4.5 \left( \frac{\theta}{\theta_p} \right)^2 + 8.6 \left( \frac{\theta}{\theta_p} \right)^3, \quad 0.1 \leq \frac{\theta}{\theta_p} \leq 0.6$$

$$\frac{Nu_{dn}(\theta)}{Nu_{dn}} = 0.41 + 0.35 \left( \frac{\theta}{\theta_p} \right) + \left( \frac{\theta}{\theta_p} \right)^2, \quad 0.1 \leq \frac{\theta}{\theta_p} \leq 0.6 \quad (39-5)$$

The correlations are valid to an internal Rayleigh number ( $Ra'$ ) of  $10^{16}$  for the oxide pool (References 39-4 and 39-6).

The heat transfer from the metal layer to the vessel wall is calculated from the Churchill-Chu correlation (Equation 39-6), which is valid to an external Rayleigh number of  $10^{13}$  for the metal pool (Reference 39-7).

$$Nu = 0.076 Ra^{1/3} \quad (39-6)$$

The heat transfer from the metal layer to the horizontal interfaces is calculated from the Globe-Dropkin correlation (Equation 39-7), which is valid in the range  $3 \times 10^5 < Ra < 7 \times 10^9$  (Reference 39-8).

$$Nu = 0.059 Ra^{1/3} \quad (39-7)$$

The Rayleigh numbers of the AP1000 in-vessel debris pool can be estimated given the mass of materials (see Table 39-1) and geometry of the AP1000 reactor vessel. Assuming 50-percent zirconium oxidation and decay heat in the oxide pool at 2 hours after shutdown (29.6 MW, including loss of volatile fission products from pool), the Rayleigh number of the oxide pool is  $10^{16}$ . The Rayleigh number for the metal pool is on the order of  $10^{10}$ .

The conditions in the AP1000 are within the valid range of the Angelini-Theofanous and Churchill-Chu correlations. The extrapolation of the Globe-Dropkin correlation to this application is modest, as it is less than one order of magnitude, and pertains to the thick metal layer condition, which is not challenging. Therefore, the correlations are considered to be appropriate for modeling the heat transfer from the molten debris to the vessel wall in the AP1000 IVR analysis.

### 39.6.2 Vessel Wall to External Cooling Water Heat Transfer

The heat transfer from the vessel wall to the cooling water is limited by the transition to film boiling at the external surface of the vessel wall. The maximum heat flux that can be removed prior to the transition to film boiling is the critical heat flux. In Section 39.4 it is shown that as long as the heat flux from the debris pool to the wall is less than the critical heat flux, the vessel maintains sufficient strength to carry the load on the vessel. At heat fluxes above the critical heat flux, the external wall temperature increases significantly, the strength of the wall is lost, and the vessel fails.

In the AP600 IVR ROAAM (Reference 39-1), the critical heat fluxes at the various points on the lower head downward-facing, curved surface were determined in the ULPU experiments (References 39-1 and 39-5). ULPU-2000 Configuration III (Figure 39-3) had a baffle and exit restriction to model the AP600-specific insulation configuration. The critical heat flux is described by the ULPU correlation (Equation 39-8):

$$q_{cr} = 490 + 30.2\theta - 0.888\theta^2 + 1.35 \times 10^{-3}\theta^3 - 6.65 \times 10^4 \frac{\text{kW}}{\text{m}^2} \quad (39-8)$$

The local angle on the lower head,  $\theta$ , is entered in degrees. The angle at the bottom of the lower head is  $0^\circ$ . The angle of the top of the oxide pool and the bottom of the metal pool is the same angle and is calculated from the height of the oxide pool,  $H$ , and the radius of the lower head,  $R$ , using the equation:

$$\cos \theta = \frac{R - H}{R} \quad (39-9)$$

The AP600 IVR ROAAM results showed that the heat fluxes generated by the debris pool in the lower plenum were on the order of 55 percent of the critical heat flux or lower at each point on the vessel surface.

The heat fluxes produced by the AP1000 IVR phenomena do not produce significant margin-to-failure with respect to the critical heat flux as defined by the ULPU correlation. Figure 39-1 presents a bounding quantification of the heat fluxes expected for the AP1000,

calculated using a conservative mass of stainless steel in the debris bed, 75 percent zirconium oxidation, and non-volatile fission product decay heat in the debris for 1.5 hours after shutdown. While the peak heat flux at the top of the oxide layer and in the metal layer is less than the critical heat flux calculated by the ULPU correlation, it provides little margin. This critical heat flux limit as defined for the AP600 cannot be extended to the AP1000. Therefore, a different ex-vessel geometry that will increase the heat removal capacity of the water is required for the AP1000.

Testing has been performed with UPLU-2000 Configuration IV (Figure 39-3) which demonstrates the feasibility of increasing the critical heat flux by constructing a hemispherical baffle outside the lower head to channel the cooling water flow. ULPU Configuration IV tests (Reference 39-9) produced peak critical heat fluxes in excess of  $1800 \text{ kW/m}^2$  and provided evidence to suggest that CHF in excess of  $2000 \text{ kW/m}^2$  could be achieved with proper baffle design.

ULPU-2000 Configuration IV also demonstrated the need to achieve a sufficiently high flooding level in the containment outside the reactor vessel to develop the high velocity circulation through the baffle needed to increase the critical heat flux. The circulation produced by the venting of steam alone (pool boiling) from the insulation is not sufficient to reach the critical heat fluxes required for the AP1000. To circulate water through the reactor vessel insulation and provide adequate reactor vessel cooling, the cavity water level above the lower head needs to be deep enough to produce two-phase flow through the vent from the cavity. The two-phase flow creates a density difference that drives the flow through the baffle and increases the critical heat flux on the outer surface of the AP1000 reactor vessel (Figure 39-4). The ULPU-2000 Configuration IV results show that, given the successful flooding and proper insulation and vent design, significant enhancement of the critical heat flux can be achieved (Figure 39-5). The critical heat flux at the elevation of the top of the oxide and at the metal layer is increased 30 to 40 percent.

The AP1000 employs a reactor vessel insulation design that provides water inlet, steam venting and a baffle around the lower head to enhance the heat removal and increase the critical heat flux on the reactor vessel external surface. The insulation is vented from the annulus between the insulation and vessel to the vessel nozzle gallery at the 98-ft elevation.

### 39.7 Quantification of Margin to Failure of the Reactor Vessel Wall

The heat load to the lower head of the AP1000 reactor vessel is calculated using the same methodology as outlined in Reference 39-1. The method assumes that the debris bed forms the metal-over-oxide debris bed configuration (called the final bounding state in Reference 39-1). The volatile fission products, and their contribution to the decay heat, are vaporized and transported out of the debris. All of the heating from the non-volatile fission products is assumed to be in the oxide layer. The reactor vessel is depressurized, and there is no water cooling of the surface of the debris bed metal layer. Only radiation heat transfer to the upper internals and reactor vessel wall is credited. The emissivity of the top surface of the metal layer is taken as a lower bound value of 0.4 (Reference 39-1).

### 39.7.1 Zirconium Oxidation Fraction Input Probability Distribution

Zirconium oxidation impacts the heat fluxes to the reactor vessel by changing the ratio of the metal to oxide. Higher oxidation fractions increase the mass of the oxide, producing a lower volumetric heat rate in the oxide layer but thinning the metal layer, thus increasing the heat flux to the wall from the metal layer. These competing effects are accounted for by providing a probability distribution of zirconium oxidation fraction over a credible range.

For the bounding IVR case, all the water in the core region boils away and there is no reflood inside the vessel. The reactor coolant system is depressurized. This case is a boil-off type scenario such as a large loss-of-coolant accident (LOCA). Reference 39-1 and Chapter 41 of the AP600 PRA (Reference 39-3) provide zirconium oxidation probability distributions for such sequences that are very similar. The probability distribution from the AP600 PRA was selected for use in this analysis since it is slightly more conservative (higher upper bound). The zirconium probability density function provides a probability of 0.89 evenly distributed for oxidation fractions from 40 to 60 percent of the total zirconium mass, 0.10 for fractions from 60 to 75 percent of the zirconium, and 0.01 for fractions from 75 to 100 percent of the zirconium.

Figure 39-6 shows the zirconium oxidation input probability distribution for the IVR analysis.

### 39.7.2 Steel Mass Input Probability Distribution

The mass of steel in the lower plenum debris bed is important since it impacts the thickness of the metal layer. The more steel that there is in the debris pool, the thicker the metal layer will be. A thicker metal layer reduces the heat flux to the vessel wall from the metal layer. So a smaller mass is conservative with respect to the heat flux to the wall from the metal layer.

The AP1000 lower support plate sits relatively low in the vessel, below the top of the lower head. Only a 65 to 70 percent of the oxidic debris is needed in the lower plenum to subsume the lower core support plate into the debris. The core shroud is held in place by the lower support plate. Given a significant relocation of oxidic debris to the lower plenum, the lower support plate, including the inlet nozzles of the fuel assemblies, and core shroud will be melted into the debris bed along with the lower supporting structures, which are in the lower plenum. This provides the lower bound mass of steel in the debris of 51 metric tons.

Prior to relocating to the lower head, the core melts inside the core barrel and accumulates above the core support plate. It is estimated that up to 25 percent of the core barrel mass may be melted by the debris prior to core relocation with decreasing probability with increasing mass. Therefore, a probability of 90 percent is distributed decreasing linearly from 51 metric tons (the minimum mass) up to 62 metric tons to account for the mass of the core barrel. A probability of 0.10 is assigned with linearly decreasing probability from 62 to 70 metric tons to account for any additional debris that could be melted in from the upper internals and upper core region.

Figure 39-7 shows the steel mass input probability distribution for the IVR analysis.

### 39.7.3 Final Bounding State Timing Input Probability Distribution

When the molten debris reaches the lower plenum, a metal-over-oxide debris bed configuration is formed and the decay heat in the oxide pool produces a strong natural circulation flow. According to Reference 39-1, this steady-state configuration is the physically reasonable final bounding state for the melt relocation expected in the advanced passive plant.

It is estimated that the core debris can achieve the final bounding state approximately 1 hour after rapid oxidation of the cladding begins. Accident Classes 3BE, 3BL and 3D comprise the IVR cases that can achieve the dry vessel configuration. Accident class 3BE has a conditional probability of 0.50 within this subset of plant damage states, and is comprised of early core melt sequences. Accident class 3D has a conditional probability of 0.35 and is comprised of both early and late core melt sequences. Accident class 3BL has a conditional probability of 15 percent and is comprised of late core melt sequences. Based on the level 1 PRA frequencies for these cases, their relative contribution and their expected timing to core uncover, a probability distribution for the time to reach final bounding state has been developed. A probability of 0.70 is distributed linearly increasing from 1.5 to 2.0 hours, and a probability of 0.30 is distributed linearly decreasing from 2.0 to 4.0 hours.

Figure 39-8 shows the timing input probability distribution for the IVR analysis.

### 39.7.4 Critical Heat Flux

The heat fluxes to the vessel wall from the molten debris pool are calculated at three locations of interest: the bottom of the lower head, the top of the oxide layer and the bottom of the metal layer. The bottom of the lower head has the lowest value of critical heat flux, and the top of the oxide layer and the bottom of the metal layer are the potential locations for the least margin to failure. The heat fluxes are normalized by the local critical heat fluxes and presented as probability distributions for each of the three locations.

The local critical heat flux at each location,  $q_{\text{chf}}(\theta)$ , is calculated using the correlation developed from the UPLU-2000 Configuration III testing presented in Reference 39-1 (Equation 39-8).

For the AP1000 IVR analysis, the critical heat flux from Equation 39-8 is “enhanced” to account for the improved heat removal for the AP1000 ex-vessel geometry using the results from the ULPU-2000 Configuration IV testing (see Figure 39-5). At the bottom of the lower head, the critical heat flux is increased by a factor of 1.2, and at the top of the oxide and the bottom of the metal layer, the critical heat flux is increased by a factor of 1.3.

### 39.7.5 Results and Conclusions of Heat Flux Quantification

The results of the heat flux quantification are presented in Figures 39-9 through 39-14. The heights of the oxide and metal pools are presented as probability distributions in Figures 39-9 and 39-10. The probability distribution of the decay power density in the oxide debris pool is presented in Figure 39-11. The range of the oxide pool  $Ra'$  number (Figure 39-12) and the

metal pool Ra number (Figure 39-13) show that the correlations are appropriate for the AP1000 calculation.

The probability distributions of the heat fluxes normalized by the local critical heat fluxes are presented in Figure 39-14. The peak heat flux occurs at the top of the oxide layer at 70 percent of the critical heat flux.

The results of the analysis show that, with the AP1000 insulation designed to increase the cooling limitation at the lower head surface and the cavity adequately flooded, the AP1000 provides significant margin-to-failure for IVR via external reactor vessel cooling.

Based on the results of the UPLU-2000 Configuration IV testing and analysis, vessel failure probability is considered to be zero in the AP1000 PRA provided the following conditions are met:

- The reactor coolant system is depressurized.
- The vessel is adequately submerged to promote two-phase natural circulation flow through the baffle surrounding the lower head.
- Reactor vessel reflective insulation remains structurally sound under the pressure loads produced by the external boiling, allows water inlet at the bottom and venting of steam at the top, and provides the proper baffling to increase the critical heat flux on the external surface of the vessel lower head.
- The reactor vessel external surface promotes the wetting phenomena identified as the surface cooling mechanism in the UPLU testing (Reference 39-5).

The probability of each of these conditions is discussed and quantified in the following sections.

### 39.8 Reactor Coolant System Depressurization

Reactor coolant system pressure is determined at node DP (see Chapter 36) on the containment event tree. Sequences that proceed downstream from node DP are depressurized to an RCS pressure close to containment atmospheric pressure. Success at node DP is required for successful IVR. Therefore, sufficient reactor coolant system depressurization is attained at all sequences considered for in-vessel retention.

### 39.9 Reactor Cavity Flooding (Node IR)

Reactor cavity flooding is considered at node IR on the containment event tree. Adequate cavity flooding is required for the success of IVR. Cavity flooding is accomplished through either the progression of the accident or through operator action to manually drain the IRWST water into containment.

Some accident sequences flood the cavity through the progression of the accident. Core damage occurs as a result of failure to recirculate water to the core once the water is drained

from the IRWST, or because injection occurs but is not sufficient or soon enough to prevent core damage. Such sequences guarantee success at node IR.

If the water does not drain from the IRWST during an accident, the operator is able to flood the cavity by opening the motor-operated valves and squib valves in the recirculation lines between the IRWST and the containment recirculation screens, as shown in Figure 39-15. The operator action is prescribed by the first step in the AFR.C-1 functional restoration guideline entered when the core-exit thermocouples reach 1200°F. The water floods the containment by flowing out of the recirculation screens, filling the containment floodable region of the containment, shown in Figure 39-16, to at least the 107' 2" elevation, shown in Figure 39-17.

This section discusses the evaluation of successful cavity flooding to prevent vessel failure at node IR for each of the AP1000 accident classes.

### 39.9.1 Node IR Success Criteria

The question that is considered at node IR to determine success or failure of cavity flooding for in-vessel retention is:

Does the water from the IRWST fill the reactor cavity to submerge the reactor vessel above the 98 foot elevation within 70 minutes of the core exit thermocouples reaching 1200°F?

To achieve the critical heat flux levels needed to cool the AP1000 lower head, the water level must be sufficient to promote the steam venting from the insulation to entrain water out of the vent. The vents from the AP1000 reactor vessel insulation exit to the vessel nozzle gallery at the 98-ft elevation. It is conservatively assumed that the water level in the containment needs to reach the 98 ft elevation within 70 minutes after the core exit temperature exceeds 1200°F.

This level requirement is conservative since it does not account for the void fraction that increases the mixture level inside the insulation. Seventy minutes is approximately the time after the core-exit temperature exceeds 1200°F required to melt and relocate the entire core to the lower head, vaporize the water in the lower head, and melt the core support plate and shroud into the debris pool.

The AP600 procedures instruct the operator to flood the reactor cavity at the end of AFR.C-1, before entering the severe accident management guidelines. The AP1000 requires the cavity to be flooded deeper and more quickly than the AP600. Therefore, as a result of this analysis, the operator action to flood the reactor cavity has been moved to the entry to AFR.C-1 for the AP1000 emergency operating procedures.

#### 39.9.1.1 Water Elevations Success Criteria

Since one of the conditions for successful IVR is a depressurized RCS (success at containment event tree (CET) node DP), it can be assumed that the AP1000 reactor cavity is full of reactor coolant system water prior to the manual cavity flooding action. Therefore, the initial water level prior to cavity flooding is above the 83-ft elevation in the containment.

Calculations of the flow rate from the IRWST to the containment floodable region for one and two trains of recirculation lines are performed using the Bernoulli equation. The flow rates from both train A and train B are calculated separately and together, taking into account resistance differences due to layout. The results are presented in Figure 39-18, and show that one train is sufficient to flood the containment to the proper level within the required time with margin for operator action time.

Therefore, successful opening of one of two containment flooding lines is sufficient to successfully submerge the vessel for accident classes that do not have injection of the IRWST through normal injection lines.

### 39.9.1.2 Manual Action Success Criteria

The operator action to flood the AP1000 cavity is determined in functional restoration guideline AFR.C-1. The operator floods the reactor cavity at step one, upon entry into the procedure. This is earlier than the AP600 functional restoration guideline indicates cavity flooding. Due to the need for deeper flooding for successful IVR in the AP1000, the action has been moved to an earlier step.

Flooding rates for 1 and 2 cavity flooding lines open are presented in Figure 39-18. With the single highest resistance flooding line open, the 98' elevation is reached within 65 minutes of opening the valves. For the lower resistance line the 98' elevation is reached within 50 minutes. A minimum of 5 minutes are available for the operator to open the cavity flooding valves after the core-exit thermocouples reach 1200°F.

The criterion used for operator action to flood the cavity is the manual opening of at least 1 of 2 cavity flooding lines within 5 minutes of a core-exit thermocouple reading of 1200°F.

## 39.9.2 Cavity Flooding Scenario Dependencies

### 39.9.2.1 Accident Class 3BE

Accident class 3BE contains core damage sequences in which the reactor coolant system is fully depressurized but gravity injection is failed. Since the IRWST water injection fails, an operator action is required to flood the reactor cavity. Fault tree IWF (see Chapter 12) is linked to node IR in accident class 3BE to evaluate the probability of hardware and human action failure in cavity flooding.

In a significant fraction of the 3BE frequency, a direct vessel injection (DVI) line is failed and the intact injection line is plugged or the injection valves fail to open. In these sequences, the IRWST water may drain from the broken side of the direct vessel injection line, through the drain from the valve vault to the floodable region of the containment, as discussed in Chapter 38 for containment event tree node RFL. The manual action to flood may not be required in this case, but conservatively, only the operator action to flood the cavity is credited at node IR for accident class 3BE.

**39.9.2.2 Accident Class 3BL**

Accident class 3BL contains severe accident sequences in which long-term recirculation of the IRWST water fails. In these cases, the IRWST water has successfully injected into the cavity before core damage, but is unable to recirculate. Cavity flooding to cool the reactor vessel is guaranteed by progression of the accident sequence. A failure probability of zero is assigned to node IR for accident class 3BL.

**39.9.2.3 Accident Class 3A**

Accident class 3A contains anticipated transient without scram sequences that damage the core. To reach the IR node in the containment event tree, node DP is successful for accident class 3A, which means that the reactor coolant system is intact throughout the pressure transient, and the passive residual heat removal system provides long-term heat removal. Core damage is assumed, although it would be very limited, and no core debris is accumulated in the lower head. Although there is no cavity flooding, success is achieved by successfully mitigating debris relocation to the lower head. A failure probability of zero is assigned to node IR for accident class 3A.

**39.9.2.4 Accident Class 3C**

In accident class 3C, the vessel is failed below the intact core as a result of the initiating event. Since vessel rupture produces core damage regardless of safety system availability, the failure of the automatic depressurization system (ADS) and gravity injection has negligible frequency in accident class 3C. Core damage is caused by the inability to reflood the core until the reactor cavity is filled. Cavity flooding is achieved through progression of the accident sequence. A failure probability of zero is assigned to node IR for accident class 3C.

**39.9.2.5 Accident Class 3BR**

Accident class 3BR contains large LOCA sequences in which the accumulators fail to inject and reflood the core. The core makeup tanks and IRWST water inject, but are not sufficient to prevent minor core damage without the accumulators. The IRWST water injects due to the progression of the accident sequence and floods the reactor vessel and cavity. A failure probability of zero is assigned to node IR for accident class 3BR.

**39.9.2.6 Accident Classes 1D and 3D**

Accident classes 1D and 3D contain core damage sequences in which depressurization is insufficient to allow adequate safety injection, but sufficient to prevent vessel failure if the cavity is flooded. Some limited injection may occur, but not at a rate that will prevent core damage or flood the cavity without operator action. Fault tree IWF (Chapter 12) is linked to node IR in accident classes 3D and 1D to evaluate the probability of hardware and human action failure in cavity flooding.

### 39.9.2.7 Accident Classes 1A and 1AP

Accident classes 1A and 1AP contain core damage sequences in which the ADS is completely failed, preventing injection from the IRWST. In these sequences, an operator action to depressurize adequately to allow core recovery is posed at node DP. In-vessel retention is not credited if node DP is failed. If depressurization succeeds at node DP, it is assumed that the IRWST injection into the vessel succeeds. The contribution to the release frequency from the failure of injection is extremely small and does not have an impact on the results (i.e., the release frequency does not change significantly). Therefore, full injection recovery of the cavity is assumed to occur at node IR for accident classes 1A and 1AP. A failure probability of zero is assigned to node IR for accident classes 1A and 1AP.

### 39.9.2.8 Accident Class 6

Accident class 6 contains core damage sequences from steam generator tube rupture (SGTR) initiated accidents. Steam generator tube rupture sequences that reach node IR have successful ADS actuation and injection from the IRWST. This ensures depressurization and gravity injection. A failure probability of zero is assigned to node IR for accident class 6.

## 39.10 Reactor Vessel Insulation Design Concept

With respect to in-vessel retention severe accident management, the goal of the reactor vessel insulation is to ensure that there will always be an adequate flow of water layer in contact with the reactor vessel to promote nucleate boiling heat transfer from the reactor vessel wall. In the event of a severe accident, the AP1000 reactor vessel reflective insulation promotes the natural circulation of water through the vessel annulus to provide cooling water for the lower head. The cooling of the vessel in a severe accident is accomplished by providing:

- A means of allowing water free access to the region between the reactor vessel and insulation.
- A support frame that provides sufficient structural integrity of the insulation surrounding the lower head and lower vessel cylinder where the in-vessel debris bed can be in contact with the wall to maintain the baffling geometry for the water flow next to the vessel.
- A means to vent steam generated by the water cooling the vessel wall from the insulation surrounding the reactor vessel.
- A support frame to prevent the insulation panels above the lower vessel from breaking free and blocking water from cooling the reactor vessel exterior surface.

### 39.10.1 Description of Reactor Vessel Insulation and Venting

A schematic (not to scale) depiction of the reactor vessel, the vessel insulation, the insulation water inlet and steam/water discharge paths, and the reactor vessel cavity are shown in Figure 39-19. The insulation is a reflective metal type insulation and is typically 4 inches thick. The insulation is made in panel sections that are bolted to a structural steel frame. The

steel frame is supported from the reactor cavity structural walls and floor. The insulation panels around the reactor vessel lower head are constructed so that they form a hemispherical shape that conforms to the shape of the lower head, while the insulation panels around the vessel cylindrical section are positioned to create an annular space between the insulation and the vertical vessel side wall. The space between the insulation and the vessel outside surface is nominally 6 inches (15 cm) wide. The space between the outer insulation vertical surface and the closest point on the octagonal reactor cavity walls is nominally 2 inches (5 cm).

At the bottom of the insulation, below the center of the lower head, is a water inlet that consists of a perforated plate, and a number of buoyant stainless steel balls and an equal number of guides. Each ball normally rests in its guide atop one of the holes in the perforated plate. The balls are heavy enough so that the air that is normally blown into the cavity for normal ventilation cannot lift the balls. However, the balls will float when the cavity fills with water, unblocking the holes and allowing water to flow into the space between the insulation and the vessel surface. The flow area through the perforated plate is sized to assure low water inlet velocity, and to minimize the inlet pressure drop.

Near the top of the reactor vessel cylindrical section there are four (4) steam/water flow paths from the space between the insulation and the vessel wall. These flow paths complete the natural circulation flow path from the space between the insulation and vessel wall to the containment flood-up water. These flow paths are embedded in the concrete shield that makes up the vessel cavity and terminate in the vessel nozzle gallery at elevation 98'. These flow paths enter the nozzle gallery vertically and are covered by a light-weight, buoyant cover that will be opened by the steam/water flow through the flow path, or the flood-up water. These covers serve to prevent the accumulation of dust or debris in the steam/water flow paths.

With the above insulation arrangement, the air that is blown into the reactor vessel cavity during normal operation cannot flow between the insulation and the reactor vessel since the inlet path is closed (the balls are blocking the inlet holes). The ventilation air therefore flows between the insulation and the cavity walls, and exits the cavity by flowing through the reactor vessel supports into the nozzle gallery area, and then vents into the loop compartments. Thus, the normal air flow keeps the cavity wall concrete, the ex-core instrumentation, and the reactor vessel supports cool.

For an event that results in the flood-up of the containment, the reactor vessel cavity will flood, floating the inlet balls and opening the inlet into the space between the insulation and the vessel surface. Water can now contact the lower head and provide heat removal by steaming, with the steam being vented to the vessel nozzle gallery through the four steam/water flow paths near the top of the cylindrical section of the vessel. As the containment flood-up level increases, the static head of the flood up water will raise the collapsed water level in the space between the insulation and vessel surface. Then, as a result of the heat transfer from the vessel head, two phase flow will be initiated with steam and water being carried up to the nozzle gallery elevation. When the flood up water exceeds the 98' elevation and floods the nozzle gallery; a natural circulation flow path is established from the containment flood up water, into the vessel cavity, into the space between the insulation and the vessel, upward along the vessel surface, through the steam/water flow paths to the

nozzle gallery, and out into the loop compartments which are part of the containment flood up region.

### 39.10.2 Design Analysis of the Insulation and Support Frame

The AP1000 reactor vessel insulation requirements to achieve the in-vessel retention function are:

- Reactor vessel lower head insulation that is shaped to conform to the hemispherical lower head which creates a smooth flow path transition to the annular space between the vessel cylindrical section and its surrounding insulation.
- A frame that maintains the insulation a specified minimum and maximum distance from the reactor vessel outer surface.
- A means of allowing flood-up water free access into the space between the insulation and the reactor vessel outer surface at the center bottom of the lower head.
- A flow path to allow the water and steam mixture created by heat transfer from the vessel surface to circulate from the space between the vessel and the surrounding insulation to the containment flood-up water.
- A support frame that prevents the insulation panels from breaking free and blocking the water/steam flow to/from the space between the vessel and insulation.

The detailed mechanical analysis of the insulation and support frame for the in-vessel retention loading conditions will verify that:

- The insulation support frame will retain the vertical insulation panels to prevent blockage of the water/steam flow path under maximum loads both toward and away from the reactor vessel.
- The insulation support frame for the insulation around the vessel lower head will prevent buoyancy-related movement of the lower panels toward the reactor vessel.
- Pressurization within the insulation/vessel surface flow path will not cause the water inlet device to close or impede flow into the space between the insulation and vessel surface.
- Movement (flexing) of the insulation during the time that water is boiling to remove heat from the vessel wall, will be restricted to prevent the venting of large steam volumes from between the insulation and the vessel.
- When there is maximum pressure acting on the insulation in the direction toward the reactor vessel, the insulation and support frame will maintain a minimum distance between the insulation and the vessel wall.

### 39.11 Reactor Vessel External Surface Treatment

The reactor vessel lower head surface ensures that the surface is well wetted. A well-aged, well-oxidized surface provides good wetting. Any surface coating that is applied to protect the base metal will promote the wetting of the outer vessel lower head surface.

### 39.12 Reactor Vessel Failure (Node VF)

#### 39.12.1 Node VF Success Criteria

The question considered at node VF to determine success or failure of reactor vessel integrity is:

Is the core debris maintained inside the reactor vessel?

Success is credited at node VF if debris is maintained in the reactor vessel and relocation to the containment is prevented. Based on the analysis of in-vessel retention, an intact reactor vessel remains intact if the reactor coolant system is depressurized (success at node DP) and the reactor vessel is adequately submerged (success at node IR). However, in accident class 3C, the vessel rupture initiating event, the vessel is failed prior to core damage and relocation. In this case, success is credited if vessel failure does not allow debris relocation to the cavity.

Success criteria are as follows:

- For all accident classes except 3C, success of node DP and node IR results in success at node VF.
- For accident class 3C, success at node DP and node IR, and maintaining the debris inside the faulted reactor vessel, result in success at node VF.

In accident class 3C, the vessel is failed below the intact core as a result of the initiating event. Since vessel rupture produces core damage, regardless of safety system availability, the failure of ADS and gravity injection has negligible frequency in accident class 3C. Core damage is caused by the inability to reflood the core until the reactor cavity is filled. AP1000 has the cavity flooding feature that, once the cavity is filled up to the break, water can reflood back into the vessel as the containment compartments fill to arrest core damage before full core relocation. Only a limited amount of debris is likely to relocate to the lower head. The most likely failure for the reactor vessel initiating event is a local failure above the top of the lower head hemisphere at the beltline of the vessel. This location has the highest fluence and brittleness from exposure. Debris relocated into the lower head is guaranteed to be water cooled in the vessel. Therefore, for accident class 3C, a scalar failure probability value of 0.1 for the probability of a break that allows debris relocation to the containment is assigned to node VF. Sensitivity to this value is investigated and discussed in Chapter 43.

### 39.13 Summary

In-vessel retention of molten core debris via external reactor vessel cooling can be accomplished in the AP1000, however enhancements over the AP600 IVR strategy are required to accommodate the uprated power level.

- The reactor vessel insulation must provide a structurally-sound baffle around the lower head and lower cylinder of the vessel to channel the flow between the vessel and insulation. An insulation design that provides the proper water inlet, steam venting and flow baffling is specified for the AP1000.
- The reactor cavity must be flooded to a higher elevation prior to the onset of the steady-state heat flux to the vessel wall from the debris to produce the two-phase natural circulation flow required to enhance the critical heat flux on the vessel surface. The operator action to flood the cavity has been moved to an earlier point in the emergency operating procedures to help accomplish adequate flooding.

The fault trees and scalar values linked for nodes IR and VF are summarized in Tables 39-2 and 39-3, respectively.

### 39.14 References

- 39-1 Theofanous, T. G., et al., *In-Vessel Coolability and Retention of a Core Melt*, DOE/ID 10460, July 1995.
- 39-2 Theofanous, T. G., et al., *Lower Head Integrity Under In-Vessel Steam Explosion Loads*, AP600 IVE ROAAM, June 1996.
- 39-3 *AP600 Probabilistic Risk Assessment Report*, GW-GL-022, Westinghouse Electric Corporation, August 1998.
- 39-4 Theofanous, T. G. and S. Angelini, "Natural Convection for In-Vessel Retention at Prototypic Rayleigh Numbers," *Nuclear Engineering and Design*, 200, 1 – 9 (2000).
- 39-5 Angelini, S., et al., "The Mechanism and Prediction of Critical Heat Flux in Inverted Geometries," *Nuclear Engineering and Design*, 200, 83 – 94 (2000).
- 39-6 Theofanous, T. G., "In-Vessel Retention as a Severe Accident Management Strategy," Plenary Lecture, *Proceedings of the Eighth International Topical Meeting on Nuclear Reactor Thermal Hydraulics, NURETH-8*, Kyoto, Japan (1997).
- 39-7 Churchill, S. W., and H. S. Chu, "Correlating Equations for Laminar and Turbulent Free Convection from a Vertical Plate," *International Journal Heat Mass Transfer* 18, 1323 – 1329 (1975).
- 39-8 Globe, S. and D. Dropkin, "Natural Convection Heat Transfer in Liquids Confined by Two Horizontal Plates and Heated from Below," *Journal Heat Transfer* 81, 24 (1959).

- 39-9 Theofanous, T. G., et al., *Quantification of Limits to Coolability in ULPU-2000 Configuration IV*, CRSS-01/11, Center for Risk Studies and Safety, Santa Barbara, CA (2001).
- 39-10 Theofanous, T. G., et al., "Premixing of Steam Explosions: PM-ALPHA Verification Studies," DOE/ID-10504, September 1996.
- 39-11 Theofanous, T. G., et al., "Propagation of Steam Explosions: ESPROSE.m Verification Studies," DOE/ID-10503, August 1996.
- 39-12 Theofanous, T. G., Volume 1 – "Appendices E, F, and G to DOE/ID-10541," and Volume 2 – "Addenda to DOE/ID-10541, -10503, -10504," October 1997, and Volume 3 – "Addenda to DOE/ID-10503 and -10504," December 1997.

Table 39-1			
MATERIAL INVENTORIES IN AP1000 REACTOR VESSEL			
Component	Material	Mass (kg) x 10 <sup>-3</sup>	Volume (m <sup>3</sup> ) <sup>(1)</sup>
<b>Core</b>			
Fuel	UO <sub>2</sub>	95.9	10.97
Active core cladding	Zircaloy	17.9	2.92
Additional zirconium <sup>(2)</sup>	Zircaloy	4.8	0.78
Control rods	Silver/Indium/cadmium	3.9	0.58
<b>Lower Internals (below top of active fuel)</b>			
Core barrel	Stainless steel	19	2.7
Lower support plate <sup>(3)</sup>	Stainless steel	25	3.4
Core shroud	Stainless steel	12	1.7
Shroud support structure	Stainless steel	9	1.3
Lower plenum energy absorber	Stainless steel	3	0.4

**Notes:**

1. In liquid state
2. Including zircaloy plugs at lower end of fuel rods
3. Including the lower nozzles of the fuel assemblies

Table 39-2

**SUMMARY TABLE FOR REACTOR CAVITY FLOODING (CET NODE IR)**

Accident Class	Failure Probability
1A	0
1AP	0
1D	IWF
3A	0
3BR	0
3BE	IWF
3BL	0
3C	0
3D	IWF
6E	IWF
6L	0

Table 39-3

**SUMMARY TABLE FOR DEBRIS RELOCATION TO CAVITY (CET NODE VF)**

Accident Class	Failure Probability
1A	0
1AP	0
1D	0
3A	0
3BR	0
3BE	0
3BL	0
3C	0.1
3D	0
6E/6L	0

AP1000 Base Case In-Vessel Retention of Molten Core Debris

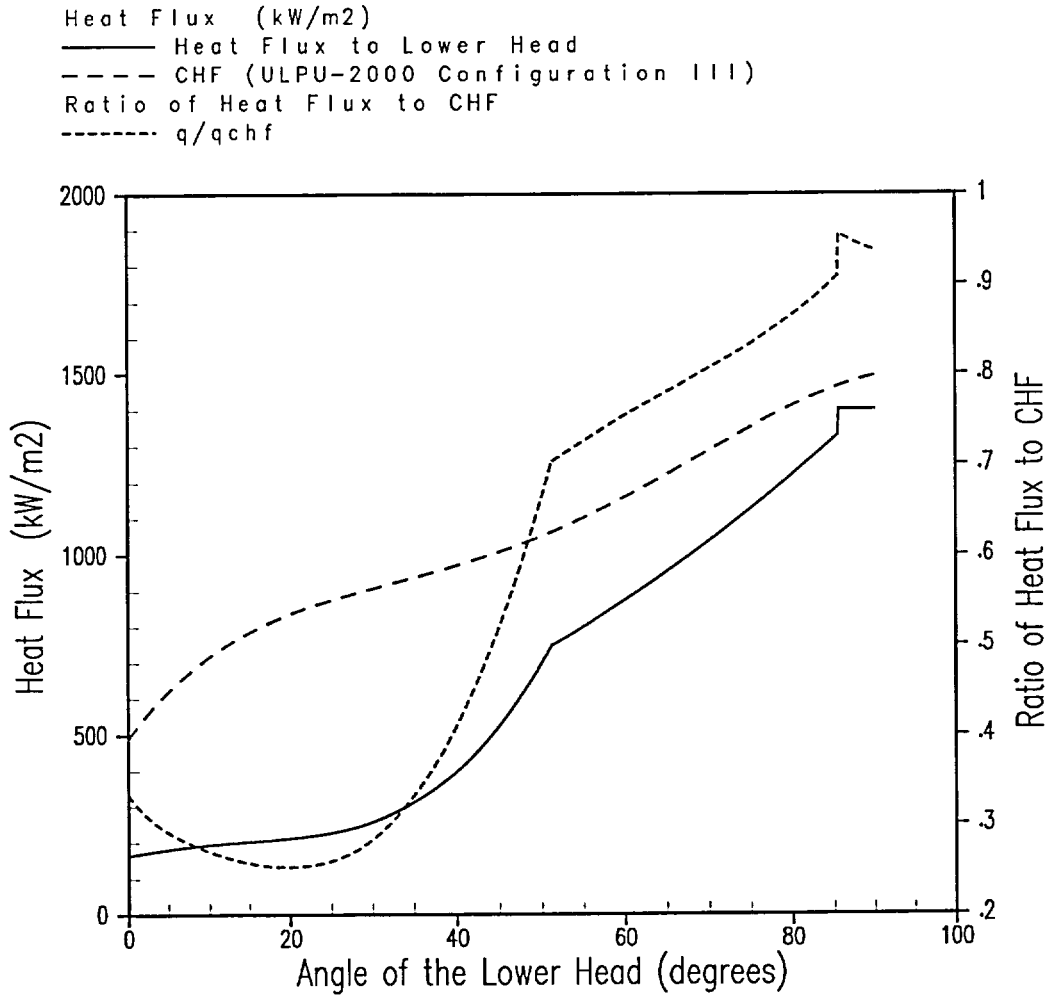


Figure 39-1

AP1000 Base Case In-Vessel Retention of Molten Core Debris

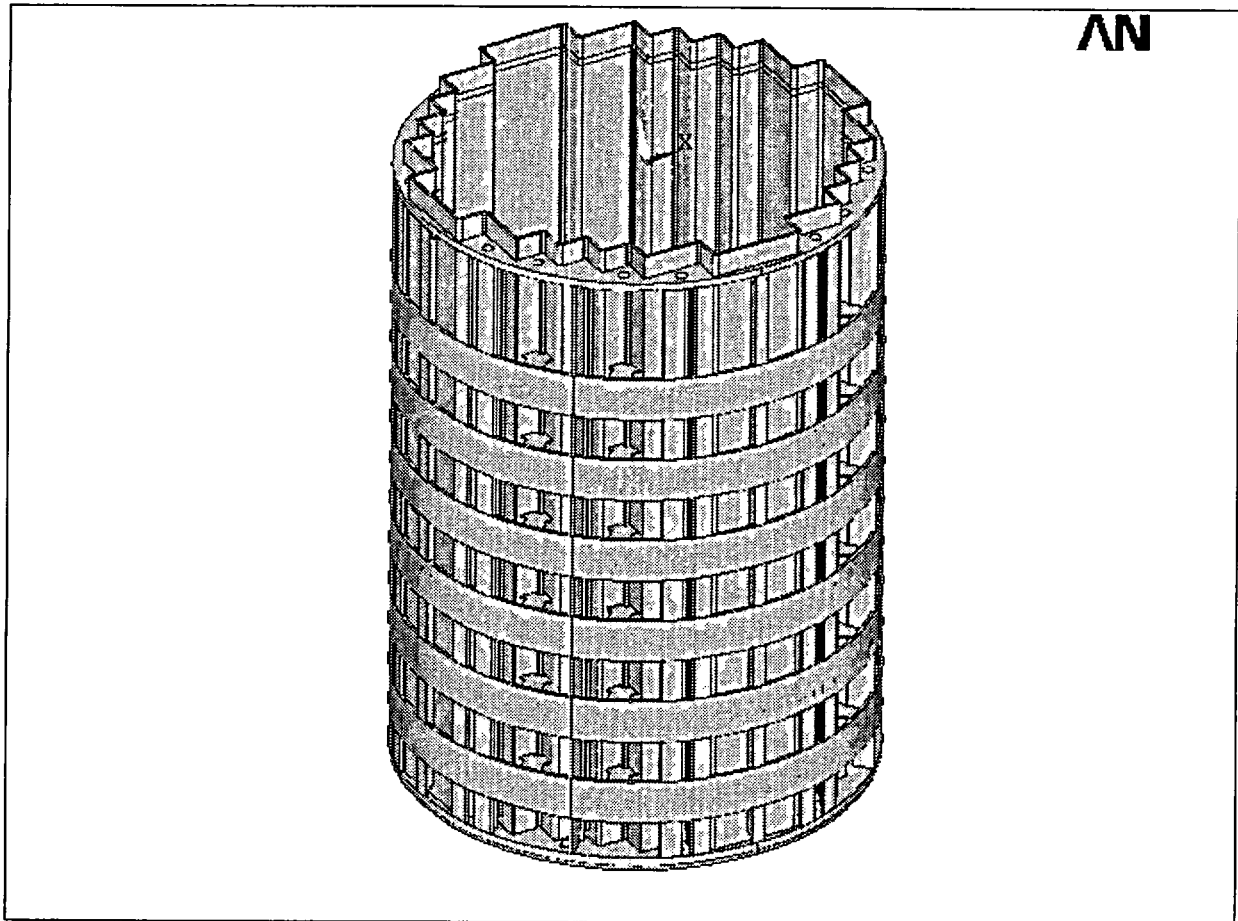


Figure 39-2

AP1000 Core Shroud

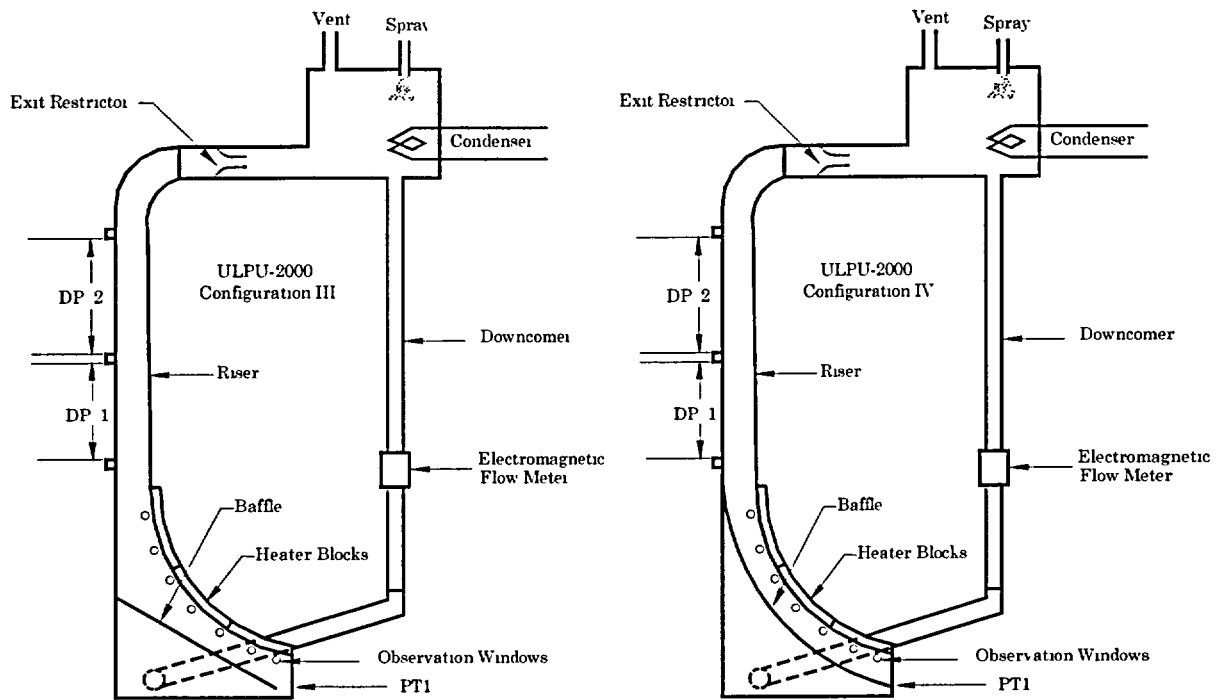


Figure 39-3

Comparison of ULPU-2000 Configuration III and ULPU-2000 Configuration IV

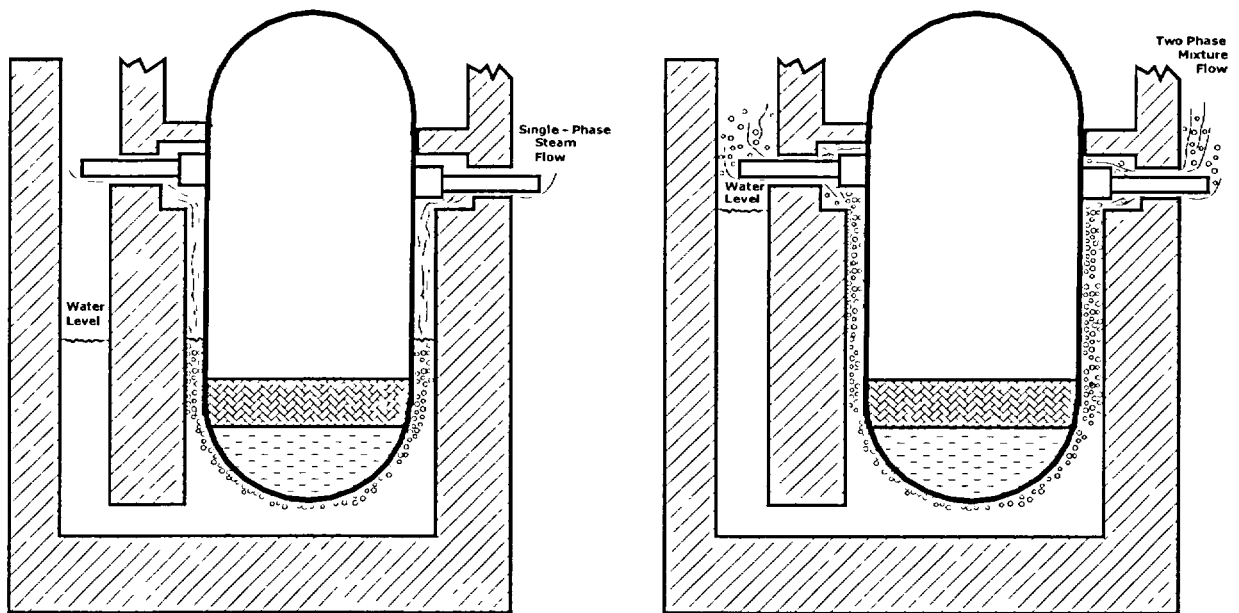
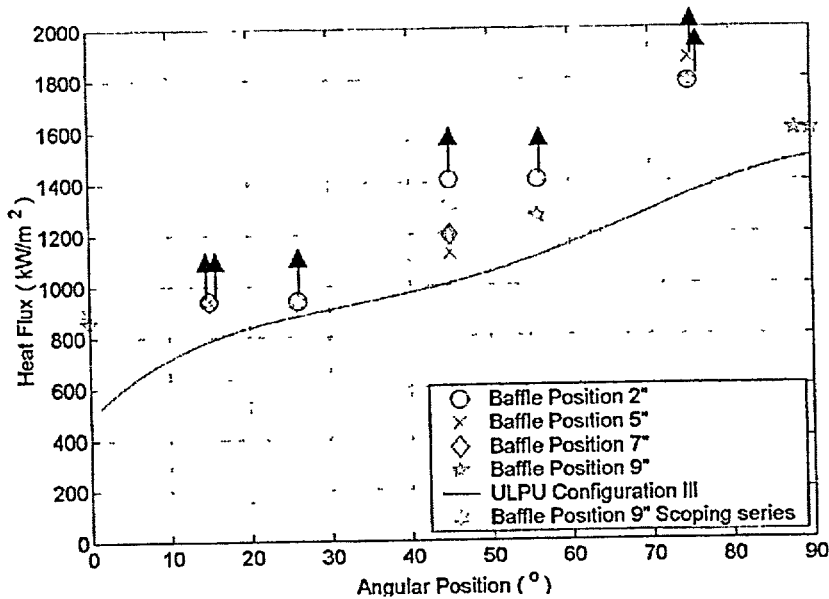
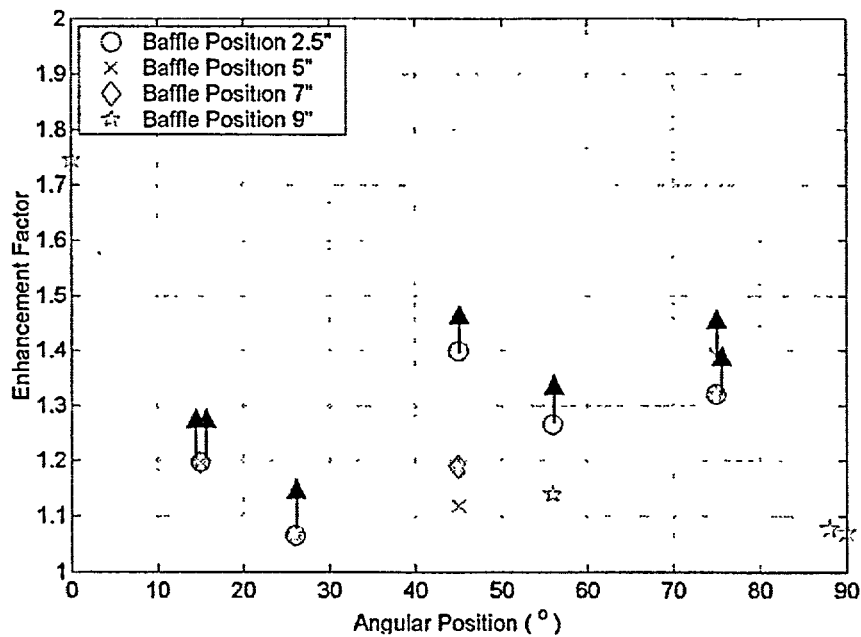


Figure 39-4

Effect of Water Level on Water Circulation During IVR



Maximum heat flux measured in the ULPU-2000 Configuration IV runs in the presence of natural circulation flow.



Enhancement factor in the ULPU-2000 Configuration IV runs (compared to AP-600 Configuration III). Recirculating flow.

Figure 39-5

ULPU-2000 Configuration IV Results (Reference 39-4)

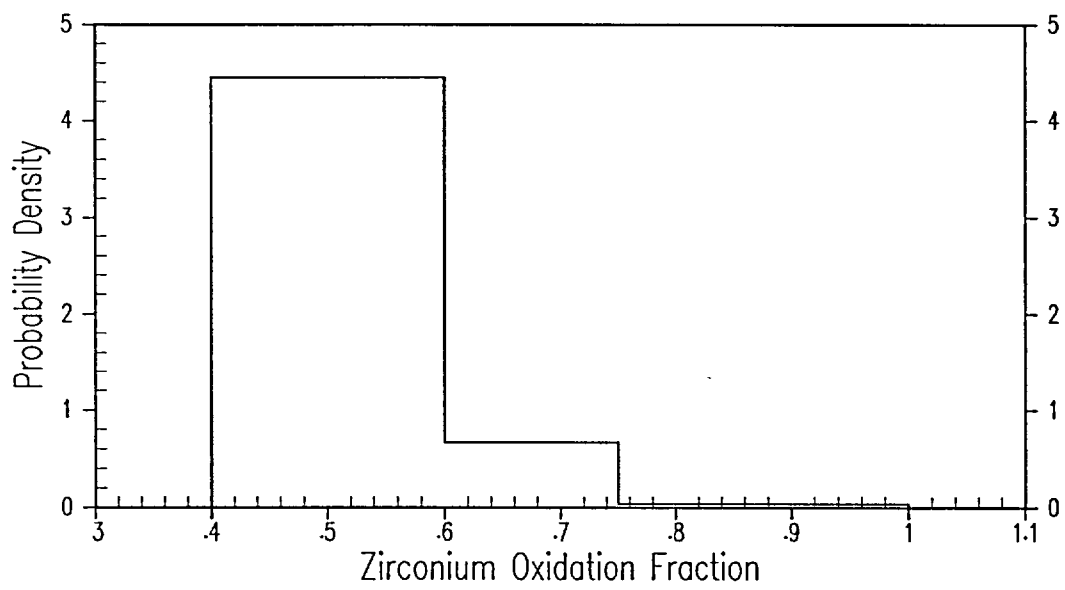


Figure 39-6

**AP1000 In-Vessel Retention of Molten Core Debris Quantification  
Zirconium Oxidation Fraction Input Probability Distribution**

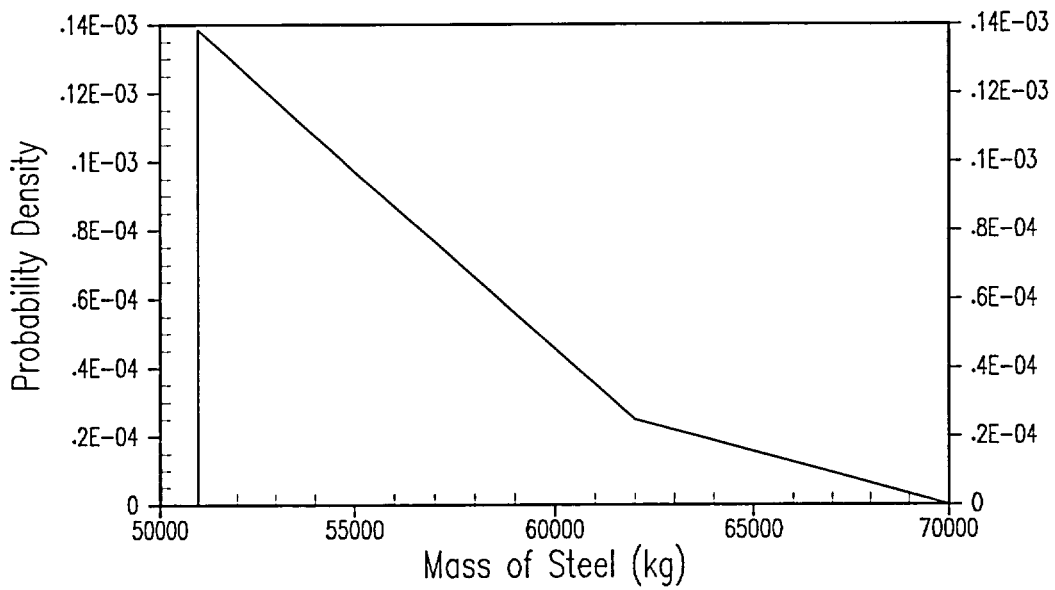


Figure 39-7

**AP1000 In-Vessel Retention of Molten Core Debris Quantification  
Mass of Steel in Debris Input Probability Distribution**

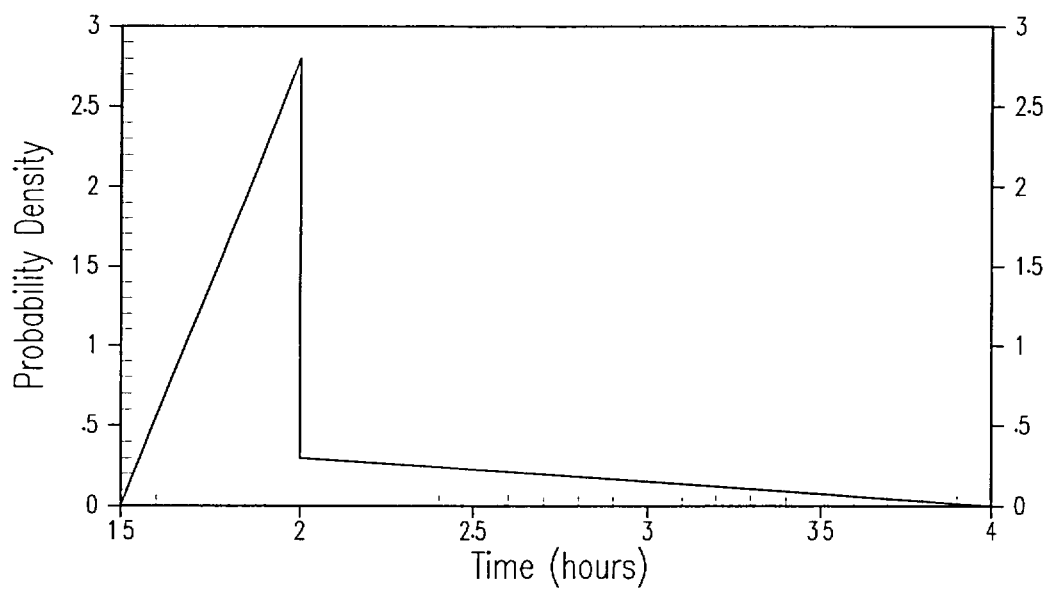


Figure 39-8

**AP1000 In-Vessel Retention of Molten Core Debris Quantification  
Time of Final Bounding State Input Probability Distribution**

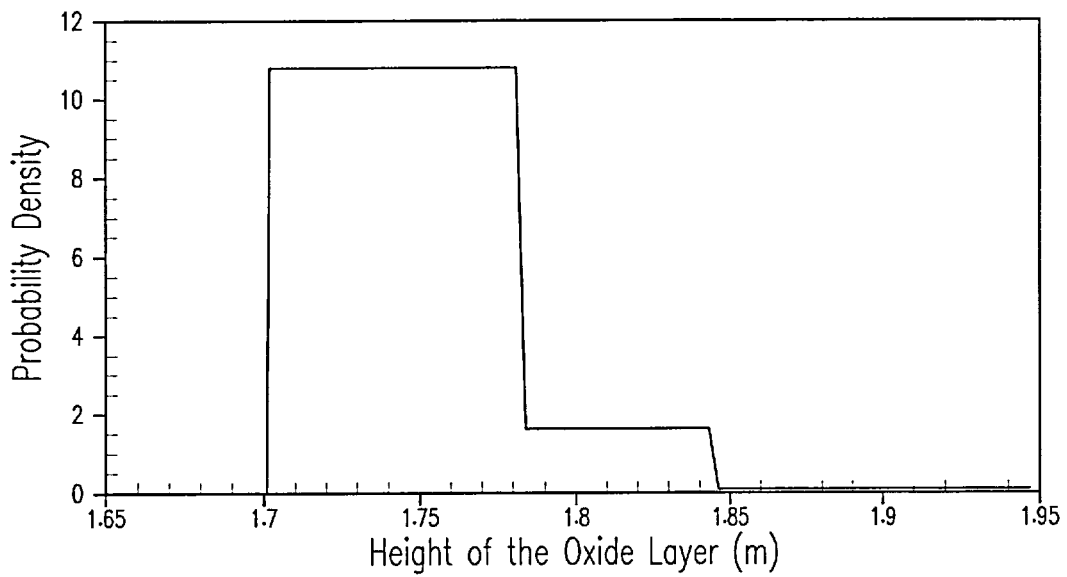


Figure 39-9

**AP1000 In-Vessel Retention of Molten Core Debris Quantification  
Height of the Oxide Layer**

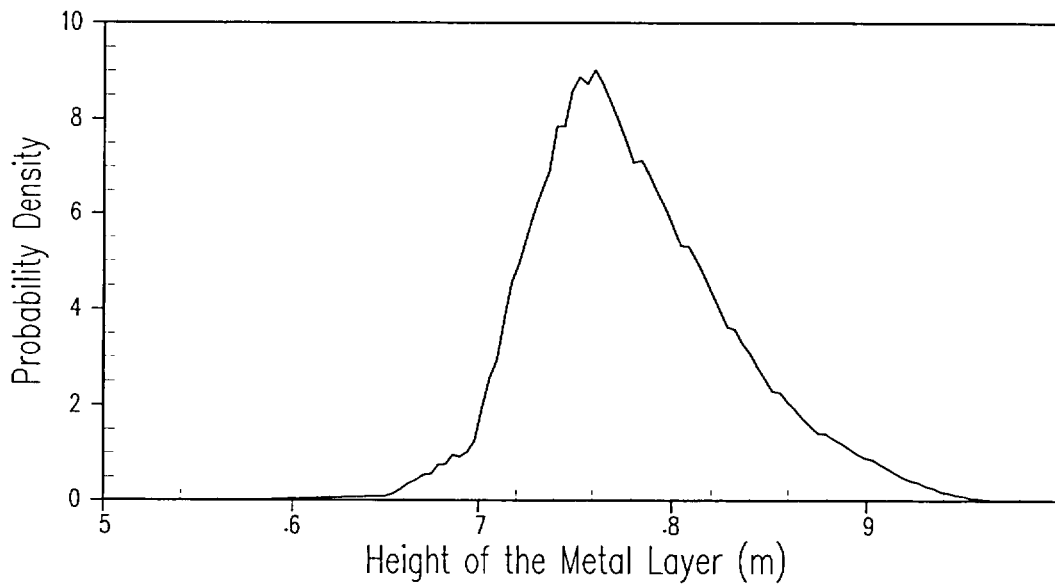


Figure 39-10

AP1000 In-Vessel Retention of Molten Core Debris Quantification  
Height of the Metal Layer

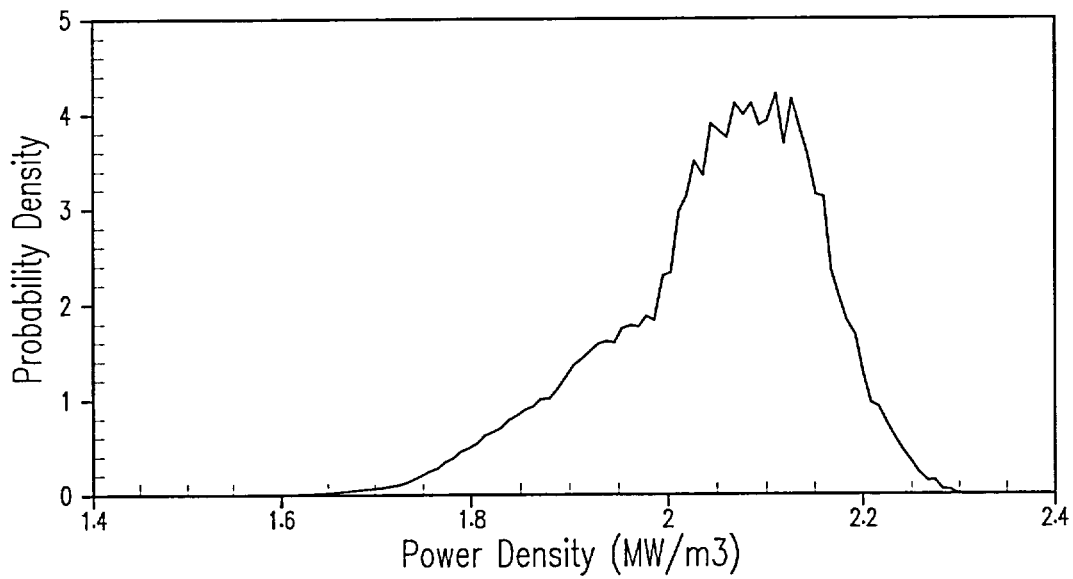


Figure 39-11

**AP1000 In-Vessel Retention of Molten Core Debris Quantification  
Power Density in Oxide Debris**

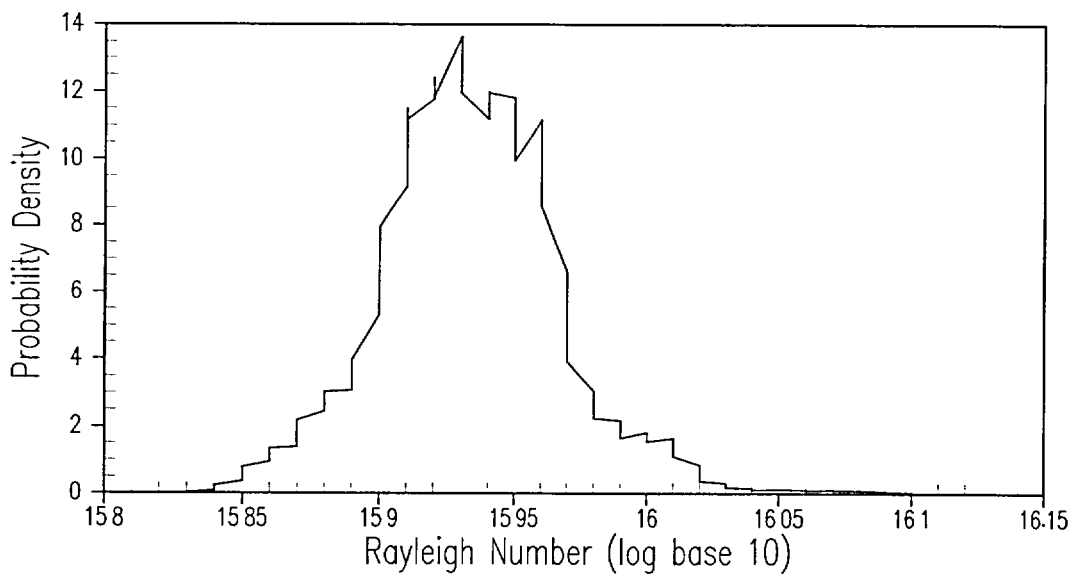


Figure 39-12

**AP1000 In-Vessel Retention of Molten Core Debris Quantification  
Internal Rayleigh Number in the Oxide Layer**

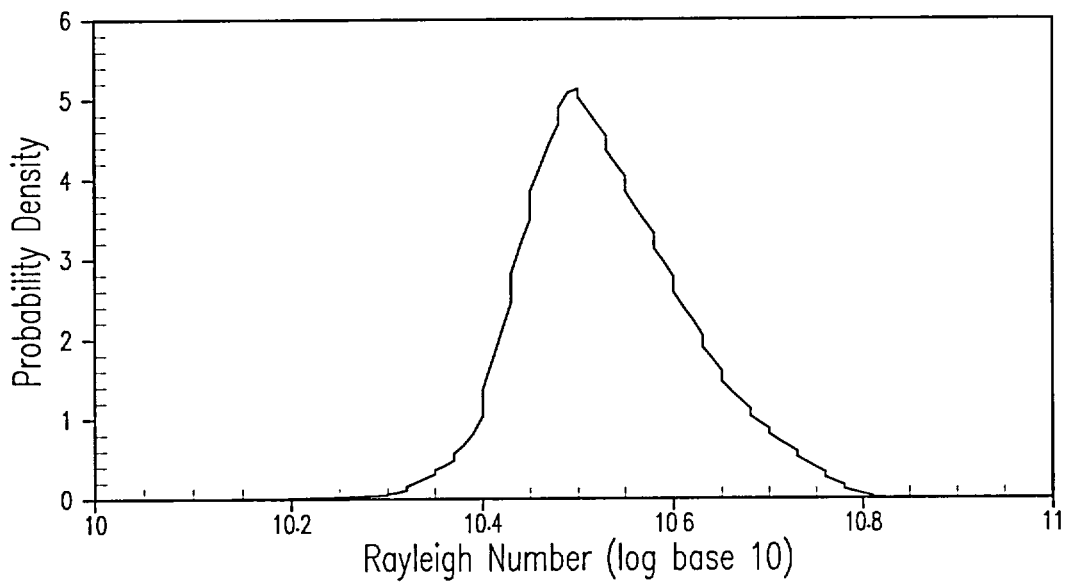


Figure 39-13

**AP1000 In-Vessel Retention of Molten Core Debris Quantification  
External Rayleigh Number in the Metal Layer**

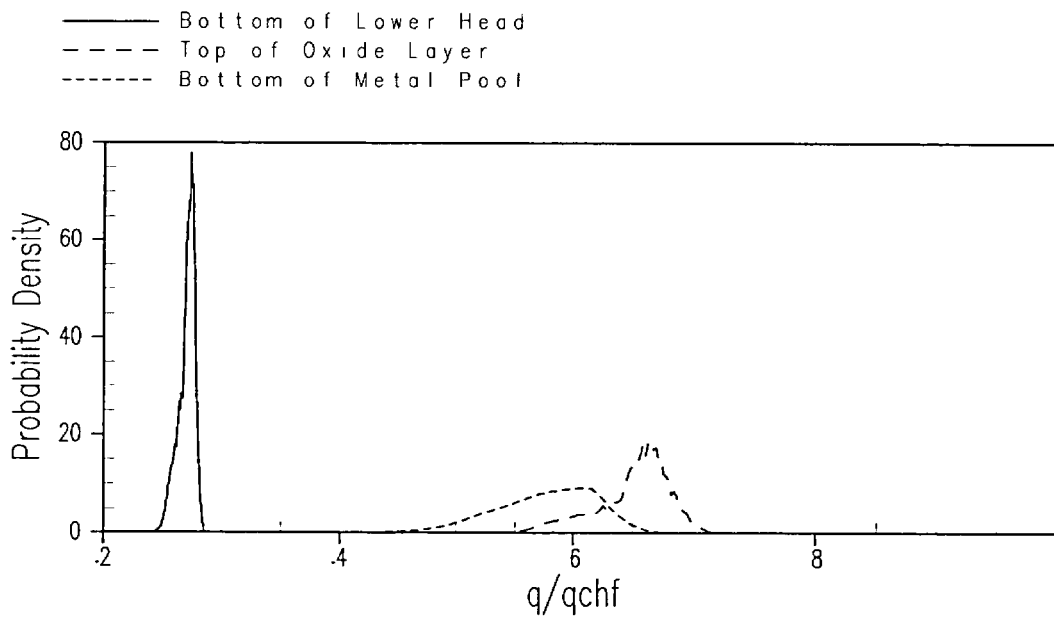


Figure 39-14

AP1000 In-Vessel Retention of Molten Core Debris Quantification  
Normalized Heat Fluxes

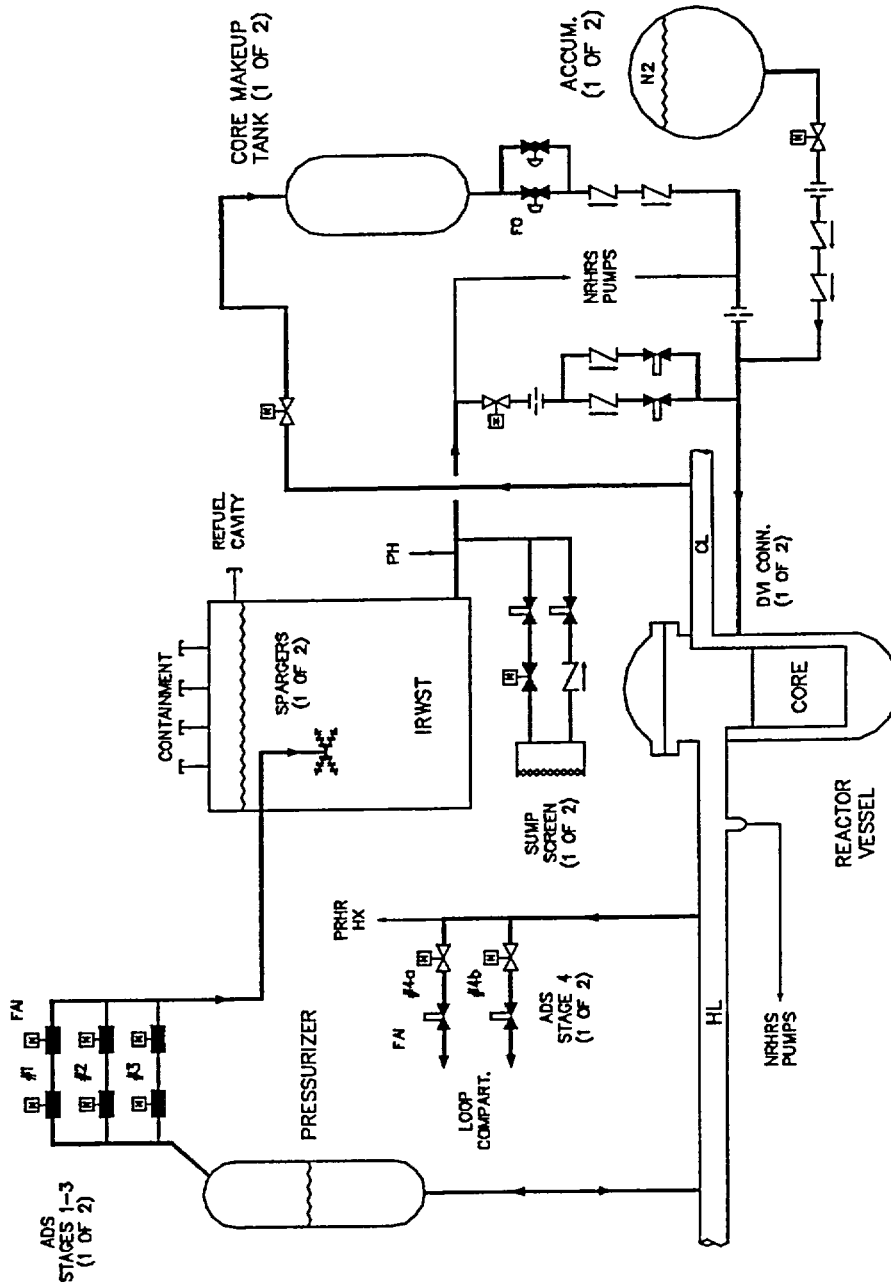


Figure 39-15

AP1000 Passive Core Cooling System

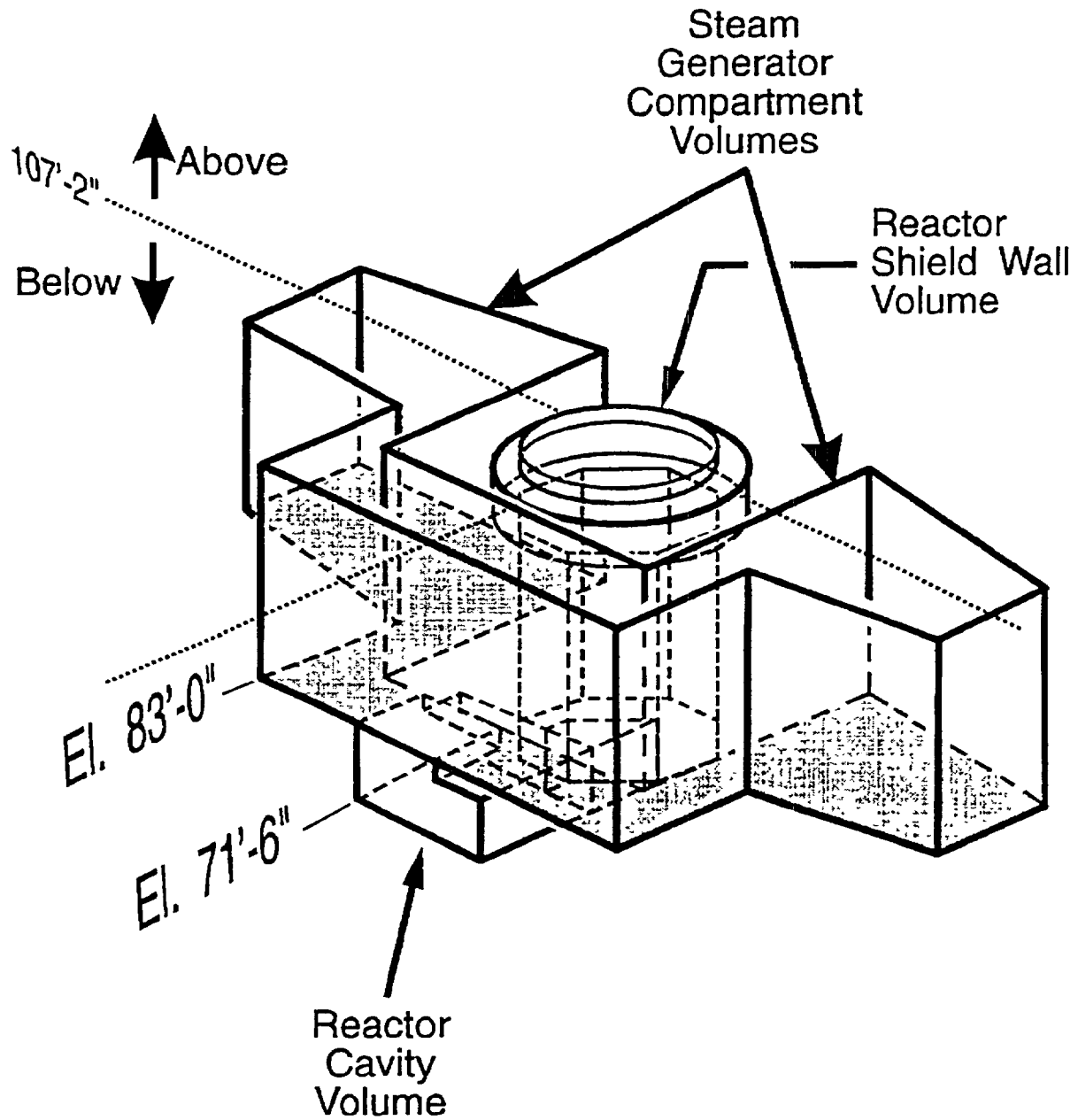


Figure 39-16

Containment Floodable Region

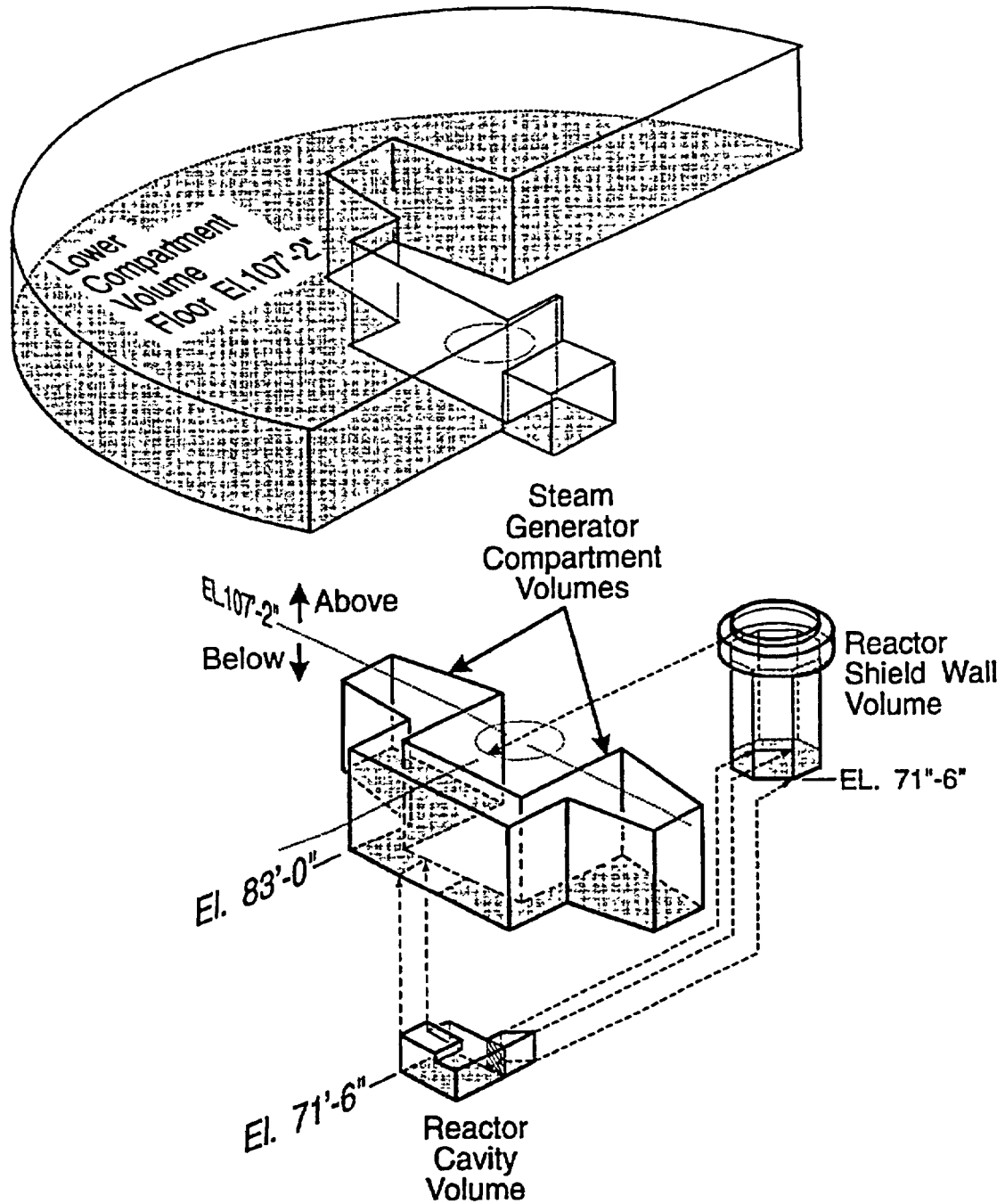


Figure 39-17

Containment Floodable Region – Exploded View

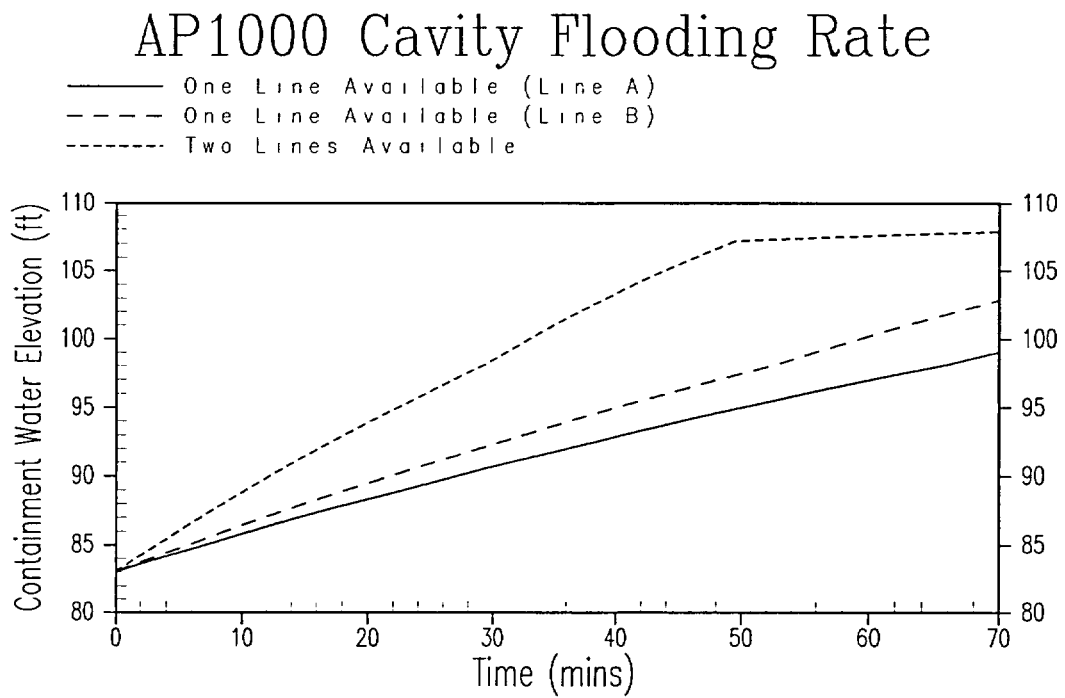


Figure 39-18

AP1000 Cavity Flooding Rate

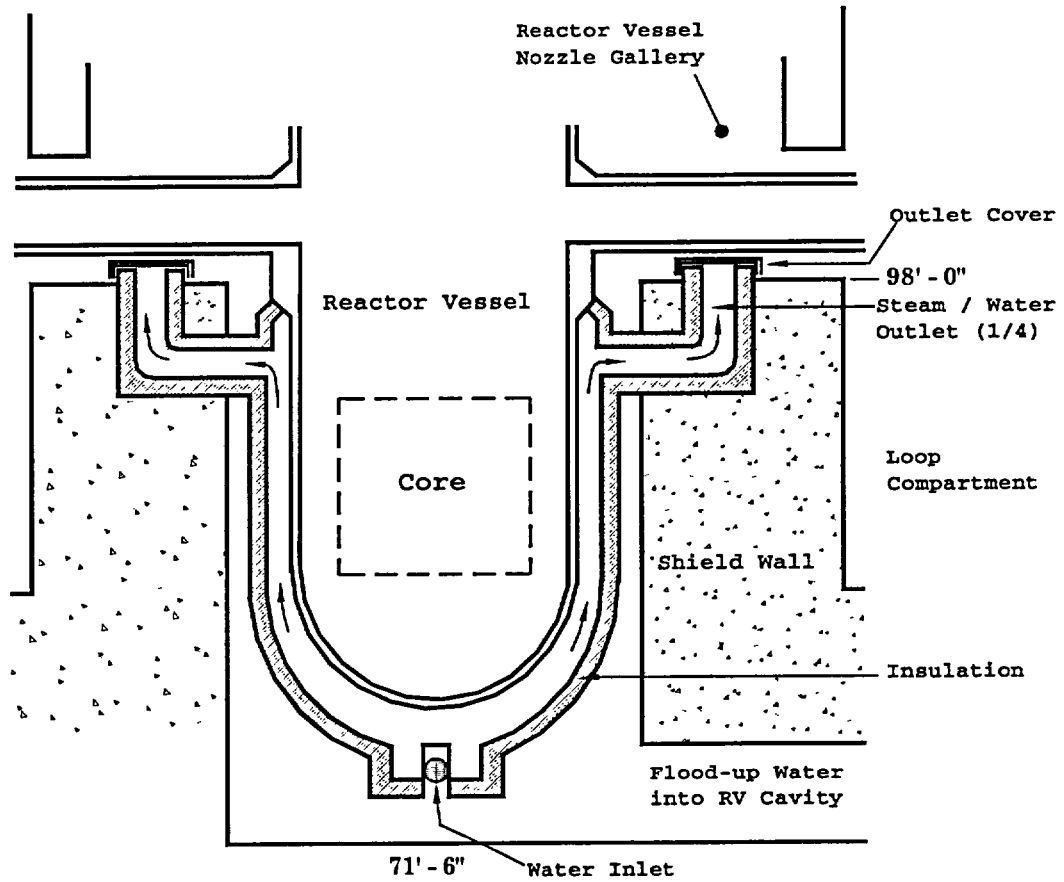


Figure 39-19

Schematic of the AP1000 Reactor Vessel, Vessel Cavity, Vessel Insulation, and Vents

**ATTACHMENT 39A****AP1000 IN-VESSEL CORE MELTING RELOCATION****39A.1 Introduction**

The phenomena associated with melting the core and the relocation of the molten debris to the lower plenum play an important role in the composition and configuration of the debris pool (Reference 39A-1). In turn, the characteristics of the debris pool significantly impact the heat loading to the lower head wall and the challenge to lower head integrity (Reference 39A-2). Therefore, understanding the melting and relocation scenarios plays an important role in the assessment of in-vessel retention of molten core debris in the lower plenum. This section investigates the core melting and relocation in detail, considering the impact of the AP1000 specific geometry, and determines the timing and interactions of the various debris materials in the formation of a lower plenum debris bed.

**39A.2 Phenomenological Issues****39A.2.1 Focusing Effect**

Lower plenum debris bed configurations, with a thin metallic layer on top of a molten oxide pool, are postulated to produce a focusing effect in the metal layer (Reference 39A-2) that can fail the reactor vessel. A large mass of metal incorporated into the lower plenum debris bed thickens the metal layer and distributes the metal pool heat load over a larger area of the vessel wall. This reduces the heat flux. The stainless steel of the lower support plate and core shroud, when incorporated in the debris pool before lower head debris dry out, will mitigate the focusing effect in the AP1000. This analysis will address the timing of lower plenum debris contacting the lower support plate and the potential for a large heat loading to the vessel wall from a thin metal layer.

**39A.2.2 Material Interaction**

Reference 39A-3 identifies potential debris interactions that could impact the formation of the lower head debris bed. This analysis considers the potential for interaction between molten zirconium and oxide debris as the core melt progresses in the AP1000 reactor vessel geometry.

**39A.3 AP1000 Reactor Vessel Lower Internals Geometry**

The initial lower internal geometry is presented in Figure 39A-1. The AP1000 reactor vessel has an inside diameter of 157 inches (4 m) and a hemispherical lower head (inside radius of 2 m). The vessel bottom head is 6 inches (15 cm) thick, and the vessel wall is 8 inches (20 cm) thick.

The AP1000 core consists of one-hundred fifty-seven 14-foot (4.27 m) 17x17 fuel assemblies. The bottom of the active fuel is 2 meters above the inside bottom of the reactor vessel. The flow area through the core is 3.88 m<sup>2</sup>.

The core is surrounded by a 7/8-inch (2.2 cm) thick core shroud (Figure 39A-2). The shroud panels conform tightly to the outside perimeter of the core. The shroud supporting structure is comprised of a top plate and a bottom plate, six 12.5-inch (32 cm) high ring assemblies spaced 12.5 inches (32 cm) apart vertically and radial ribs that tie the panels to the rings. The core shroud sits inside the cylindrical core barrel. The core barrel has an inner diameter of 133.75 inches (3.4 m) and is 2 inches (5.1 cm) thick. The volume between the core barrel and the core shroud has a cross-sectional area of 1.5 m<sup>2</sup>. The lower core support plate is welded to the bottom of the core barrel, and the core barrel hangs from the flange of the reactor vessel.

The 15-inch (38.1 cm) thick lower core support plate supports the core and the shroud. The support plate is welded to the 2-inch (5.1 cm) thick core barrel that hangs from the flange of the reactor vessel. The bottom of the support plate is nominally 55.3 inches (1.4 meters) above the inside bottom of the vessel. Four radial keys are welded to the support plate to prevent the support plate from moving radially and give the lower support plate a total outer diameter of 148.25 inches (3.77 m). An energy absorber structure is present in the lower plenum to support the lower support plate from below if it drops. The energy absorber is mounted to the bottom of the lower support plate and nominally sits 1 inch (2.54 cm) above the bottom of the lower head.

A detail of the bottom of the shroud and support plate is presented in Figure 39A-3. The bottom plate of the core shroud is 4-inch thick stainless steel that rests on the support plate. It has sixteen 0.781-inch diameter holes through the lower plate that provide cooling flow to the shroud/barrel annulus (core bypass flow). The flow is directed from the region below the core between the lower core support plate and the bottom of the active fuel. The masses of the reactor vessel lower internal components are in Table 39A-1.

### **39A.4 Modeling of Core and Reactor Vessel Lower Internals Heatup**

#### **39A.4.1 MAAP4 Model**

The MAAP4 code investigates core uncover and heatup in the AP1000 accident sequence. The MAAP4 code models the uncover, melting, relocation, and freezing of the fuel. It models the in-vessel debris pool formation and predicts the failure of the crust. It tracks the amount of sensible and decay heat in the debris and accounts for the release of fission products from the fuel, which decreases the decay power density in the debris.

For the MAAP4 analysis, the active core region is partitioned into 90 nodes (15 axial rows by 6 radial rings). The unfueled region below the core is modeled with four axial rows representing (from bottom up) the core support plate, the fuel assembly nozzles, the fuel rod zirconium plugs, and the lower plenum of the fuel rods. The unfueled region above the active core is modeled with one axial row.

Two axial power profiles are modeled: top-skewed and chopped-cosine (Figure 39A-4). The radial power profile is relatively flat and is shown in (Figure 39A-5).

The MAAP4 code models the core initially as a solid cylinder and the core shroud and core barrel together as one lumped stainless steel cylindrical heat sink surrounding the core. The

vessel wall is a second carbon steel cylindrical heat sink surrounding the core shroud/barrel heat sink.

The MAAP4 modeling is not capable of fully modeling the complexities of the actual shroud/barrel geometry, which is not lumped, and is not a concentric cylinder around the core. The behavior of the core melting and relocation is insensitive to the heat sink modeling, but the response of the core shroud and barrel to the core melt is difficult to accurately model with the lumped cylindrical model. In the AP1000 MAAP4 model in this analysis, the core shroud/barrel heat sink was set up to conserve the total radial heat capacity and mass of the actual shroud and barrel. The mass of the core shroud panels and supporting structures in the active fuel region of the core is 17,650 kg. The mass of the core barrel in the active fuel region of the core is 18,320 kg. Therefore, the total mass of the shroud and core barrel together provides a heat sink mass of 35,970, or 2400 kg per each of the 15 axial rows of nodes in the active core model. The inside radius of the heat sink model is set to be 1.648 meters (ID = 129.75 inches). The actual inside radius is 133.75 inches. The modeled radius maintains the outer radius of the core barrel (OD = 137.75 in), but makes the total thickness of the heat sink 4 inches. The increased thickness over the actual total thickness of 2.875 inches increases the thermal resistance of the heat sink model due to thermal conductivity; however, it cannot completely account for the total thermal resistance due to the radiation heat transfer between the shroud panel and the core barrel.

#### 39A.4.2 Finite Difference Modeling

To overcome the limitations of the MAAP4 code in the modeling of the core shroud and barrel, an additional analysis of the core heatup was performed using a finite difference model of the core. The finite difference model captures the geometric characteristics of the reactor vessel internals. The major limitation of the finite difference model is that the melting, relocation, and freezing of the core cannot be modeled, so care must be taken to use the results conservatively. The model makes assumptions with respect to the oxidation energy input to the cladding and neglects steam cooling due to the boiling in the lower region of the core. However, all the sequences are at low pressure and the steaming rate is low during the core melting phase of the accident sequence when the core is uncovered, so the amount of steam cooling is limited.

The results of the finite difference model (see Figures 39A-6 and 39A-7), along with the MAAP4 results, form the basis of the AP1000 core and lower internals heatup and melting calculation.

#### 39A.4.3 Relocation of In-Core Debris to Lower Plenum

An analysis of the molten pool relocation to the lower plenum was performed using the methodology from Reference 39A-1 to calculate the progressive melting of the core barrel and using initial conditions defined from the finite difference calculation.

#### 39A-5 Base Core Damage Sequence for In-Vessel Retention

The limiting core damage accidents for heat transfer from the core debris to the vessel wall are sequences that progress to core damage quickly and do not reflood the core debris inside

the reactor vessel. Due to decay heat considerations, the accident that proceeds the most quickly to core melting and relocation is conservative. Water cooling of the core and any core debris extends the time of the core melting, potentially arrests the relocation, and significantly limits the heat flux to the vessel wall from relocated debris.

In-vessel retention sequences are assumed to have successful reactor coolant system (RCS) depressurization through at least two of four, stage 4 automatic depressurization system (ADS) valves to reduce stresses on the reactor vessel wall and successful reactor cavity flooding to submerge the vessel. Therefore, the base core damage sequence is initiated by a large loss-of-coolant accident (LOCA). The reactor coolant system is depressurized, but the failure of the gravity injection leads to core melting early in the accident sequence. In the scenario, the cavity is flooded manually by the operator after the core-exit gas temperature exceeds 1200°F, as instructed by the functional restoration guidelines. The vessel is not reflooded through the break.

This type of accident sequence is classified as accident class 3BE in the AP1000 Probabilistic Risk Assessment (PRA). Typically, a large LOCA will reflood the core when the water level in the containment submerges the break. The largest LOCA that can reasonably be postulated with no reflooding is a spurious actuation of a stage 4 ADS valve. The ADS-4 valves have a large flow area from the reactor coolant system to the containment, and open to an elevation above the maximum water level in the containment. This prevents vessel reflooding. Therefore, the sequence timing considered in this analysis is based on an accident initiated by the spurious opening of a stage 4 ADS valve that proceeds to an accident class 3BE severe accident. This sequence will provide the conservatively fastest timing for establishing a lower plenum debris pool.

The MAAP4 results for the in-vessel retention base case for the top-skewed power shape case are presented in Figures 39A-8 through 16, and for the chopped cosine power shape case, in Figures 39A-17 through 25.

### 39A.5.1 Core Heatup and Formation of In-Core Molten Debris Layers

The analysis of the in-core molten pool formation determines the composition, volume, and power density of the debris that can relocate to the lower head, and the timing of the relocation. The lower plenum debris pool needs to contact the lower support plate to melt it and, thus, include sufficient metal in the debris to mitigate the focusing effect. Therefore, the less initial mass that can relocate is conservative.

Based on the results of the MAAP4 code, the top of the active fuel uncovers at 2300 seconds after the initiation of the accident. The uncovered portion of the core begins to heat up from the decay heating of the fuel, and the vessel mixture level continues to decrease, uncovering more of the core. Oxidation of the zircaloy cladding begins at 3000 seconds, signaling the onset of core damage and causing the core to heat up more rapidly. Unoxidized cladding and other metals in the core (such as control rod material) melt first and drain downward to the cooler regions of the core and refreeze where the temperature is less than the metal melting temperature, ~1600 to 2100 K. The melting and draining of the metal is followed by the melting of the uranium dioxide fuel and oxidized cladding, which has a much higher melting temperature, 2850 to 3100 K.

Based on the MAAP4 analyses, at the time of the onset of core damage, the water/steam mixture level in the reactor vessel is 1 meter above the bottom of the active fuel (3 m above the inside bottom of the vessel). The core temperature below this elevation is initially low due to the water cooling, and the heatup rate is relatively slow because the power density of the fuel and cladding oxidation rates are lower in this region. Thus 1 meter above the bottom of the active fuel is considered to be the highest elevation in the core where the bottom of the in-core molten debris pool with a refrozen oxide crust will form. The high pool assumption is conservative with respect to the mass of debris available for the initial relocation to the lower plenum.

At the time of the onset of oxidation in the core, the mass of water in the core region between the bottom of the active fuel and the top of the mixture level is 1840 kg, considering an average void fraction of 0.5. If 100 percent of this water reacts with the cladding, the maximum cladding oxidation is 26 percent of the cladding in the active core region, or 34 percent of the cladding above the initial water level.

The metal control rods and unoxidized zirconium in the core melt first, and drain downward into the cooler regions of the core below 1 meter, and continue to melt and drain as the lower regions uncover and heat up. The molten metal eventually refreezes at the top of the support plate, in the fuel assembly bottom nozzles, and bottom of the fuel rods, which are unfueled, are water-cooled, and have a significant heat sink mass. Assuming maximum cladding oxidation, the total mass of unoxidized zirconium in the active core is 13265 kg, or 2.2 m<sup>3</sup> of zirconium. The control rod material has a volume of 0.59 m<sup>3</sup>. The cross-sectional flow area of the intact core is 3.88 m<sup>2</sup>. The volume between the top of the lower support plate the bottom of the active fuel has a height of 0.2 meters and a total volume of 0.8 m<sup>3</sup>. Therefore, the height of the metal blockage extends 54 cm above the bottom of the active core.

The fuel assemblies on the periphery of the core are cooled by radiation heat transfer to the shroud and core barrel, and they have a lower than average power density. The finite difference model predicts that a significant fraction of these peripheral fuel assemblies are coolable and, thus, do not participate in the initial pool formation. Based on the finite difference calculation, it is assumed that half of the mass of the peripheral assemblies above the bottom of the in-core pool does not melt, and is held up from participating in the initial relocation of molten debris.

The sideward crust of the molten pool is expected to form in these outermost fuel assemblies of the core. The crust contains the debris and prevents debris relocation until the in-core debris pool develops superheat to melt the sideward crust. Given the maximum cladding oxidation, and assuming that half of the peripheral fuel assembly UO<sub>2</sub> or ZrO<sub>2</sub> melts initially, the total mass of the oxide that melts to form the molten oxide pool and crust is 72,600 kg.

The height from the top of the metal blockage to the bottom of the in-core pool at 1 meter is 48 cm. The total volume fills with molten oxide, which refreezes 15,700 kg of oxide material to form the bottom crust of the in-core debris pool.

When the crust fails, the molten debris drains to the volume between the core shroud and barrel (Figure 39A-26), filling the volume and draining any molten metal from the top of the in-core debris pool. The small bypass flow area through the shroud bottom plate is plugged

with metal that melted from the shroud and barrel and froze in the holes. The outlets of the bypass holes are plugged with metal frozen below the active core. This "pocket" volume between the shroud and core barrel has a cross-sectional area of 1.5 m<sup>2</sup> and will fill with debris from the molten pool. The pocket volume is initially filled with 0.35 m<sup>3</sup> of structure and approximately 5000 kg molten stainless steel from the melting of the shroud and core barrel during the melting (based on MAAP4 results). The volume of oxide debris that relocates into the pocket between the shroud and barrel is 0.7 m<sup>3</sup> and holds up 5730 kg of oxide.

Therefore, 51,772 kg of oxide with a volume of 6.1 m<sup>3</sup> is molten and available to form the superheated oxide pool and participate in the initial relocation to the lower head.

The time that it takes to form the molten debris pool is estimated from the decay heat and the oxidation energy, and the mass of the zirconium, UO<sub>2</sub>, and zirconium. An adiabatic heatup calculation of the time to melt this fraction of the core is 2575 seconds. Added to the average uncover time of 2650 seconds, the time is 5225 seconds. Based on the results of the finite difference calculation, the minimum time that 50 percent of the core UO<sub>2</sub> is melted is 6000 seconds. The MAAP4 model predicts the relocation of approximately 6 m<sup>3</sup> of molten debris to the lower plenum to occur at approximately 6000 seconds. Therefore, the crust failure is predicted to occur at 6000 seconds after accident initiation or 3000 seconds after the onset of core damage.

At 6000 seconds, the power density of the oxide debris in the pool is 2.9 MW/m<sup>3</sup> assuming the top-skewed power shape and ANS 79 decay heat + 2 sigma uncertainty. The power density in the molten debris considers the loss of the decay heat contained in volatile fission products released from the fuel (Reference 39A-2), which is 27.5 percent of the total decay heat at 6000 seconds after scram. The fraction of volatile fission product released from the debris as taken from Reference 39A-2 is conservative with respect to the releases of barium and strontium from the debris, which can release an addition 10 percent of the decay heat from the oxide.

### 39A.5.2 Melting of Core Shroud and Core Barrel

The AP1000 core shroud and core barrel are predicted to sustain significant damage in the elevations at the top of the in-core pool after core uncover and during the melting and relocation before the crust failure. The finite difference calculation, in the region above where the molten debris pool is expected to form, predicts that the core shroud melts before the UO<sub>2</sub> starts melting (Figure 39A-27 and Figure 39A-28) and that the core barrel melts significantly at the same elevation soon after the UO<sub>2</sub> melting begins.

The MAAP4 modeling also predicts that the core shroud melts at the 1.5- to 2-meter elevations in the core (Figure 39A-28), but later in time than the finite difference model. At the time that MAAP4 predicts the debris to relocate to the lower plenum, the mass of the shroud and much of the core barrel has melted away. The remaining mass equates to a core barrel thickness of approximately 0.5 inches, with the inner surface temperature at the melting temperature of the stainless steel and the outer surface temperature at approximately 1500 K (2300°F).

As discussed in Section 39A.4, MAAP4 models the shroud and barrel as one lumped cylindrical heat sink, which does not model the resistance due to radiation between the components. Therefore, the whole mass heat ups more uniformly with respect to the finite difference model, delaying the time that the inner "shroud part" of the heat sink reaches the melting temperature with respect to the finite difference modeling.

Once the shroud panels melt, the radiation heat transfer from the core is directly to the core barrel. This reduces the thermal resistance to the core barrel. Once melting of the inner shroud fraction of the lumped heat sink has occurred, MAAP4 models this effect and effectively models the heat sink. The mass and heat capacity of the shroud, the supporting structures, and the barrel are preserved in the MAAP4 model. So it is concluded that the MAAP4 results, as modeled in this analysis with the proper sideward mass and heat capacity, provide reasonable results with respect to the core barrel temperature and melting at the various elevations at and below the pool elevation.

### 39A.5.3 Initial Relocation of Molten Core Debris to Lower Plenum

The maximum heat load from the in-core debris pool to the crust occurs along the sidewall of the crust, and the heat load downward is predicted to be much less (Reference 39A-1) than sideward. The crust of the in-core debris pool will fail from the side once the pool develops significant superheat. Based on the MAAP4 results, the water level in the vessel does not decrease significantly below the bottom of the active fuel until after debris relocates into the lower plenum. The bottom of the metal blockage and the lower core support plate are cooled with water before the initial debris relocation, and not significantly heated from above. The blockage will not fail, and it prevents a downward relocation of the molten pool into the lower plenum.

After the relocation of molten debris into the pocket volume between the core shroud and core barrel, the debris pool has a volume of  $6.1 \text{ m}^3$ . The total cross-sectional area in the vessel between the shroud and barrel, and inside the remaining peripheral fuel assemblies is  $7 \text{ m}^2$ . Therefore, the pool is anticipated to contact the core barrel up to an elevation of 1.9 m above the bottom of the active fuel.

Based on the MAAP4 results, the core shroud/barrel is thinned and weakened in the elevation 1.5 to 2.0 meters above the bottom of the active fuel (see Figures 39A-13 through 15 and 39A-22 through 24). Below this elevation, the barrel is predicted to be overheated, yet fully intact. The heat flux from the molten pool will be highest at the top of the pool, and the core barrel failure occurs azimuthally where the barrel is initially thinned near the top of the debris pool. The azimuthal length limitation is imposed by the supporting structure of the core shroud that runs vertically along the inside of the core barrel. The initial failure is postulated to occur between a vertical rib and the pinch point between the remaining peripheral assemblies and the barrel, an azimuthal distance of 1.3 m. The limiting length in the AP1000 is approximately the same as the limiting length of 1.4 m used to estimate the core barrel failure size in the AP600 analysis (Reference 39A-1). Thus, the failure of the core barrel by the molten debris pool, and subsequent relocation to the lower head, occurs essentially via the same mechanism as postulated in the AP600 (Reference 39A-1).

The geometry of the core barrel (inner diameter, thickness, and material) is the same as the AP600 and the mechanism for core barrel failure is the same as the AP600. The core barrel in the AP1000 is thinned and significantly overheated, while the core barrel in the AP600 was cooler due to the presence of the reflector. Therefore, the degree of superheat in the debris needed to fail the AP1000 core barrel is bounded by the superheat in the debris that failed the AP600 core barrel (Reference 39A-1). The debris pour is oxide in composition and has a superheat on the order of 150 K. The initial relocation of 52,000 kg of debris into the lower plenum of the reactor vessel occurs over a duration of 500 seconds (Figure 39A-30).

The geometry and material composition of the reactor vessel wall and lower head of the reactor vessel are the same as the AP600. The debris composition and mass flow rate are also the same. The superheat in the debris is bounded by the superheat predicted for the AP600. Therefore, the results and conclusions of the jet impingement analysis performed for AP600 are applicable to the AP1000, and thus, the AP1000 vessel is not predicted to fail from jet impingement to the vessel wall during the relocation of molten debris to the lower plenum.

#### 39A.5.4 Lower Plenum Debris Pool Formation

The purpose of examining the lower head debris pool formation is to determine the rate, timing, and composition of material that enters the debris pool, and whether oxide debris in the lower plenum subsumes the lower support plate before failing the lower head.

The lower core support plate hangs from the core barrel, which supports the weight of the core and lower internal structures. The core barrel is significantly overheated and thinned from melting before debris relocation and stressed by the weight it is supporting. When the debris contacts the core barrel, the core support plate will drop 1 inch until it is supported from below by the energy absorber structure in the lower plenum of the reactor vessel. When core debris begins to pour into the lower plenum, the energy absorber structure is submerged in molten oxide and melts quickly. The lower core support plate drops and rests on the radial keys (see Figure 39A-1). The keys maintain a 9 cm gap between the vessel wall and the core support plate. The volume below the collapsed lower support plate is, at most, 8.0 m<sup>3</sup>. The volume of the molten oxide debris predicted to fill the lower plenum during the initial relocation after the crust fails is 6.1 m<sup>3</sup>. Therefore, the initial relocation does not reach the lower core support plate.

After the initial relocation, the debris above the lower support plate will continue to melt due to the decay heating in each of the regions. There are several debris regions considered to be the initial condition for modeling the subsequent debris relocation that occurs after the initial debris relocation (see Figure 39A-31). The adiabatic heatup and melting timing of these regions is calculated and compared to the timing of the water depletion rate in the lower head, which is estimated conservatively.

The debris layers are lumped into four masses above the lower core support plate, which are, from top to bottom:

- Peripheral fuel assemblies, which are assumed to collapse onto the top of the blockage after the initial relocation

- Oxide crust, which has frozen around unmelted UO<sub>2</sub> fuel
- Upper zirconium crust, which has frozen around unmelted UO<sub>2</sub> fuel
- Zirconium crust, below the bottom of the active fuel and the lower support plate

#### 39A.5.4.1 Modeling Melting and Relocation of Layers

##### 39A.5.4.1.1 Peripheral Fuel Assemblies

The remaining mass of the peripheral fuel assemblies is assumed to collapse onto the top of the oxide crust upon the initial relocation of the molten pool to the lower head. This assumption is reasonable given that the oxide pool subsumes the bottom portion of the peripheral fuel assemblies during the time between crust failure and the core barrel failure. The initial temperature is estimated to be 2700 K. The temperature is based on the average temperature between the 2300 K cold edge of the temperature profile in the peripheral assemblies as calculated in the finite difference model and the 3113 K melting temperature of UO<sub>2</sub>, which defines the hot edge of the assemblies.

The time for the peripheral assemblies to heat up to the melting temperature is found from the equation:

$$t_{mp} = \frac{m_p C_p (T_{mp} - T_i)}{Q_p V_p} + t_0 \quad (39A-1)$$

where:

- $t_{mp}$  = time to the melting point (secs)
- $m_p$  = mass of the oxide in the peripheral assemblies (kg)
- $C_p$  = heat capacity of the oxide in the peripheral assemblies (kJ/kg-K)
- $T_{mp}$  = melting temperature of the UO<sub>2</sub> (K)
- $T_i$  = initial temperature of the peripheral assemblies (K)
- $Q_p$  = power density in peripheral assemblies (kW/m<sup>3</sup>)
- $V_p$  = volume of the oxide debris (m<sup>3</sup>)
- $t_0$  = time of the initial relocation (sec)

The melting rate of the peripheral assemblies is:

$$\dot{V}_p = \frac{Q_p * V_p}{h_{LH-P} * \rho_{ox}} \quad (39A-2)$$

where:

- $\dot{V}_p$  = melting rate (m<sup>3</sup>/sec)
- $h_{LH-p}$  = latent heat of melting (kJ/kg)
- $\rho_{ox}$  = the volume averaged density of the UO<sub>2</sub> and ZrO<sub>2</sub> eutectic

The oxide latent heat of melting is found from the latent heats of UO<sub>2</sub> and ZrO<sub>2</sub> using the following equation:

$$h_{LH-p} = \frac{f_{UO_2} MW_{UO_2} h_{LH-UO_2} + f_{ZrO_2} MW_{ZrO_2} h_{LH-ZrO_2}}{f_{UO_2} MW_{UO_2} + f_{ZrO_2} MW_{ZrO_2}} \quad (39A-3)$$

where:

- $MW_{UO_2}$  = the molecular weight of UO<sub>2</sub>
- $MW_{ZrO_2}$  = the molecular weight of ZrO<sub>2</sub>
- $f_{UO_2}$  = the molecular fraction of UO<sub>2</sub>
- $f_{ZrO_2}$  = the molecular fraction of ZrO<sub>2</sub>
- $h_{LH-UO_2}$  = the latent heat of melting of UO<sub>2</sub>
- $h_{LH-ZrO_2}$  = the latent heat of melting of ZrO<sub>2</sub>

#### 39A.5.4.1.2 Oxide Crust

The oxide crust consists of previously molten oxide material that is frozen around unmelted fuel, and the mass of the debris that has accumulated in the pocket volume between the shroud and core barrel. The oxide crust and unmelted fuel is treated as a lumped mass, and the initial temperature is estimated to be 2800 K. This is a low bound value based on the relocated mass temperature and latent heat, and the unmelted UO<sub>2</sub> temperature from the finite difference calculation.

The melting rate of the oxide crust is found using the same method as the peripheral fuel assemblies. The total power density is found from the volume averaged power density of the previously molten fuel and the unmelted fuel.

#### 39A.5.4.1.3 Upper Metal Crust

The metal crust above the bottom of oxide fuel, or the upper metal crust, consists of a layer of zirconium frozen around unmelted fuel rods. The initial temperature of 1800 K is estimated conservatively high from the temperature of the UO<sub>2</sub> in level 2 from the finite difference calculation.

The melting rate of the zirconium and UO<sub>2</sub> is calculated using the same lumped heat capacity methodology as above. Initially, the UO<sub>2</sub> and zirconium heat up as a lumped mass to the zirconium melting temperature. Then all the decay heat goes into melting the zirconium. After zirconium melting is completed, the UO<sub>2</sub> begins to heat up again from the zirconium melting temperature until it reaches the UO<sub>2</sub> melting temperature.

#### 39A.5.4.1.4 Support Plate and Metal Crust Below Bottom of Active Fuel

The metal crust below the bottom of the active fuel, or the lower metal crust, consists of a layer of zirconium and control rod material frozen around the bottom plenum and zirconium plugs of the fuel rods, the stainless steel fuel assembly lower nozzles, and the stainless steel lower core support plate. There is no decay heat in this layer, and the initial temperature is 400 K since the layer is cooled by water.

For success, the lower plenum debris pool must contact the bottom of the support plate before the debris dries out. The support plate begins to heat up after contact and when the debris dries out. The upward heat flux from the lower plenum oxide debris bed is 1.2 MW/m<sup>2</sup>, and the area for heat transfer is assumed to be 11.1 m<sup>2</sup>, the upward facing area of the oxide pool at the elevation of the bottom of the support plate. The support plate and frozen metal are assumed to heat up as a lumped mass. The support plate is considered to fail when the metal is fully molten.

#### 39A.5.4.2 Lower Head Integrity Success Criterion for In-Vessel Melting and Relocation

The lower head integrity success criterion for the in-vessel melting and relocation is based on the following question:

Does the debris contact the lower core support plate before the water in the lower plenum boils away and the debris heats back up to a superheated condition?

The time to boil the water away is calculated conservatively by assuming that all of the decay heat and sensible heat in the debris goes into the water. The volume of debris that contributes to the boiling is conservatively assumed to be the entire volume below the lower core support plate. Note that there is a cancellation effect on the oxide latent heat of fusion in calculating the dry out time.

$$t_{\text{dry-out}} = \frac{M_w h_{fg} - Q_{\text{latent,ox}} - Q_{\text{sens,ox}} + Q_{\text{latent,ox}}}{QV_{\text{LSP}}} + t_0 = \frac{M_w h_{fg} - V_{\text{LSP}} \rho_{\text{ox}} C_{p\text{-ox}} \Delta T_{\text{SH}}}{QV_{\text{LSP}}} + t_0 \quad (39A-4)$$

where:

- $t_{\text{dry-out}}$  = the dry out time
- $M_w$  = the initial mass of water in the lower head (kg)
- $h_{fg}$  = the heat of vaporization of water (kJ/kg)
- $V_{\text{LSP}}$  = the volume below the lower core support plate (m<sup>3</sup>)
- $\rho_{\text{ox}}$  = the density of the oxide debris (kg/m<sup>3</sup>)
- $C_{p\text{-ox}}$  = the heat capacity of the molten oxide (kJ/kg-K)
- $\Delta T_{\text{SH}}$  = the superheat in the debris (K)

The superheat in the debris is volume-averaged between the volume of the initial relocation debris ( $V_1$ ), which has a superheat of +150 K ( $\Delta T_{SH-1}$ ), and the volume of debris required to fill the lower plenum, which has a superheat of +0 K.

$$\Delta T_{SH} = \frac{V_1 \Delta T_{SH-1}}{V_{LSP}} \quad (39A-5)$$

#### 39A.5.4.3 Results

The mass distributions for the top-skewed and chopped cosine power shapes are presented in Tables 39A-2a and 39A-2b, and the results of the relocation analysis are presented in Tables 39A-3a and 39A-3b. The material properties used in the calculations are presented in Table 39A-4.

In both cases, the debris subsumes the lower core support plate before the water boils away in the lower plenum. There is a period when zirconium is melting at the same time as oxide from the peripheral fuel.

#### 39A.6 Potential for Debris Interaction

If molten metal debris is mixed with molten oxide debris, it is postulated that there is potential for the debris to interact and produce a uranium/zirconium metal layer that may sink to the bottom of the lower plenum debris bed.

The upper metal layer consists of zirconium frozen around unmelted  $UO_2$  at the bottom of the core. A fraction of the zirconium is predicted to melt during the relocation of the oxide crust or peripheral assemblies. The zirconium blockage is below the oxide crust, contained in a crucible formed by the core barrel and bottom metal blockage. Its melting temperature is much lower than the melting temperature of the oxide, maintaining the crust between the layers. Even if a fraction of the zirconium were molten, there is no pathway for it to flow to the lower plenum, where it could potentially interact with the oxide. Therefore, there is no mechanism to cause significant mixing of the metal and oxide layers even if they were melted at the same time.

#### 39A.7 Conclusions from Analysis of AP1000 In-Vessel Core Melting and Relocation

The important conclusions from the analysis of the lower plenum debris pool formation analysis are:

- The lower plenum debris bed is cooled with water during the entire relocation process before contact with the support plate. Transient debris configurations are not predicted to threaten vessel integrity.
- The lower plenum oxide debris subsumes the lower core support plate before dry out in the lower plenum occurs. If the relocated debris is assumed to be instantaneously quenched in the lower plenum water, the oxide debris contacts the lower support plate before the debris can return to a superheated condition. Therefore, the lower core support plate, the core shroud, and a sizeable fraction of the core barrel are subsumed in the debris bed. The focusing effect is mitigated.

- The lower plenum debris bed is predicted to form a metal layer over oxide pool configuration.
- The potential for debris interaction, creating a bottom metal pool of uranium dissolved in zirconium, is expected to be small.
- The earliest time to achieve the fully molten, circulating debris bed in the lower plenum is 2.7 hours after shutdown. The timeline of events is presented in Table 39A-5.

#### 39A.8 References

- 39A-1. Theofanous, T. G., et al., Lower Head Integrity Under In-Vessel Steam Explosion Loads, DOE/ID-10541, June 1996.
- 39A-2. Theofanous, T. G., et al., In-Vessel Coolability and Retention of a Core Melt, DOE/ID-10460, July 1995.
- 39A-3. Rempe, J. L., et al., Potential for AP600 In-Vessel Retention through Ex-Vessel Flooding, INEEL/EXT-97-00779, December 1997.

Table 39A-1

**CORE AND LOWER INTERNALS MATERIAL INVENTORIES IN  
AP1000 REACTOR VESSEL**

Component	Material	Mass (kg) x 10 <sup>-3</sup>	Volume (m <sup>3</sup> ) <sup>(1)</sup>
<b>Core</b>			
Fuel	UO <sub>2</sub>	95.9	10.97
Active core cladding	Zircaloy	17.9	2.92
Additional zirconium <sup>(2)</sup>	Zircaloy	4.8	0.78
Control rods	Silver/indium/cadmium	3.9	0.58
<b>Lower Internals (below top of active fuel)</b>			
Core barrel	Stainless steel	19	2.7
Lower support plate <sup>(3)</sup>	Stainless steel	25	3.4
Core shroud	Stainless steel	12	1.7
Shroud support structure	Stainless steel	9	1.3
Lower plenum energy absorber	Stainless steel	3	0.4

**Notes:**

1. In liquid state
2. Including zircaloy plugs at lower end of fuel rods
3. Including the lower nozzles of the fuel assemblies

Table 39A-2a

**MASS AND POWER DISTRIBUTIONS OF DEBRIS LAYERS IN  
TOP-SKEWED POWER SHAPE CASE**

	Mass	Fraction (%)	Height	Volume	Power Density
Mass of UO <sub>2</sub> in peripheral assemblies	6548	6.8		0.7	
Mass of ZrO <sub>2</sub> in peripheral assemblies	561		1.63	0.1	
TOTAL	7108			0.8	2.2
Mass of UO <sub>2</sub> relocated to lower plenum	47687	49.7		5.5	
Mass of ZrO <sub>2</sub> relocated to lower plenum	4085			0.7	
TOTAL	51772			6.1	2.9
Mass of relocated UO <sub>2</sub> in pockets	5281	5.5		0.6	
Mass of relocated ZrO <sub>2</sub> in pockets	452			0.1	
TOTAL	5734			0.7	2.9
Mass of relocated UO <sub>2</sub> in crust	13910	14.5		1.6	
Mass of relocated ZrO <sub>2</sub> in crust	1191		0.46	0.2	
TOTAL	15102			1.8	2.9
Mass of unmelted UO <sub>2</sub> in crust	10383	10.8		1.2	
Mass of unmelted ZrO <sub>2</sub> in crust	0		0.46	0.0	
TOTAL	10383			1.2	2.7
Mass of UO <sub>2</sub> in metal blockage	12090	12.6		1.4	1.2
Mass of Zr in metal blockage	12488		0.54	2.1	
Mass of zircaloy relocated	786			0.1	
Mass of control rod material	3900			0.6	
Mass of zircaloy below core	4800			0.8	0.0
Mass of fuel assemblies lower nozzles	760		0.22	0.1	
Mass of support plate	25000			1.6	

Table 39A-2b

**MASS AND POWER DISTRIBUTIONS OF DEBRIS LAYERS IN  
CHOPPED COSINE POWER SHAPE CASE**

	Mass	Fraction (%)	Height	Volume	Power Density
Mass of UO <sub>2</sub> in peripheral assemblies	6548	6.8		0.7	
Mass of ZrO <sub>2</sub> in peripheral assemblies	561		1.63	0.1	
TOTAL	7108			0.8	2.1
Mass of UO <sub>2</sub> relocated to lower plenum	47687	49.7		5.5	
Mass of ZrO <sub>2</sub> relocated to lower plenum	4085			0.7	
TOTAL	51772			6.1	2.8
Mass of relocated UO <sub>2</sub> in pockets	5281	5.5		0.6	
Mass of relocated ZrO <sub>2</sub> in pockets	452			0.1	
TOTAL	5734			0.7	2.8
Mass of relocated UO <sub>2</sub> in crust	13910	14.5		1.6	
Mass of relocated ZrO <sub>2</sub> in crust	1191		0.46	0.2	
TOTAL	15102			1.8	2.8
Mass unmelted UO <sub>2</sub> in crust	10383	10.8		1.2	
Mass of unmelted ZrO <sub>2</sub> in crust	0		0.46	0.0	
TOTAL	10383			1.2	3.3
Mass of UO <sub>2</sub> in metal blockage	12090	12.6		1.4	1.2
Mass of Zr in metal blockage	12488		0.54	2.1	
Mass of zircaloy relocated	786			0.1	
Mass of control rod material	3900			0.6	
Mass of zircaloy below core	4800			0.8	0.0
Mass of fuel assemblies lower nozzles	760		0.22	0.1	
Mass of support plate	25000			1.6	

Table 39A-3a

RESULTS OF TOP-SKEWED POWER SHAPE CASE

	Material	Mass (kg)	Mole Fraction	Molten Vol (m3)	Qdk (kW/m3)	Init Temp (K)	Start Time Heatup (s)	Time to MP (s)	Time fully melted (s)
Peripheral fuel rods	UO <sub>2</sub>	6548	0.84	0.7	2189.2	2700	6000	6572	7804
	ZrO <sub>2</sub>	561	0.16	0.1					
Oxide crust and pockets	UO <sub>2</sub>	19192	0.89	2.2	2908.7	2800	6000	6274	7194
	ZrO <sub>2</sub>	1644	0.11	0.3					
Unmelted UO <sub>2</sub> in UO <sub>2</sub> crust	UO <sub>2</sub>	10383		1.2	2656.6				
Unmelted UO <sub>2</sub> in zirc crust	UO <sub>2</sub>	12090		1.4	1160.9	2125	8599	12579	
Zirc in the active fuel region	Zr	12488		2.0		2000	6000	6850	8599
Zirc below active fuel region	Zr	5586	0.10	0.9					
Support plate and nozzles	SS	29660	0.90	4.2		400	6888	8942	9662
Initial relocation						q <sub>up</sub> (kW/m <sup>2</sup> )		vol under LSP (m <sup>3</sup> )	Contact time LSP (s)
Molten debris in lower plenum	UO <sub>2</sub>	47687	0.84	5.5	2908.7	1200		8.0	6718
	ZrO <sub>2</sub>	4085	0.16	0.7					
Water in RPV boils away	H <sub>2</sub> O	Mass (kg)	Vol (m <sup>3</sup> )	Debris Superheat (K)	Dry Out Time (sec)				
		11038	11.6	115	6888				
						Contact LSP (s)	Dry Out Time (sec)		
						6718	6888		

Table 39A-3b

RELOCATION RESULTS OF CHOPPED COSINE POWER SHAPE CASE

	Material	Mass (kg)	Mole Fraction	Molten Vol (m3)	Qdk (kW/m3)	Init Temp (K)	Start Time Heatup (s)	Time to MP (s)	Time fully melted (s)
Peripheral fuel rods	UO <sub>2</sub>	6548	0.84	0.7	2124.8	2700	6000	6589	7859
	ZrO <sub>2</sub>	561	0.16	0.1					
Oxide crust and pockets	UO <sub>2</sub>	19192	0.89	2.2	2823.1	2800	6000	6283	7154
	ZrO <sub>2</sub>	1644	0.11	0.3					
Unmelted UO <sub>2</sub> in UO <sub>2</sub> crust	UO <sub>2</sub>	10383		1.2	3321.7				
Unmelted UO <sub>2</sub> in zirc crust	UO <sub>2</sub>	12090		1.4	1169.3	2125	8581	12531	
Zirc in the active fuel region	Zr	12488		2.0		2000	6000	6843	8581
Zirc below active fuel region	Zr	5586	0.10	0.9					
Support plate and nozzles	SS	29660	0.90	4.2		400	6915	8969	9689
Initial relocation						q <sub>up</sub> (kW/m <sup>2</sup> )		vol under LSP (m <sup>3</sup> )	Contact time LSP (s)
Molten debris in lower plenum	UO <sub>2</sub>	47687	0.84	5.5	2823.1	1200	8.0	6707	
	ZrO <sub>2</sub>	4085	0.16	0.7					
Water in RPV boils away	H <sub>2</sub> O	Mass (kg)	Vol (m <sup>3</sup> )	Debris Superheat (K)	Dry Out Time (sec)				
		11038	11.6	115	6915	Contact LSP (s)	Dry Out Time (sec)		
						6707	6915		

Table 39A-4

**MATERIAL PROPERTIES USED IN IN-VESSEL MELTING AND RELOCATION CALCULATION**

	Material Properties Used In						
	ZrO <sub>2</sub>	UO <sub>2</sub>	Oxide	SS	Zr	Metal	Water
Melt temp	2911	3113	2973	1700	2125	1600	K
Density	5990	8740	8434	7020	6130		950 kg/m <sup>3</sup>
Solid Cp	0.645	0.535		0.64	0.356		kJ/kgK
Liquid Cp	0.815	0.485	0.502	0.835	0.458		kJ/kgK
Latent heat	856.2	274	320	280	225	2226	kJ/kg
Mole weight	123	267		56	91	18	kg/kg-mole

Table 39A-5

**DEBRIS RELOCATION TIME LINE**

Event	From Beginning of Accident (Second)	From Onset Melt	
		(Second)	(Hour)
Time of core uncover	2300	-	-
Onset of melting	3000	0	0.0
In-pool crust failure	6000	3000	0.8
Initial relocation to lower plenum starts	6000	3000	0.8
Second oxide relocation starts	6283	3283	0.9
Initial relocation to lower plenum ends	6500	3500	1.0
Lower plenum debris contacts lower support plate	6707	3707	1.0
Zircaloy blockage melting begins	6843	3843	1.1
Lower plenum dry out	6915	3915	1.1
Second oxide relocation ends	7859	4859	1.3
Zircaloy blockage melting ends	8581	5581	1.6
Lower support plate melting begins	8969	5969	1.7
Lower support plate melting ends	9689	6689	1.9
Unmelted oxide falls into pool	9689	6689	1.9

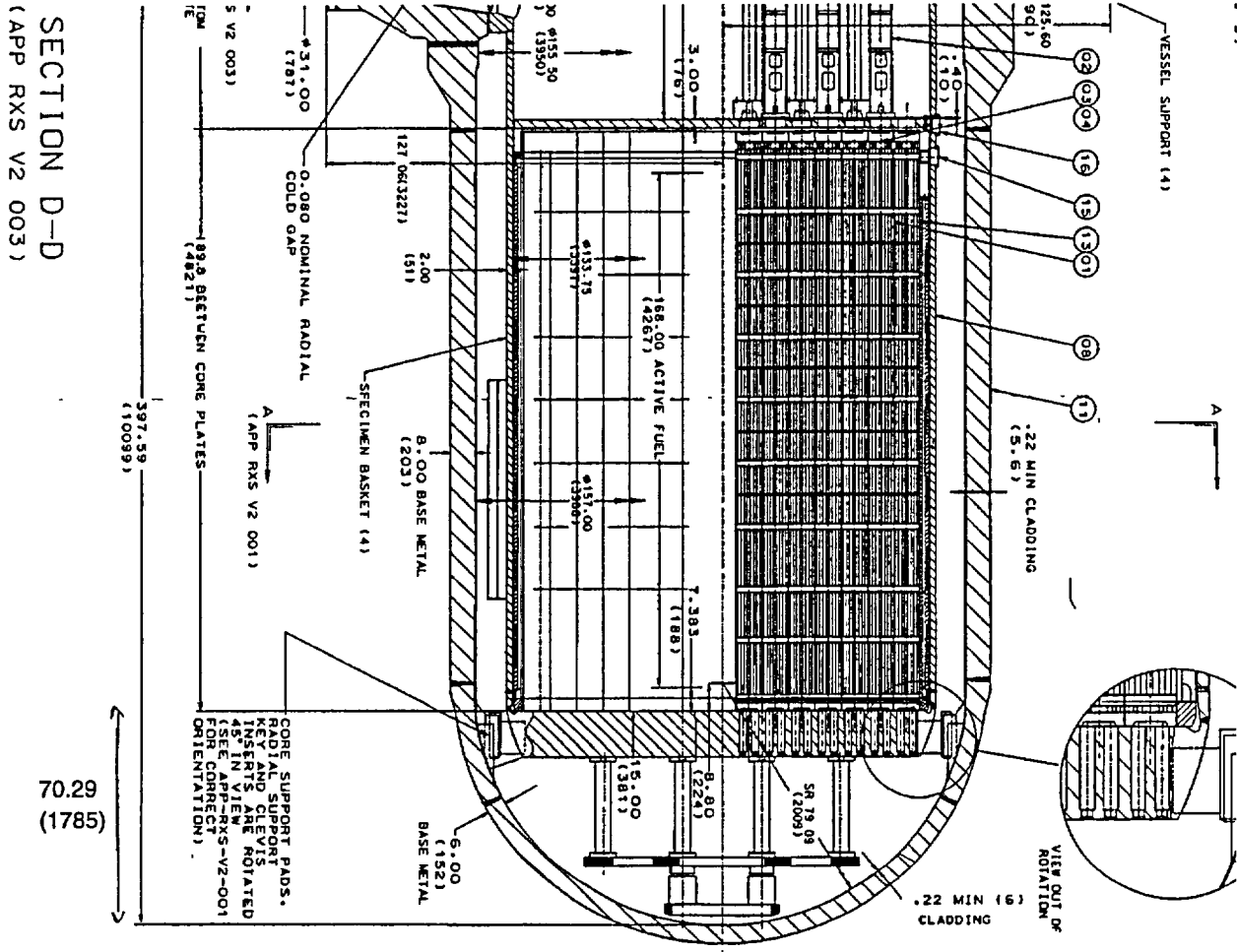
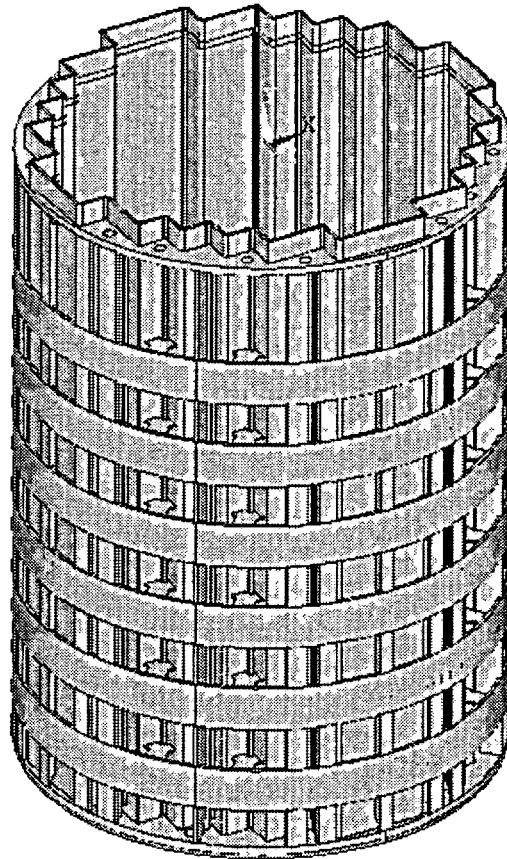


Figure 39A-1

AP1000 Reactor Pressure Vessel, Core and Lower Internals



**AN**

Figure 39A-2

Core Shroud

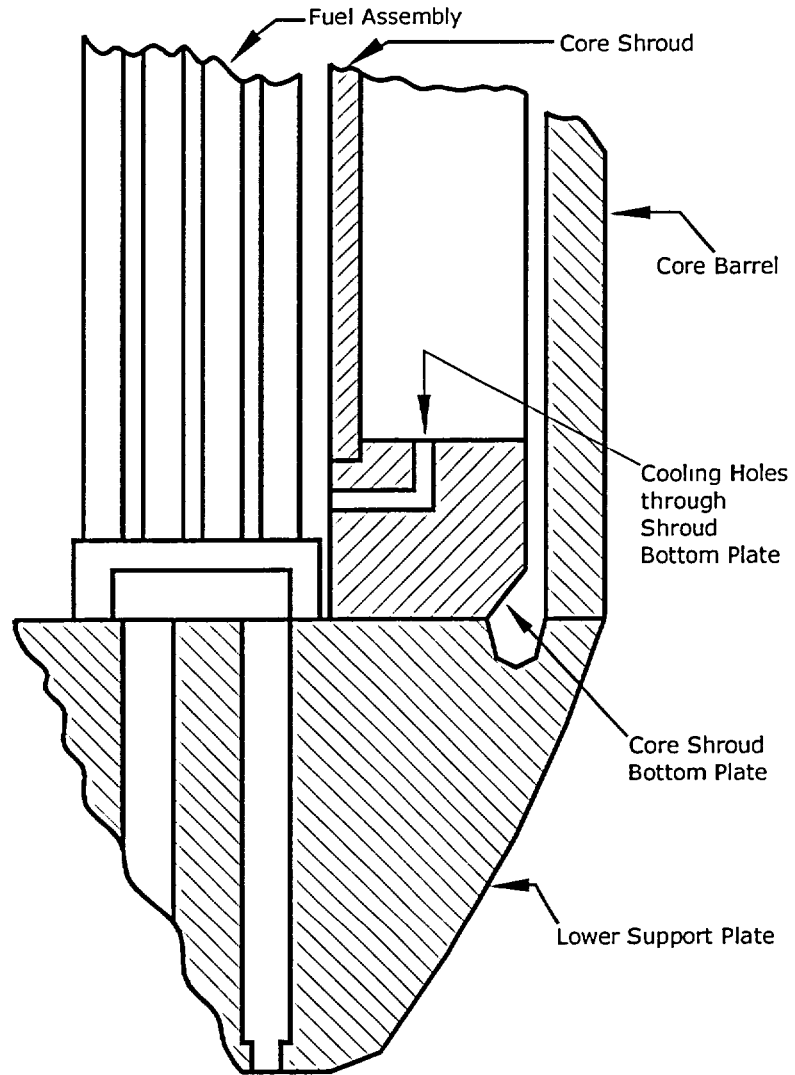


Figure 39A-3

Bottom of Core Shroud, Core Barrel, and Lower Core Support Plate (Not to Scale)

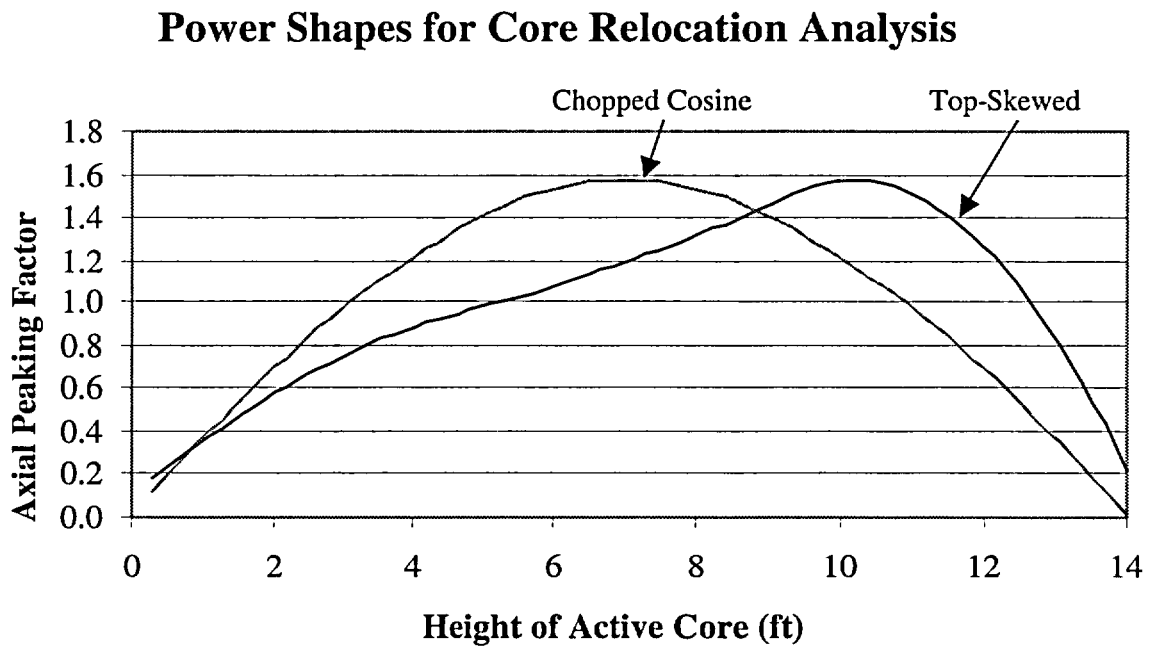


Figure 39A-4

Axial Power Shapes Used for Core Relocation Analysis

	1	2	3	4	5	6	7	8
1	(a) 0.691	(a) 0.755	(b) 0.913	(b) 0.938	(b) 0.923	(d) 1.230	(d) 1.161	(f) 0.802
2	(a) 0.755	(b) 0.953	(b) 0.953	(b) 0.844	(c) 1.113	(d) 1.176	(e) 1.021	(f) 0.640
3	(b) 0.913	(b) 0.953	(c) 1.001	(c) 1.002	(c) 1.069	(d) 1.235	(e) 1.014	
4	(b) 0.938	(b) 0.844	(c) 1.002	(c) 0.934	(d) 1.176	(d) 1.235	(f) 0.746	
5	(b) 0.923	(c) 1.113	(c) 1.069	(d) 1.176	(d) 1.288	(f) 0.867		
6	(d) 1.230	(d) 1.176	(d) 1.235	(d) 1.235	(f) 0.867			
7	(d) 1.161	(e) 1.021	(e) 1.014	(f) 0.746				
8	(f) 0.802	(f) 0.640						

Ring	(a) 1	(b) 2	(c) 3	(d) 4	(e) 5	(f) 6
# of Asmb	1.25	8	8	11	4	7
Area Fraction	0.032	0.204	0.204	0.280	0.102	0.178
Radial Peaking Factor	0.742	0.915	1.038	1.158	1.018	0.758

Figure 39A-5

Radial Power Shape Used for Core Relocation Analysis

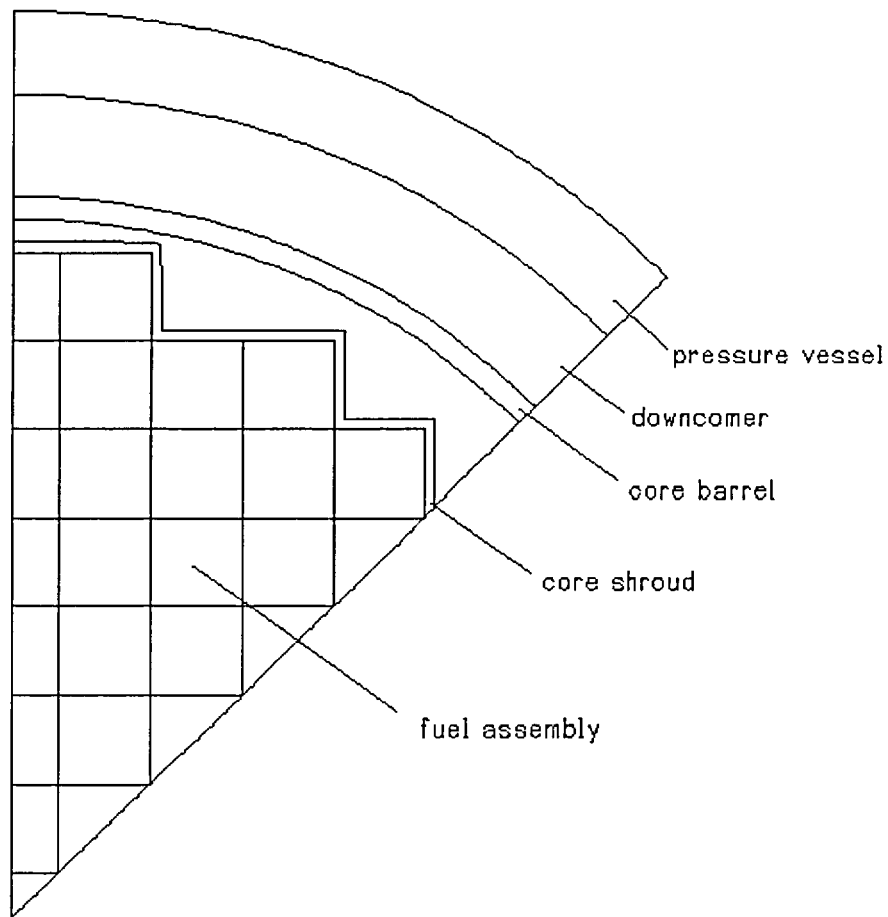


Figure 39A-6

Cross Section Geometry of Finite Difference Computational Model

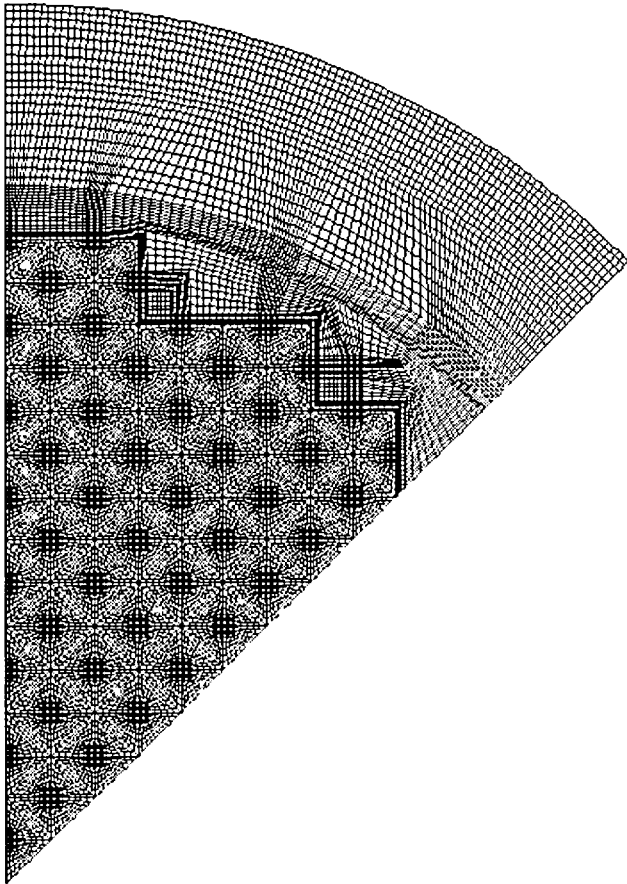


Figure 39A-7

Computational Mesh for Finite Difference Computational Model

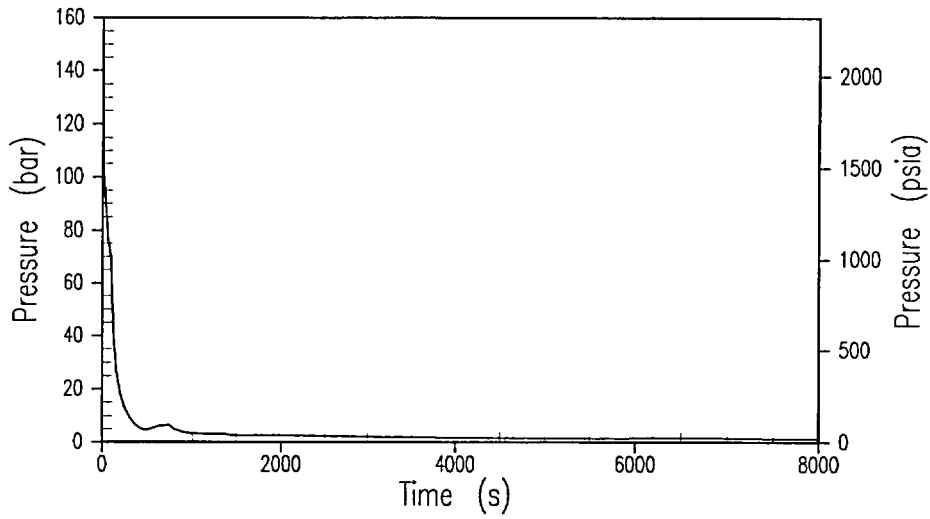


Figure 39A-8

**MAAP4 AP1000 Core Melting and Relocation,  
Top-Skewed Power Shape Reactor – Coolant System Pressure**

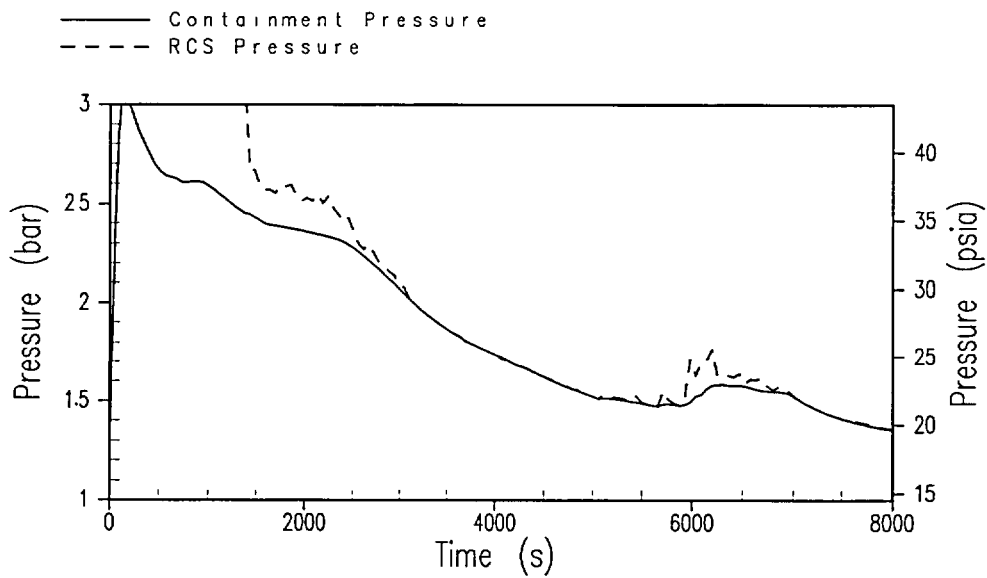


Figure 39A-9

**MAAP4 AP1000 Core Melting and Relocation,  
Top-Skewed Power Shape – Containment and Reactor Coolant System Pressure**

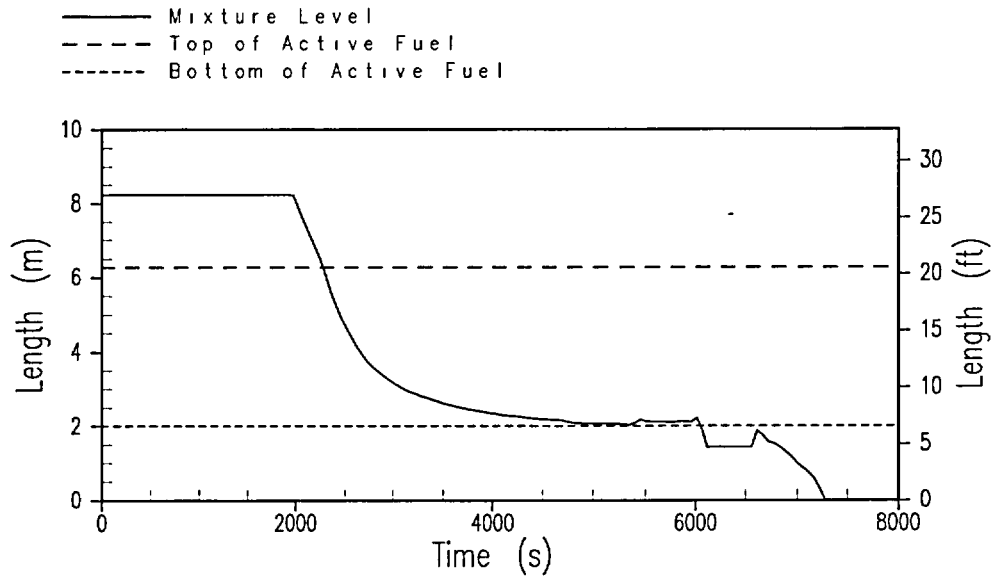


Figure 39A-10

**MAAP4 AP1000 Core Melting and Relocation,  
Chopped Cosine Power Shape – Reactor Vessel Mixture Level**

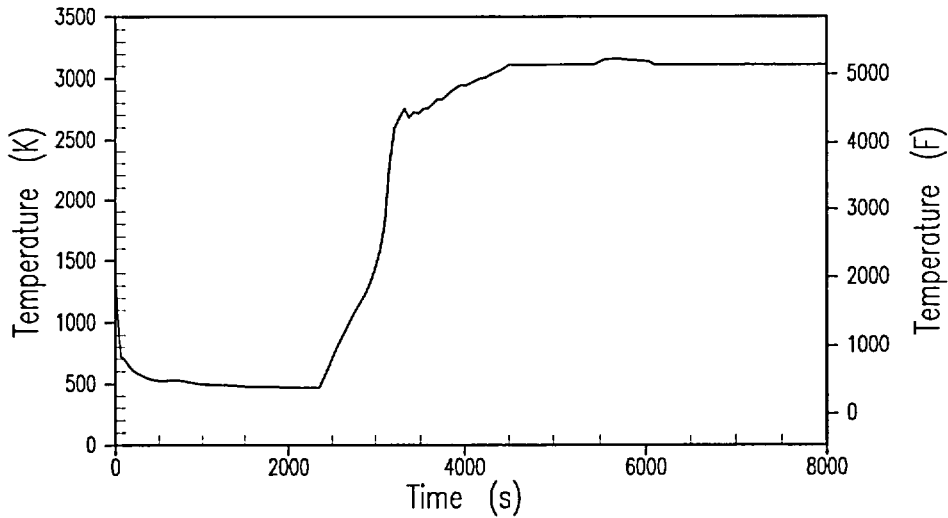


Figure 39A-11

**MAAP4 AP1000 Core Melting and Relocation,  
Top-Skewed Power Shape – Hottest Temperature in Core**

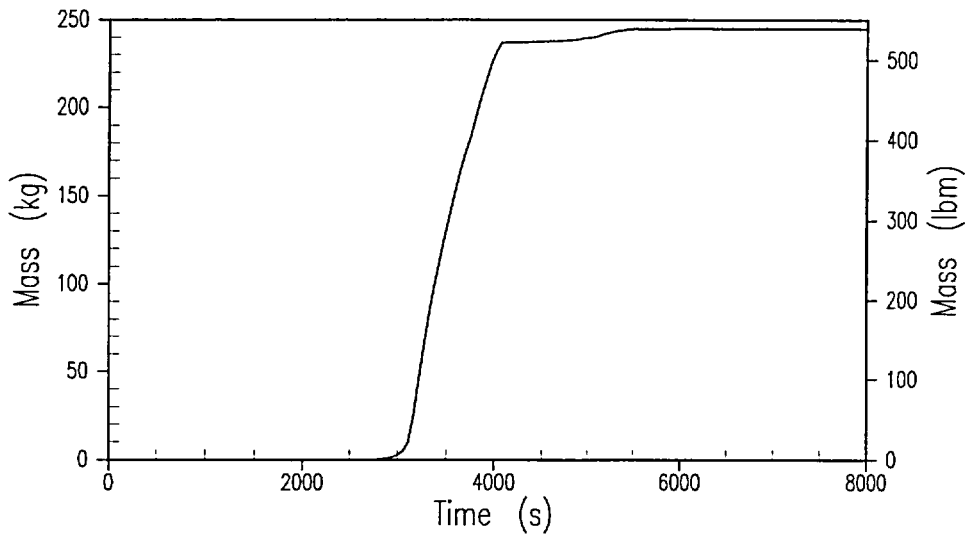


Figure 39A-12

**MAAP4 AP1000 Core Melting and Relocation, Top-Skewed Power Shape – Mass of Hydrogen Generated in Core**

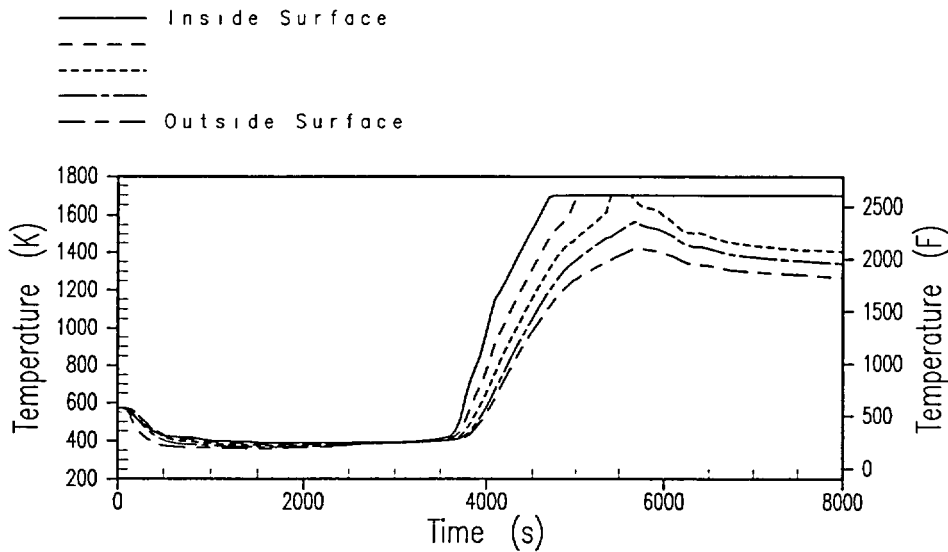


Figure 39A-13

**MAAP4 AP1000 Core Melting and Relocation, Top-Skewed Power Shape  
 Temperature of Core Shroud/Barrel (Core Elevation 1.7 – 2.0 m)**

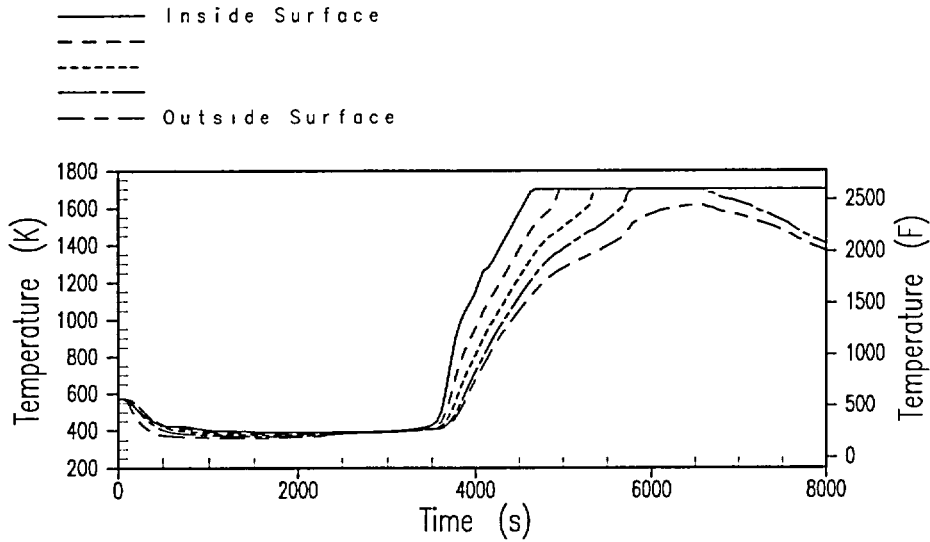


Figure 39A-14

**MAAP4 AP1000 Core Melting and Relocation, Top-Skewed Power Shape  
 Temperature of Core Shroud/Barrel (Core Elevation 2.0 – 2.3 m)**

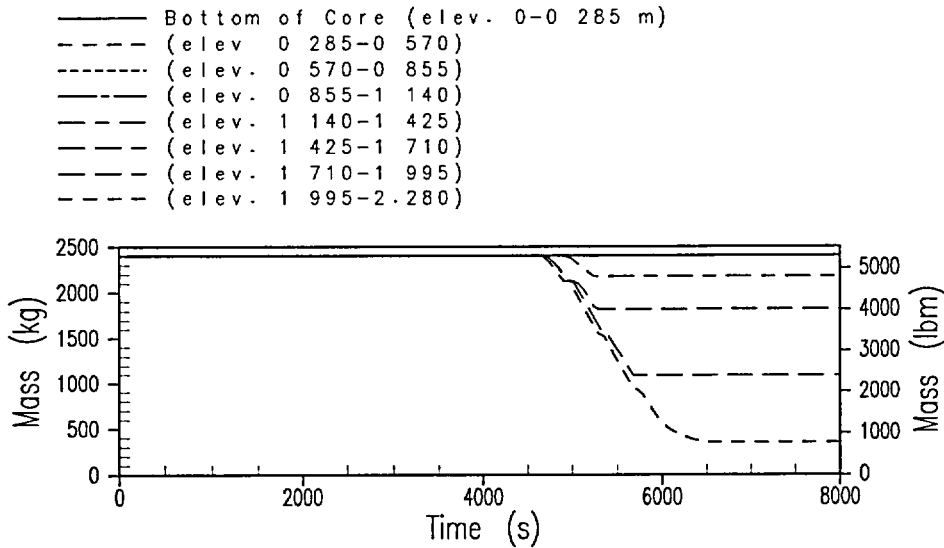


Figure 39A-15

**MAAP4 AP1000 Core Melting and Relocation,  
 Top-Skewed Power Shape – Mass of Core Shroud/Barrel**

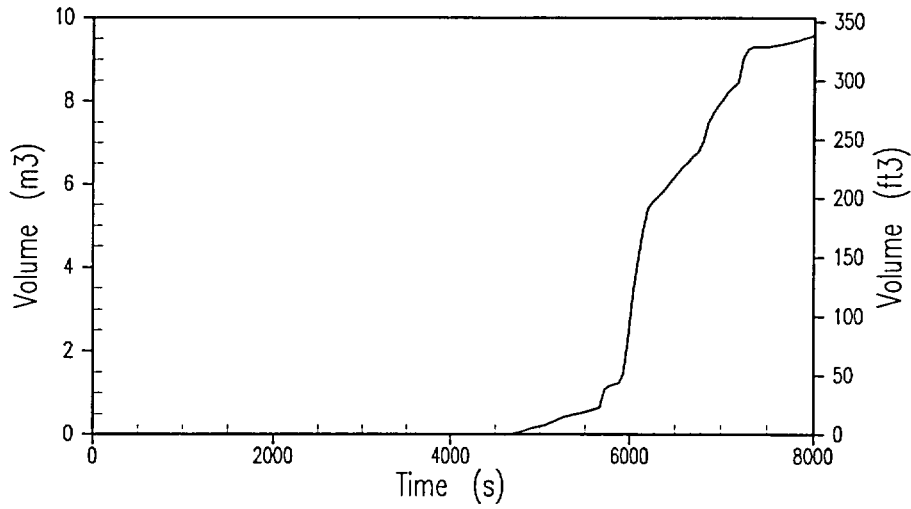


Figure 39A-16

**MAAP4 AP1000 Core Melting and Relocation, Top-Skewed Power Shape  
Volume of Debris in Reactor Vessel Lower Plenum**

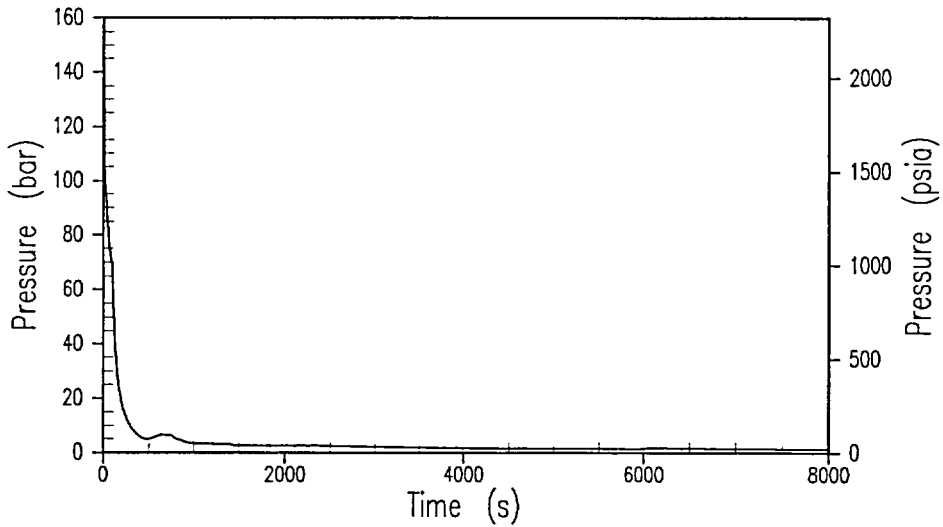


Figure 39A-17

**MAAP4 AP1000 Core Melting and Relocation,  
Chopped Cosine Power Shape – Reactor Coolant System Pressure**

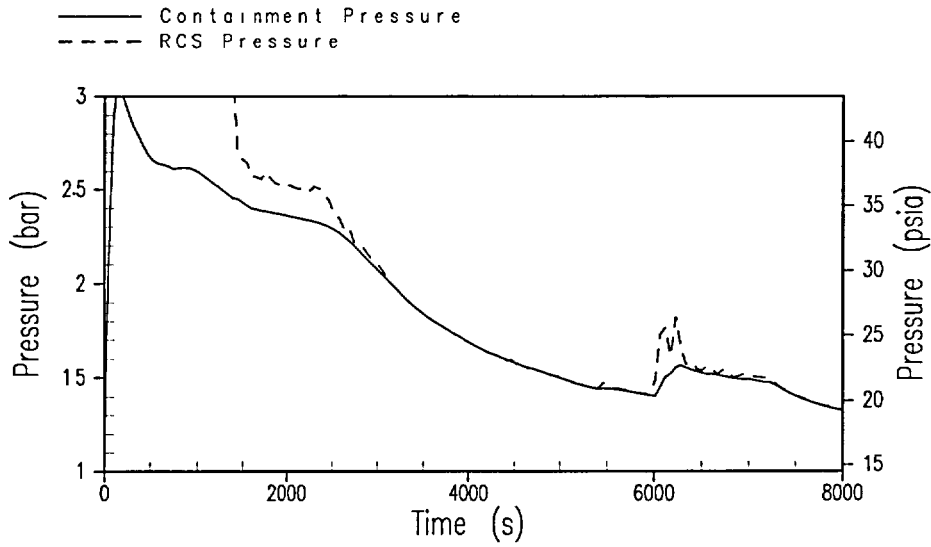


Figure 39A-18

**MAAP4 AP1000 Core Melting and Relocation,  
 Chopped Cosine Power Shape – Containment and Reactor Coolant System Pressure**

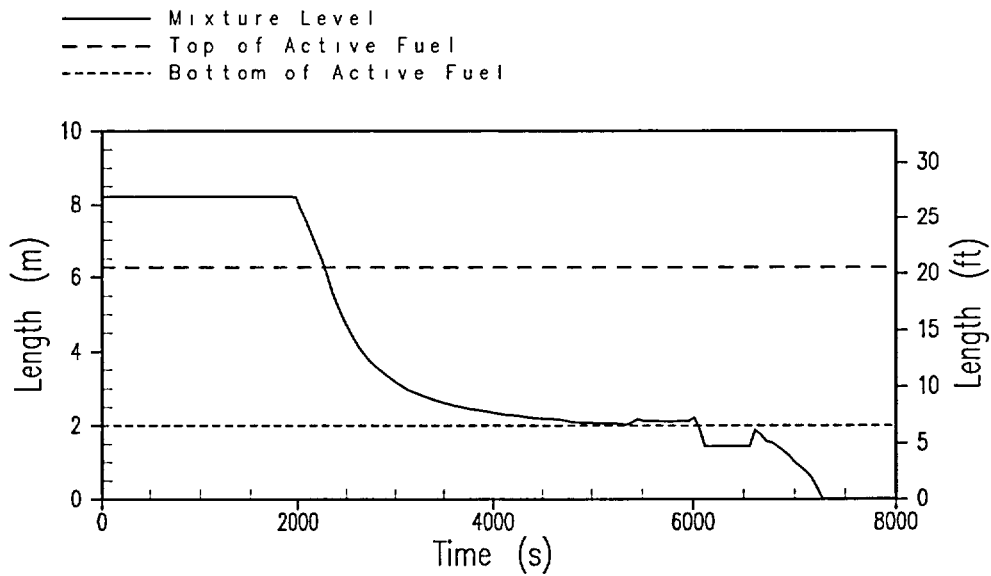


Figure 39A-19

**MAAP4 AP1000 Core Melting and Relocation,  
 Chopped Cosine Power Shape – Reactor Vessel Mixture Level**

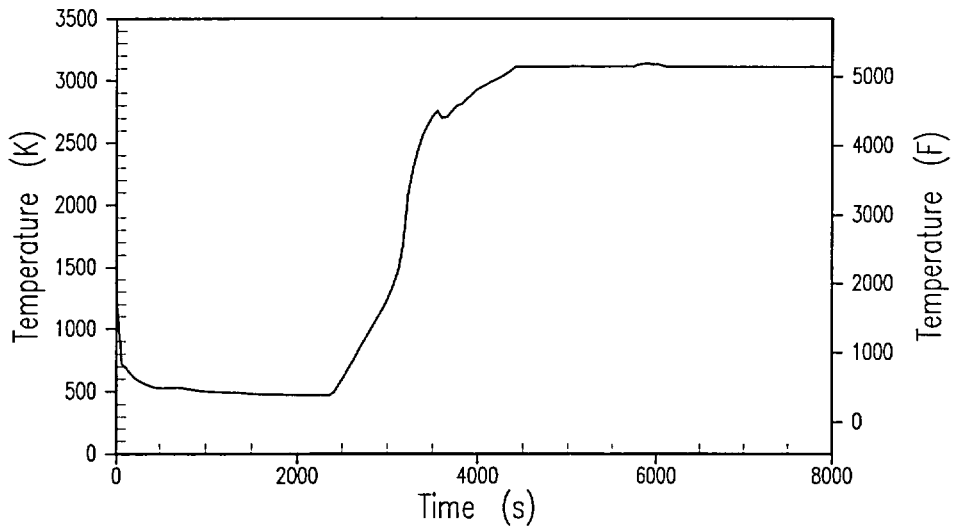


Figure 39A-20

**MAAP4 AP1000 Core Melting and Relocation,  
Chopped Cosine Power Shape – Hottest Temperature in Core**

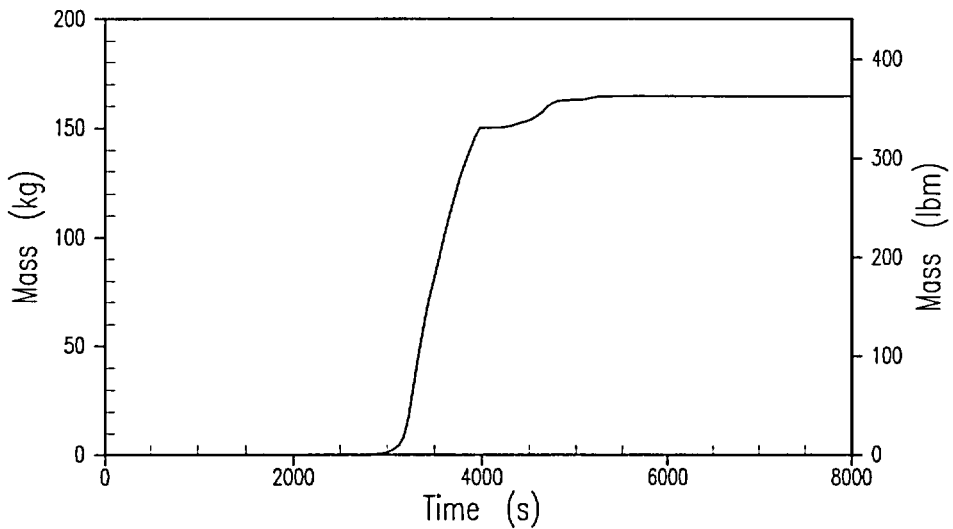


Figure 39A-21

**MAAP4 AP1000 Core Melting and Relocation,  
Chopped Cosine Power Shape – Mass of Hydrogen Generated in Core**

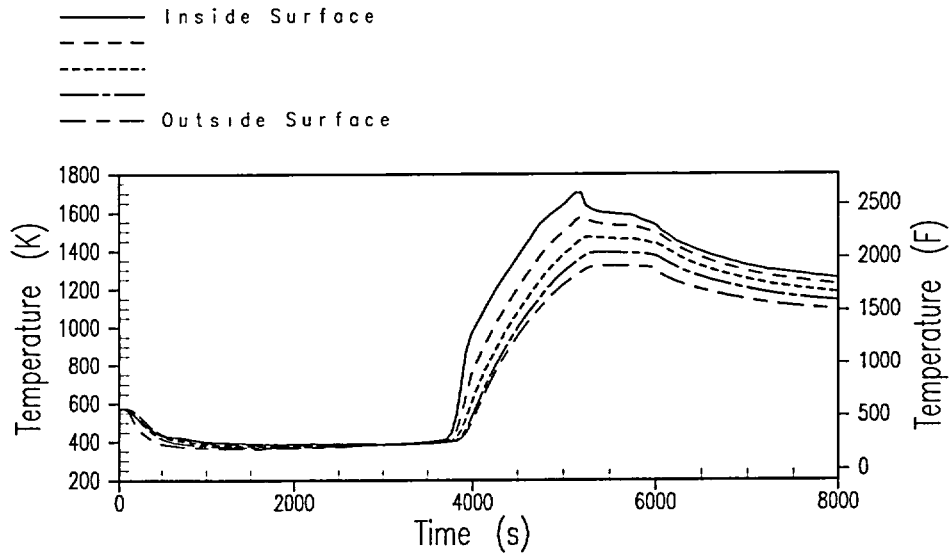


Figure 39A-22

**MAAP4 AP1000 Core Melting and Relocation, Chopped Cosine Power Shape  
Temperature of Core Shroud/Barrel (Core Elevation 1.1 – 1.4 m)**

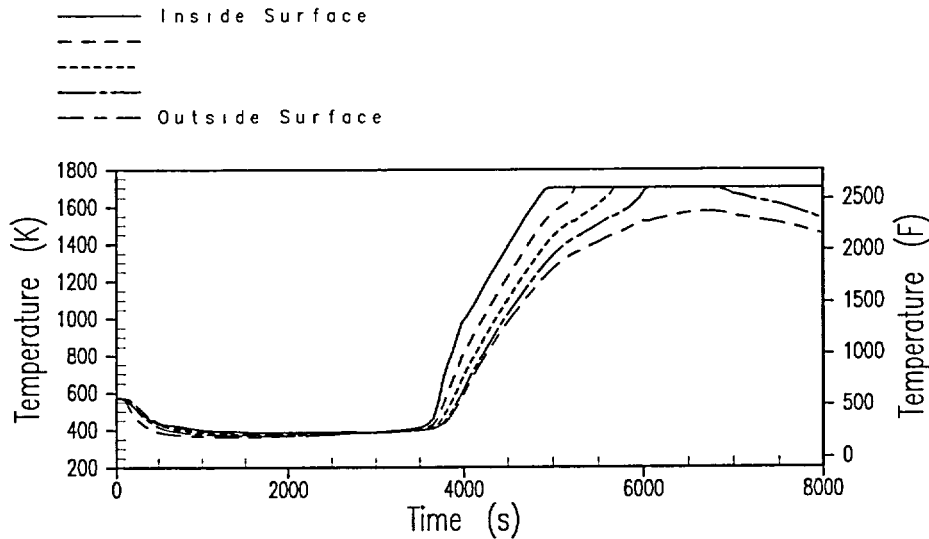


Figure 39A-23

**MAAP4 AP1000 Core Melting and Relocation, Chopped Cosine Power Shape  
Temperature of Core Shroud/Barrel (Core Elevation 1.4 – 1.7 m)**

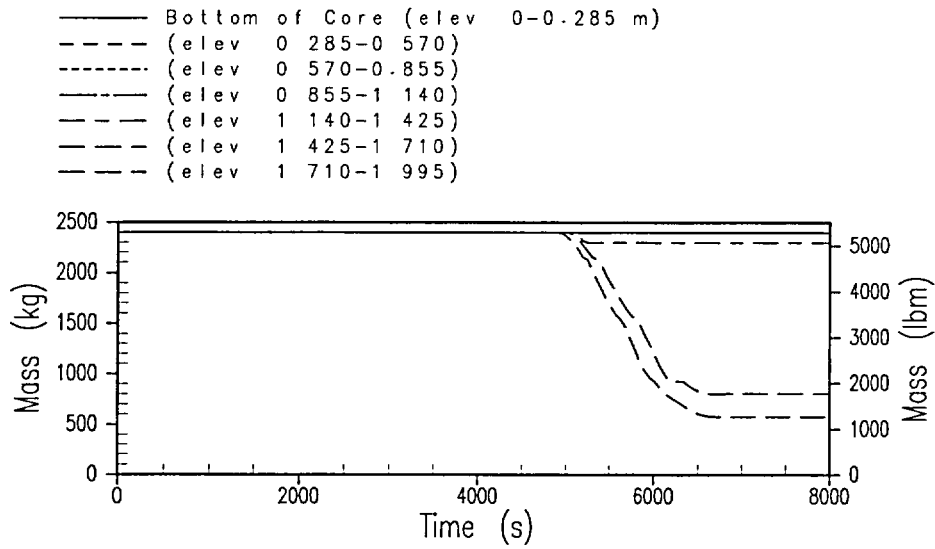


Figure 39A-24

**MAAP4 AP1000 Core Melting and Relocation, Chopped Cosine Power Shape – Mass of Core Shroud/Barrel**

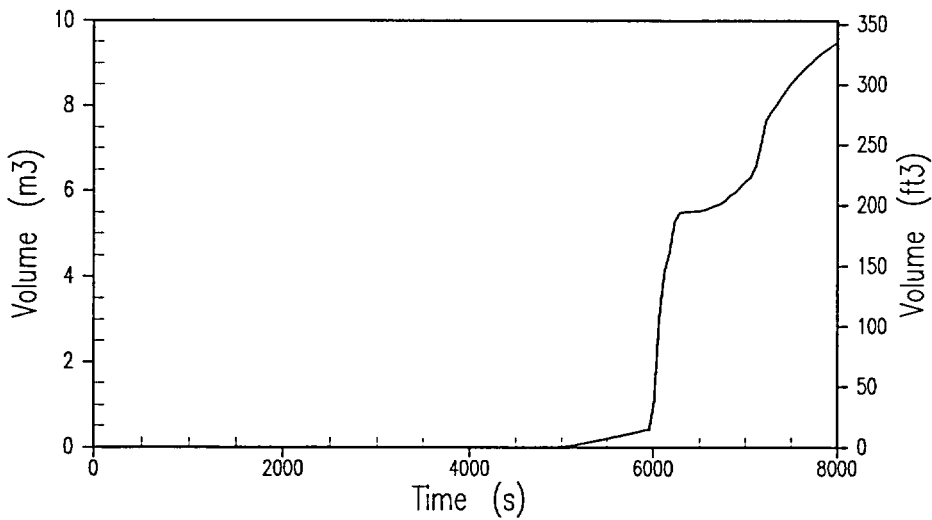


Figure 39A-25

**MAAP4 AP1000 Core Melting and Relocation, Chopped Cosine Power Shape  
Volume of Debris in Reactor Vessel Lower Plenum**

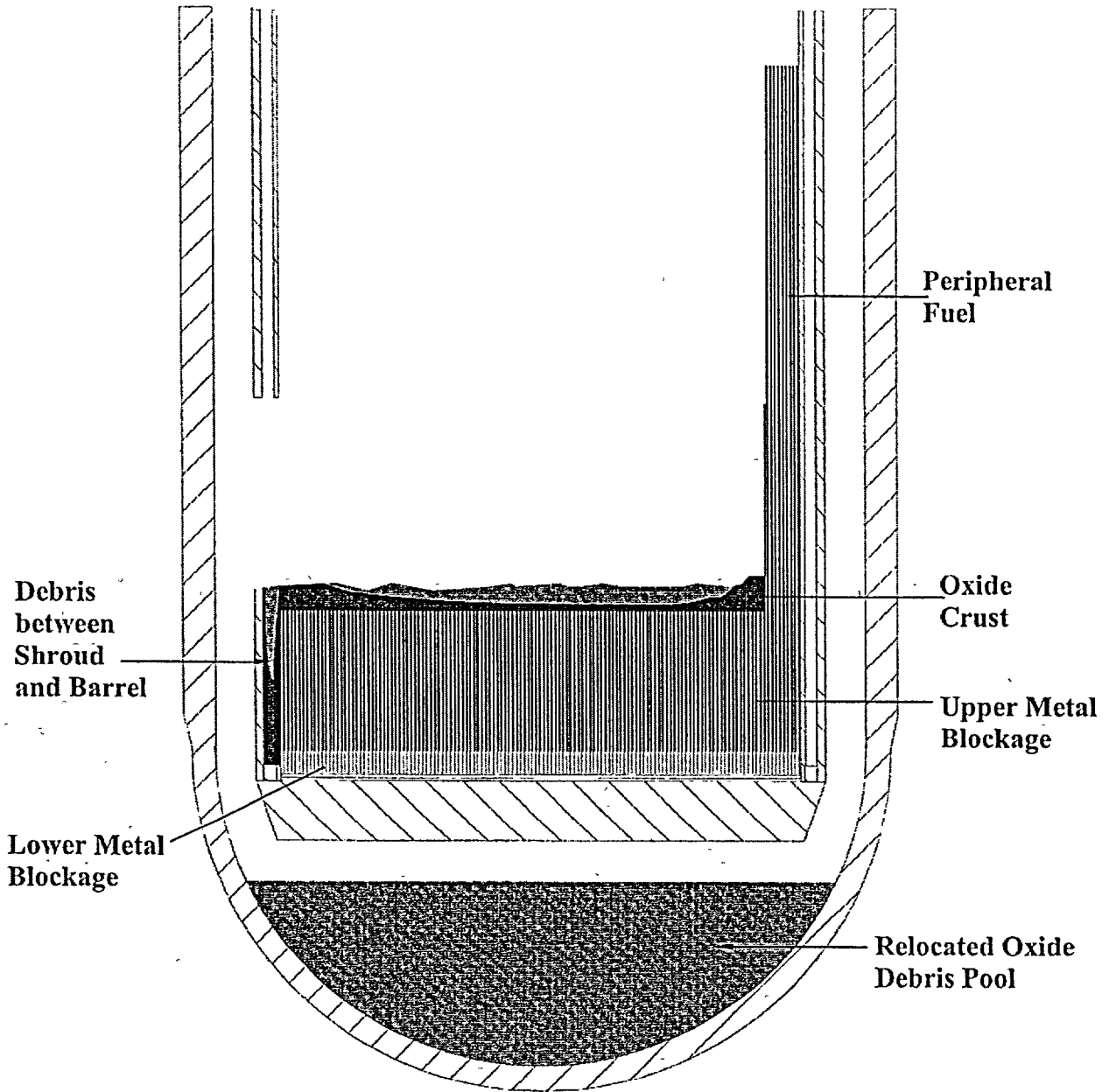


Figure 39A-26

Initial Oxide Relocation to Lower Plenum

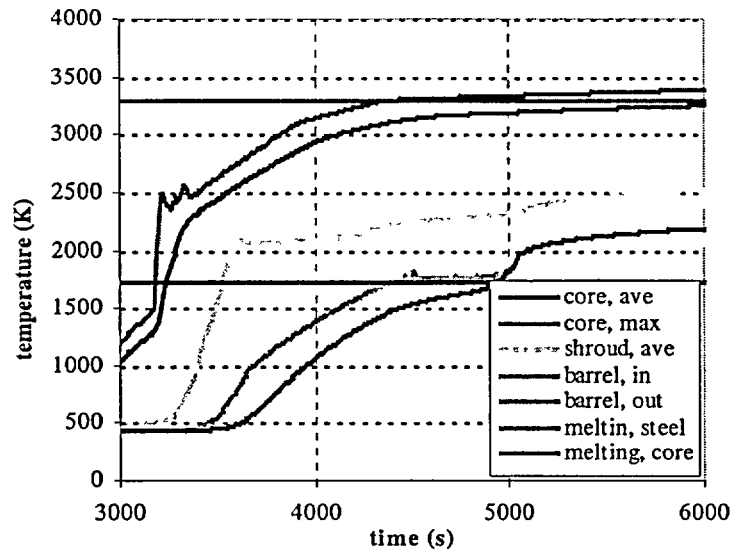


Figure 39A-27

Finite Difference Result for Top-Skewed Power Shape at Level 5

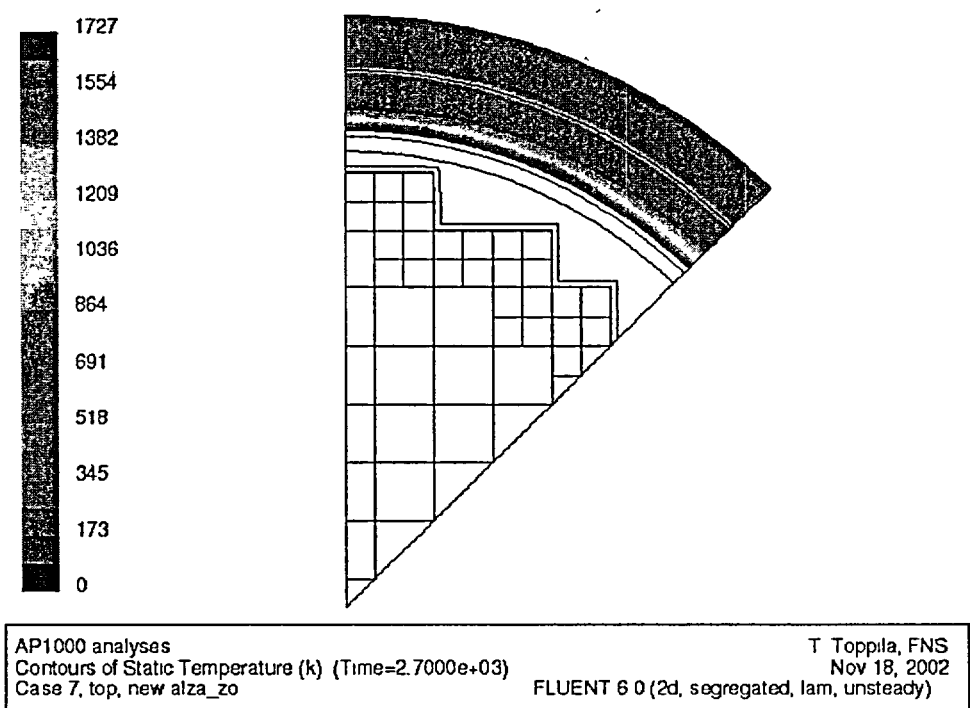


Figure 39A-28

Finite Difference Temperature Map Level 5 at 5380 Seconds for Top-Skewed Power Shape Case

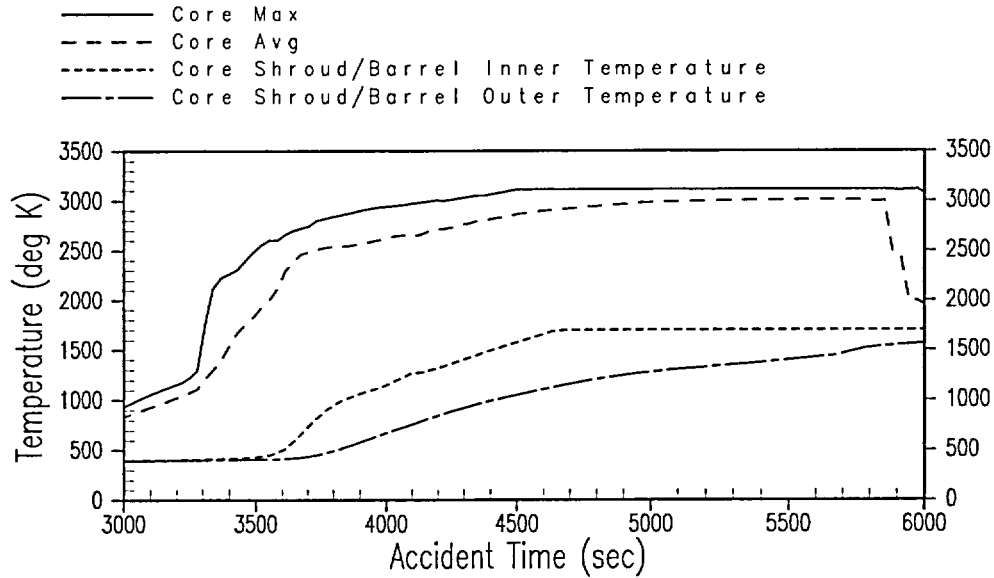


Figure 39A-29

**MAAP4 Core Temperature Profile for Top-Skewed Power Shape Core Elevation = 2.0 - 2.3 m Above Bottom of Active Fuel (Core Axial Row 12)**

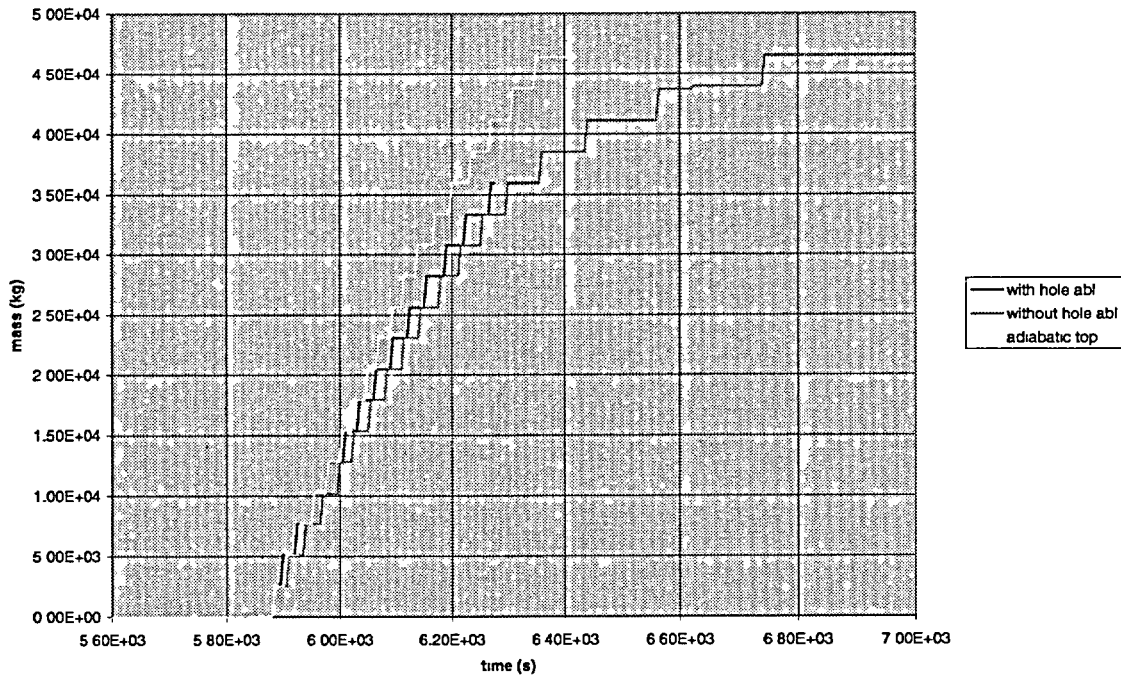


Figure 39A-30

**Relocation of Corium**

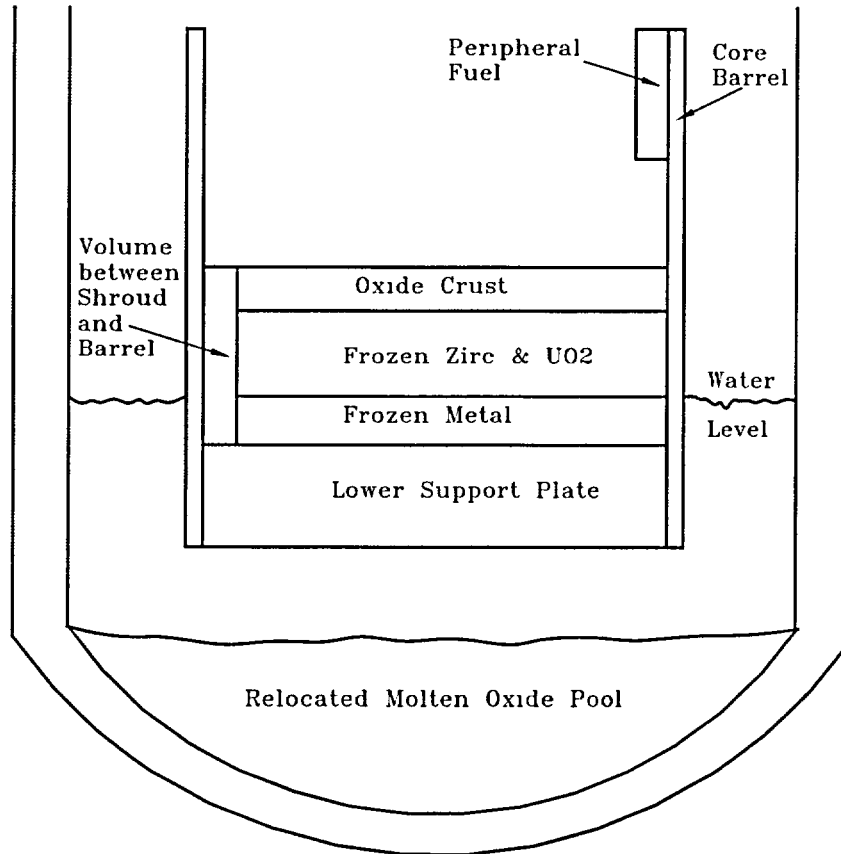


Figure 39A-31

Model for Relocation to Lower Plenum

## CHAPTER 41

### HYDROGEN MIXING AND COMBUSTION ANALYSIS

Hydrogen burning in the containment and challenging the containment integrity are considered in this analysis. As reactor vessel failure and relocation of core debris into the containment are assumed to result in containment failure on the containment event tree (CET), only hydrogen generated in-vessel is included in the analysis. Local burning of hydrogen as diffusion flames and local detonation during the hydrogen release as well as global deflagration and potential stratification, which could lead to detonation in the longer term are considered as potential containment failure modes. The probability of combustion events failing containment is quantified using decomposition event trees (DETs). The results of the decomposition event tree analyses provide input to nodes DF, DTE, DFL, and DTI on the AP1000 containment event tree. The failure probabilities for each of these CET nodes are summarized in Table 41-1 for each of the accident classes in the AP1000 Probabilistic Risk Assessment (PRA) quantification.

#### 41.1 Discussion of the Issue

In the course of a severe accident, a substantial amount of combustible gases can be generated in-vessel from the oxidation of the zirconium and other metals. The AP1000 containment is provided with nonsafety-related glow plug igniters to control the concentration of combustible gases. If the igniters operate, combustion of hydrogen plumes may present a thermal load to the containment. Combustible gas can accumulate in the containment at flammable concentrations if the igniter system fails to function. The AP1000 hydrogen analysis quantifies the threat to containment integrity with and without hydrogen igniters.

If vessel failure does not occur, the amount of hydrogen in the containment is limited to the mass generated during the in-vessel core heatup and relocation. If vessel failure occurs with water in the cavity, an additional amount of hydrogen may be generated from ex-vessel fuel-coolant interactions. Furthermore, if the debris layer in the cavity is not coolable or if insufficient water is available in the containment to cool the debris, and subsequent thermal attack of concrete occurs, additional hydrogen and other combustible gas, such as carbon monoxide, will be generated. The AP1000 containment event tree analysis assumes containment failure if vessel failure is predicted, so the evaluation of containment integrity from hydrogen combustion only considers in-vessel hydrogen generation.

Hydrogen combustion is evaluated during two time frames: early (time frame II, during the in-vessel relocation and hydrogen generation) and intermediate (time frame III, prior to 24 hours after the onset of core damage). In the early time frame, containment challenge is considered from hydrogen burning as an unmixed plume (diffusion flame) and from local detonation at high concentrations in confined compartments below the operating deck. In the intermediate time frame when the hydrogen is mixed, containment challenge from global deflagration and potential detonation due to stratification of gases is considered. Hydrogen is always assumed to burn within 24 hours of core damage.

## 41.2 Controlling Phenomena

The conditions required for combustion in the containment are flammable gas mixtures and the presence of an ignition source. Typically, a spark is sufficient to cause ignition. If the mixture temperature is above ~1000 K, auto-ignition can occur without the presence of an ignition source. The flammability limits are determined by the concentrations and temperature of the combustible gas-air-diluent mixture. Hydrogen and the oxygen in the air are the reactants in the combustion reaction. Steam, carbon dioxide, and excess nitrogen in the mixture act as inertants that may inhibit the reaction.

Hydrogen-air-steam mixtures can burn in several modes: diffusion flames, slow and accelerated deflagrations, and detonations (Reference 41-1). Burning of an unmixed hydrogen plume near the source results in a diffusion flame. Diffusion flames are stationary and result primarily in thermal loads on nearby structures or equipment. Deflagrations or detonations are burning of premixed gases. In practical terms, a slow deflagration is a flame that travels at a speed much slower than the speed of sound such that the pressure inside the containment equilibrates during the combustion. No dynamic loads are generated. Accelerated deflagrations travel fast enough to generate shock waves and dynamic loads. Detonations travel at supersonic velocities and also generate dynamic loads. The static loads that result from deflagrations can be predicted and bounded. The maximum dynamic loads from accelerated flames and detonations are difficult to calculate.

Standing diffusion flames on the in-containment refueling water storage tank (IRWST) pool or at the in-containment refueling water storage tank vents can be postulated early into an accident following core uncover for sequences in which the automatic depressurization system (ADS) stages 1 through 3 provide a primary depressurization mechanism. A standing diffusion flame at an open vent could present a thermal load to the containment steel shell, which is close to some of the vents. If the primary system break is in one of the passive core cooling system (PXS) compartments, which flood with water and submerge the break, diffusion flames can also be postulated at the vault exit in the core makeup tank (CMT) room. This location has a direct line of sight with the personnel and equipment hatches, electrical penetrations, and the containment shell, and may present a thermal loading challenge.

The static loads associated with deflagrations are limited by thermodynamics. If all of the chemical energy available in the mixture is converted to temperature and pressure, then the maximum pressure is limited by the adiabatic, isochoric (constant volume), complete combustion (AICC) pressure. The actual pressure would drop over time from this peak because of heat losses to water, structures, and equipment in containment. Dynamic pressure loads are not limited by the adiabatic, isochoric, complete combustion value because the local pressure is due to very rapid, nonequilibrium combustion.

The mode of combustion depends on the mixture concentrations, initial conditions, and boundary conditions (Reference 41-1). Near the hydrogen source, hydrogen may not be mixed significantly with the air in the containment. If ignition occurs there, then a diffusion flame may be formed. Further downstream from the hydrogen source, mixing will have occurred and a deflagration or detonation may result, depending on the hydrogen concentration and geometric boundary factors. In some cases, accelerated flames may also develop to detonations, which is called deflagration-to-detonation transition (DDT). The

occurrence of flame acceleration and deflagration-to-detonation transition is complex and not completely understood. It is dependent on a number of parameters. These include hydrogen and oxygen concentrations; nature and concentration of inertants; gas temperature and pressure before ignition; ignition source; the size and shape of the compartment in which the combustion occurs; and the number, size, and shape of any obstacles in the compartment.

In AP1000, direct initiation of detonation by high-energy sources from equipment is unlikely because ignition sources of sufficient magnitude do not exist in containment. However, mechanisms to amplify a flame to a detonation may occur. Deflagration-to-detonation transition is considered the most likely mechanism. Transition to detonation is considered in several regions of the containment for accident sequences that result in hydrogen concentrations greater than 10 volume percent. The regions are the tunnel connecting the two steam generator compartments, the core makeup tank and equipment bay, in-containment refueling water storage tank gas space, steam generator compartments, and steam generator annulus.

### 41.3 Major Assumptions and Phenomenological Uncertainties

Because of phenomenological uncertainties, a number of assumptions are necessary in the hydrogen analysis. This AP1000 analysis is based on the analysis of the AP600 hydrogen (Reference 41-2). It assumes that the plant behavior is similar.

#### 41.3.1 Hydrogen Generation

The degree to which the cladding is oxidized during the in-vessel phase of the accident sequence and the availability of water to the core determines the rate and the mass of hydrogen released to the containment during the early time phase. The rate and mass of hydrogen produced are important parameters in determining the hydrogen concentration and the flammability limits of the gas mixtures in the containment compartments. For these analyses, only in-vessel hydrogen generation is considered as reactor vessel failure and debris relocation to the containment is assumed to result in early containment failure on the containment event tree.

#### 41.3.2 Containment Pressure

The containment pressure is an important parameter in the determination of the pre-burn boundary conditions. A higher initial pressure can result in a higher peak pressure, but the increased steam mass can inert the mixture and prevent combustion. If the passive containment cooling system (PCS) water is not operational, containment pressures are greater than 45 psia (3.0 bar) (see Chapter 34) and combustion is inerted. For this reason, the passive containment cooling system water is assumed to be operational in these analyses.

#### 41.3.3 Flammability Limits

A flammable condition is determined by flammability limits. Flammability limits of a combustible gas mixture are defined as the limiting gas compositions at a given temperature and pressure in which a deflagration will propagate once ignited. There is relatively good information on flammability limits of hydrogen-air-steam mixtures at temperatures less than

149°C. For hydrogen, there are two lean propagation limits considered, upward and downward. At lean upward propagation limits, flames will propagate upward because of buoyancy. At lean downward propagation limits, flames will propagate upward and downward throughout the volume by their own reaction kinetics. Hence, the extent of flame propagation (or combustion completeness) for combustion at lean flammability limits is determined by the hydrogen concentration (Reference 41-3). The addition of steam or other inert gas has a strong effect on the hydrogen concentration and flammability (Reference 41-4).

Combustion initiated by igniters occurs at lean upward flammability limits with a small pressure rise. However, with the failure of igniters, combustion at a hydrogen concentration above the lean downward propagation limits may result in much larger pressure and temperature consequences. The global burn considered in the analysis is defined as combustion at or above the lean downward propagation limits. This definition includes the possibility that a global burn becomes a detonation, since the occurrence of a detonation requires a hydrogen concentration much above the lean downward propagation limits (Reference 41-5).

#### 41.3.4 Detonation Limits and Loads

A detonation is a supersonic combustion front that produces a dynamic load in excess of the adiabatic, isochoric, complete combustion value. The energy release from the combustion of the hydrogen-air-steam mixture sustains the shock structure that ignites and burns the mixture. The detonation limits cannot currently be predicted by any first-principles theory. Engineering correlations used to predict the limits have been developed based on a measurable quantity called the detonation cell width. For simplified discussion, the detonation cell width can be considered a characteristic length that describes the sensitivity of the mixture to detonation. The smaller the detonation width, the easier it is to get the mixture to detonate and sustain propagation. It is assumed that the likelihood of direct initiation of detonation by sufficiently high-energy sources from any objects in the containment during accident conditions does not exist. Deflagration to detonation transitions (DDT) (Reference 41-6) is considered as the only detonation mechanism.

Since the lowest hydrogen concentration for which deflagration-to-detonation transition has been observed in the intermediate-scale FLAME facility at Sandia is 15 percent (Reference 41-7), and 10 CFR 50.34(f) limits hydrogen concentration to less than 10 percent, the likelihood of deflagration-to-detonation transition is assumed to be zero if the hydrogen concentration is less than 10 percent. Containment failure is assumed if a detonation is predicted.

#### 41.3.5 Igniter System

The availability of the igniter system for each accident sequence is evaluated by fault tree VLH (Chapter 16) and linked to the containment event tree node IG for all accident sequences. The AP1000 igniter system, if operational during a severe accident, will burn hydrogen as soon as the lean upward flammability limits are met. Thus, the concentration of hydrogen is maintained, on average, at the lean upward flammability limits. However, depending on the hydrogen release rate, location and oxygen availability, locally high

concentrations may exist in the in-containment refueling water storage tank or in the subcompartment where the pipe break occurs. Hydrogen combustion due to the operation of the igniter system results in uniformly distributed hydrogen concentrations less than 10 percent and hydrogen releases to confined compartments are oxygen starved during the transient release even with the artificially high hydrogen generation rates and 100 percent active cladding reaction assumed in the analyses. Therefore, for accident scenarios in which the igniter system is operational from the onset of core damage, a zero conditional probability of global burn or detonation is assumed.

The hydrogen igniters are actuated by manual action when core-exit temperature exceeds 1200°F as directed by the emergency response guideline (ERG) AFR.C-1. The indication and actuation are done with containment conditions within the equipment qualification limits of the systems used, within the design basis of the plant and systems, and before fission-product releases to the containment, so equipment survivability of the monitoring and actuation systems during the time frame that they are required to perform is assured.

The time available for the operator to actuate the hydrogen igniters is assumed to be 10 minutes from the time the core-exit thermocouples exceed 1200°F. Sensitivities concerning the reliability of the operator action and the hydrogen control system reliability are presented in Chapter 50. The failure probability is summarized in Table 41-1.

#### 41.3.6 Other Ignition Sources

A flammable mixture will not burn without an ignition source unless the temperature of the mixture is so high (~1000 K) that auto-ignition becomes possible. Hot surfaces or random sparks from equipment or static electricity may be postulated ignition sources. High-temperature gas jets exiting from the reactor coolant system (RCS) may become an ignition source. However, the gas stream may not have enough momentum to entrain the surrounding flammable mixture, especially in the depressurized cases.

For decomposition event tree quantification, with igniter failure, the likelihood of a random ignition source is assumed to be 0.5 during the in-vessel phase with hydrogen generation to the containment. In the long term, the probability of an ignition source is assumed to be 1.

#### 41.3.7 Severe Accident Management Actions

Severe accident management guidance considered in the AP1000 PRA includes the operator action to flood the reactor cavity in the event of core damage. This action often results in the late reflooding of a damaged core. Some sequences lead to core reflooding through the natural progression of the accident. No recovery of pumped injection reflooding the core is considered in these analyses. (Pumped injection to refill the cavity or reflood the core is possible as an accident management strategy.)

#### 41.4 Hydrogen Generation and Mixing

The MAAP4 code, (Reference 41-8) was used to investigate the hydrogen generation rate in the core and releases from the reactor coolant system into the containment for the AP600 hydrogen analysis (Reference 41-2). The accident progression and containment response such as break

location, sequence timing and rate of containment flooding can have a significant effect on hydrogen generation. The overall sequence behavior for the AP1000 is essentially the same as the AP600. The AP1000 MAAP4.04 analysis results for dominant accident classes are provided in Attachment 41A. A discussion of the insights for each accident class is provided.

#### 41.4.1 Accident Class 3BE – Failure of Gravity Injection

Accident class 3BE represents accident sequences that are fully depressurized with the failure of gravity injection. The operator action to flood the reactor cavity is successful. Based on the dominant sequences in the Level 1/Level 2 interface (see Chapter 43), the applicable break locations are:

- A direct vessel injection line break in the PXS compartment,
- Loss-of-coolant accidents (LOCAs) in the floodable region (steam generator compartments), and
- Spurious ADS sequences that present no break in the RCS piping below the water elevation in the containment.

This section discusses important insights into the behavior of these sequences. Three types of cases are identified in accident class 3BE. Each case is discussed separately.

##### 41.4.1.1 Direct Vessel Injection Line Break with no PXS Compartment Flooding

Direct vessel injection (DVI) line breaks in the PXS compartment are isolated from the normal containment flooding. The PXS compartment cannot flood with the in-containment refueling water storage tank water that is intentionally drained through the recirculation lines into the floodable region of the containment. In this case, the gravity injection line in the broken DVI line is failed and does not deliver water to the PXS compartment. Water is unable to get into the reactor coolant system through the break and refill the vessel, so the core is not reflooded. The hydrogen generation occurs relatively slowly as reactor vessel water boils away from the decay heat in the covered fraction of the core. The uncovered cladding has to heat up to reach the oxidation temperatures while it is cooled by passing steam. As it heats up, the zirconium above the water line is oxidizing, melting, and relocating. The surface area available for oxidation is controlled by this self-limiting process. Steaming is limited, which limits the hydrogen production.

The reactor coolant system is depressurized prior to the hydrogen generation, so hydrogen is released to the containment as it is generated. The release pathway is through the automatic depressurization system stages 1 to 3 valves to the in-containment refueling water storage tank, through the automatic depressurization system stage 4 valves to the loop compartments and through the break to the PXS compartment. The majority of the hydrogen is released to the loop compartments through automatic depressurization system stage 4 valves, bypassing the confined compartments, and is well-mixed in the containment. However, there is potential for hydrogen concentrations in the in-containment refueling water storage tank and PXS compartments to increase during the release. The spargers in the in-containment refueling water storage tank are covered with water. The static pressure reduces the flow to the in-containment

refueling water storage tank, but the water condenses the steam from the gas flow releasing pure hydrogen to the tank. Steam concentration is low in the in-containment refueling water storage tank and high in the PXS compartment.

The containment pressure is relatively low throughout the transient, as there is no rapid steam generation from large-scale quenching.

#### 41.4.1.2 Direct Vessel Injection Line Break with PXS Compartment Flooding

DVI line breaks in the PXS compartment are isolated from the normal containment flooding. The PXS compartment cannot fill with the in-containment refueling water storage tank water that is intentionally drained through the recirculation lines into the floodable region of the containment. However, in this case, the in-containment refueling water storage tank squib valves open automatically on the low core makeup tank level and the PXS compartment floods with in-containment refueling water storage tank water drained through the broken DVI line. The water in the PXS compartment submerges the break and provides water to the reactor vessel while the relatively intact core is overheated and hydrogen generation is just beginning. Hydrogen generation occurs as sensible heat is quenched from the damaged core. Abundant steam and unreacted, overheated zirconium surface area are available, which enhances the hydrogen production. The degree of oxidation is limited by the depth of core uncover at the time of the reflood.

The reactor coolant system is depressurized prior to the hydrogen generation, so hydrogen is released to the containment as it is produced. The release pathways to the containment are through the automatic depressurization system stages 1 to 3 valves to the in-containment refueling water storage tank, through the automatic depressurization system stage 4 valves to the loop compartments and through the break to the PXS compartment. The majority of the hydrogen is released to the loop compartments through the automatic depressurization system stage 4 valves, bypassing the confined compartments, and is well mixed in the containment. However, there is potential for the hydrogen concentrations in the in-containment refueling water storage tank and PXS compartments to be increase during the release. The spargers in the in-containment refueling water storage tank are covered with water, which reduces the flow to the in-containment refueling water storage tank, but condenses the steam from the gas flow. Steam concentration is low in the in-containment refueling water storage tank.

The PXS compartment flooding submerges the break and fills the room with water. Steam from the break is condensed in the in-containment refueling water storage tank water, but the concrete walls are hot from the initial blowdown into the room and the steam concentration in the PXS compartment remains high.

The containment pressure is elevated as the quenching of the overheated core produces large quantities of steam.

#### 41.4.1.3 Loop Compartment Break with Cavity Flooding

Breaks in the loop compartment are in the floodable region of the containment. The containment is flooded with in-containment refueling water storage tank water by the operator. The hydrogen generation occurs slowly as reactor vessel water boils away from the limited

decay heat in the covered fraction of the core. The uncovered cladding has to heat up to reach the oxidation temperatures while it is cooled by passing steam. As it heats up, the zirconium above the water line is oxidizing, melting, and relocating. The surface area available for oxidation is controlled by this self-limiting process. Steaming is limited, which limits the hydrogen production. Because of the elevation of the break and the volume of the containment, the vessel reflood does not occur until after significant core damage and reduction in the surface area of the unoxidized zirconium. Therefore, although the vessel is reflooded, the hydrogen generation is similar to that of the non-reflooded cases.

The reactor coolant system is depressurized prior to the hydrogen generation, so hydrogen is released to the containment as it is produced. The release pathways to the containment are through the automatic depressurization system stages 1 to 3 valves to the in-containment refueling water storage tank, through the automatic depressurization system stage 4 valves and the break to the loop compartments. The majority of the hydrogen is released to the loop compartments, bypassing the confined compartments, and is well mixed into the containment. However, there is potential for hydrogen concentration in the in-containment refueling water storage tank to increase during the release. The PXS compartments are dead-ended and do not receive significant flow of containment gases. Therefore, the PXS compartment hydrogen concentration is lower than the rest of the containment. The spargers in the in-containment refueling water storage tank are covered with water and reduce the flow to the in-containment refueling water storage tank, but condense the steam from the gas flow. Steam concentration is low in the in-containment refueling water storage tank.

The containment pressure is elevated as the quenching of the overheated core produces large quantities of steam.

#### 41.4.1.4 Spurious ADS

Spurious ADS cases that result in full system depressurization are essentially breaks in the loop compartment above the water level in the floodable region of the containment. The containment is flooded with in-containment refueling water storage tank water by the operator. Because the elevation of the opening in the RCS (ADS stage 4) is above the water level in the containment, water is unable to get into the reactor coolant system through the break and refill the vessel. The hydrogen generation occurs relatively slowly as reactor vessel water boils away from the decay heat in the covered fraction of the core. The uncovered cladding has to heat up to reach the oxidation temperatures while it is cooled by passing steam. As it heats up, the zirconium above the water line is oxidizing, melting, and relocating. The surface area available for oxidation is controlled by this self-limiting process. Steaming is limited, which limits the hydrogen production.

The reactor coolant system is depressurized prior to the hydrogen generation, so hydrogen is released to the containment as it is produced. The release pathways to the containment are through the automatic depressurization system stages 1 to 3 valves to the in-containment refueling water storage tank, and through the automatic depressurization system stage 4 valves to the loop compartments. The majority of the hydrogen is released to the loop compartments, bypassing the in-containment refueling water storage tank (IRWST), and is well mixed into the containment. However, there is potential for hydrogen concentration in the in-containment refueling water storage tank to increase during the release. The spargers in the in-containment

refueling water storage tank are covered with water, which reduces the flow to the in-containment refueling water storage tank, but condenses the steam from the gas flow. Steam concentration is low in the in-containment refueling water storage tank. The PXS compartments are dead-ended and do not receive significant flow of containment gases. Therefore, the PXS compartment hydrogen concentration is lower than the rest of the containment.

The containment pressure is elevated as the quenching of the overheated core produces large quantities of steam.

#### 41.4.2 Accident Class 3BL – Failure of Gravity Recirculation

Accident class 3BL represents accident sequences that are fully depressurized with the failure of gravity recirculation. Based on the dominant sequences in the Level 1/Level 2 interface (see Chapter 43), the applicable break locations are loss-of-coolant accidents in the floodable region (steam generator compartments) and DVI line breaks in the PXS compartment. Cavity flooding is successful as a result of the accident progression.

This section discusses the hydrogen behavior and insights for accident class 3BL sequences.

##### 41.4.2.1 Loop Compartment Breaks

Breaks in the loop compartment are in the floodable region of the containment. Gravity injection is successful and, based on the definition of the 3BL accident class, water is unable to get into the reactor coolant system through the break or recirculation lines to refill the vessel, so the core is not reflooded. The hydrogen generation occurs slowly as reactor vessel water boils away from the limited decay heat in the covered fraction of the core. The uncovered cladding has to heat up to reach the oxidation temperatures while it is cooled by passing steam. As it heats, the zirconium above the water line is oxidizing, melting, and relocating. The surface area available for oxidation is controlled by this self-limiting process. Steaming is limited, which limits the hydrogen production.

The reactor coolant system is depressurized prior to the hydrogen generation, so hydrogen is released to the containment as it is produced. The release pathways to the containment are through the automatic depressurization system stages 1 to 3 valves to the in-containment refueling water storage tank, and through automatic depressurization system stage 4 valves and the break to the loop compartments. The majority of the hydrogen is released to the loop compartments, bypassing the in-containment refueling water storage tank, and is well mixed in the containment. There is potential for hydrogen concentration in the in-containment refueling water storage tank to be elevated during the release. The in-containment refueling water storage tank is drained prior to the hydrogen release so the spargers in the in-containment refueling water storage tank are not covered with water and the steam from the reactor coolant system is not condensed. The steam release to the in-containment refueling water storage tank drives the air out of the tank before hydrogen is generated.

The containment pressure is relatively low throughout the transient, as there is no rapid steam generation from large-scale quenching.

#### 41.4.2.2 DVI Line Break to the PXS Compartment

DVI line breaks in the PXS compartment are isolated from the floodable region of the containment. Gravity injection is successful and, based on the definition of the 3BL accident class, water is unable to get into the reactor coolant system through the break or recirculation lines to refill the vessel, so the core is not reflooded. The hydrogen generation occurs slowly as reactor vessel water boils away from the limited decay heat in the covered fraction of the core. The uncovered cladding has to heat up to reach the oxidation temperatures while it is cooled by passing steam. As it heats, the zirconium above the water line is oxidizing, melting, and relocating. The surface area available for oxidation is controlled by this self-limiting process. Steaming is limited, which limits the hydrogen production.

The reactor coolant system is depressurized prior to the hydrogen generation, so hydrogen is released to the containment as it is produced. The release pathways to the containment are through the automatic depressurization system stages 1 to 3 valves to the in-containment refueling water storage tank, and through automatic depressurization system stage 4 valves to the loop compartments and through the break to the PXS compartments. The majority of the hydrogen is released to the loop compartments, bypassing the in-containment refueling water storage tank, and is well mixed in the containment. There is potential for hydrogen concentration in the in-containment refueling water storage tank and PXS compartments to be elevated during the release. The in-containment refueling water storage tank is drained prior to the hydrogen release so the spargers in the in-containment refueling water storage tank are not covered with water and the steam from the reactor coolant system is not condensed. The steam release to the confined compartments drives the air out of the tank before hydrogen is generated.

The containment pressure is relatively low throughout the transient, as there is no rapid steam generation from large-scale quenching.

#### 41.4.3 Accident Class 3BR – Large LOCA with Accumulator Failure

Accident class 3BR represents large loss-of-coolant accident sequences that are fully depressurized with the failure of gas-charged accumulators. The reactor vessel is voided by the large loss-of-coolant accident, and the core makeup tanks and gravity injection are unable to inject fast enough to refill the vessel before core damage occurs. By definition of the accident class, the applicable breaks are large loss-of-coolant accidents in the floodable region (steam generator compartments). Cavity flooding is successful as a result of the accident progression.

Accident class 3BR sequences all have large loss-of-coolant accident breaks in the steam generator rooms. The large loss-of-coolant accident voids the reactor vessel and the accumulators fail to refill the vessel. The core overheats quickly as decay heat is high immediately after scram. Gravity injection is successful and refills the vessel after stage 4 ADS opens the injection line valves, so the core is reflooded while the relatively intact core is overheated and hydrogen generation is just beginning. Abundant steam and unreacted, overheated zirconium surface area are available, which enhances the hydrogen production. The degree of oxidation is limited.

The reactor coolant system is depressurized through the break prior to the hydrogen generation, so hydrogen is released to the containment as it is produced. The release pathways are through the large break to the loop compartment, automatic depressurization system stages 1 to 3 valves to the in-containment refueling water storage tank, and through automatic depressurization system stage 4 valves to the loop compartments. The majority of hydrogen is released to the loop compartments, bypassing the in-containment refueling water storage tank, and is well mixed in the containment. There is potential for hydrogen concentration in the in-containment refueling water storage tank to be elevated during the release. The in-containment refueling water storage tank is full and the steam is condensed in the in-containment refueling water storage tank water, so the steam concentration in the in-containment refueling water storage tank is low.

The containment pressure is elevated due to the large loss-of-coolant accident initiating event and the quenching of the overheated core by the core makeup tank water and gravity injection.

#### 41.4.4 Accident Class 3C

Accident class 3C represents accident sequences initiated by the failure of the reactor vessel below the top of the active fuel. This is a large cold side break that is expected to void the vessel, regardless of the elevation of the break. ADS and injection systems are successful, but they are unable to refill the reactor vessel above the break elevation. The core is not recovered until the water level in the cavity is above the break elevation and the vessel can be refilled through the break as the cavity fills.

The uncovered fraction of the core would overheat early in the accident since the decay heat is high and the core cannot be cooled from the onset of the accident. Therefore, once the water is able to reach the core, it is assumed that the core is reflooded while the relatively intact core is overheated. Hydrogen generation occurs as sensible heat is quenched from the damaged core. Abundant steam and unreacted, overheated zirconium surface area are available, which enhances the hydrogen production. The degree of oxidation is limited by the amount of the core that is uncovered and fraction of zirconium that is overheated.

The reactor coolant system is depressurized by the break, but the RCS is not vented until the ADS is actuated. Substantial hydrogen generation cannot occur until water is available to the core. At low pressure in the RCS, condensation is not expected in the steam generator tubes. Therefore, even with stages 1 to 3 open, containment water cannot enter through the break until the water level is at least 10 feet above the break (the depth of the sparger in the in-containment refueling water storage tank pool). The containment will not be flooded to such a depth until the in-containment refueling water storage tank injection begins. The in-containment refueling water storage tank injection squib valves open at the same time as ADS stage 4. Therefore, the RCS is fully depressurized prior to the hydrogen generation, so hydrogen is released to the containment as it is produced. The release pathways are through the automatic depressurization system stages 1 to 3 valves to the in-containment refueling water storage tank, and through automatic depressurization system stage 4 valves to the loop compartments. The majority of hydrogen is released to the loop compartments, bypassing the in-containment refueling water storage tank, and is well mixed in the containment. There is potential for hydrogen concentration in the in-containment refueling water storage tank to be elevated during the release. The in-containment refueling water storage tank is full and the steam is condensed in

the in-containment refueling water storage tank water, so the steam concentration in the in-containment refueling water storage tank is low.

The containment pressure is elevated due to the large loss-of-coolant accident initiating event and the quenching of the overheated core by the core makeup tank water and gravity injection.

#### 41.4.5 Accident Classes 3D and 1D

Accident classes 3D and 1D represent sequences that are partially depressurized. Actuation of automatic depressurization system stage 4 is assumed to fail entirely in these analyses. Based on the dominant sequences, accident class 3D/1D sequences are initiated by spurious ADS, small and medium loss-of-coolant accidents in the floodable compartments, and by direct vessel injection breaks into the PXS compartments. The operator action to flood the reactor cavity is successful.

In accident class 3D/1D sequences, gravity injection is available but the reactor coolant system is only partially depressurized, and in-containment refueling water storage tank water cannot inject. The core is not reflooded and quenched. Hydrogen generation occurs as the water level in the vessel boils off.

No stage 4 automatic depressurization system is available to release the hydrogen to the loop compartments where it can be mixed in the containment. A substantial fraction of the hydrogen generated in-vessel is released through automatic depressurization system stages 1 to 3 valves to the in-containment refueling water storage tank. The spargers are submerged and much of the steam is quenched. Very high hydrogen concentrations with relatively low steam concentrations are generated in the in-containment refueling water storage tank. If the break is in the PXS compartment, high hydrogen and steam concentrations exist there as well. The release of hydrogen and steam to the PXS compartment can also create high concentrations in the core makeup tank room to which the PXS compartments vent.

Because core is not recovered or quenched, the containment pressure is low in this accident class. The breaks tend to be small or medium sized in the 3D/1D accident sequences, and most of the energy released from the RCS is quenched in the in-containment refueling water storage tank. The hydrogen is released through the in-containment refueling water storage tank above the operating deck, and there is little flow generated below the operating deck. So the containment is not expected to be well-mixed in the 3D/1D accident sequences.

#### 41.4.6 Accident Class 1AP

Accident class 1AP represents small loss-of-coolant accident with passive residual heat removal and intermediate loss-of-coolant accident sequences in which the automatic depressurization system is failed. The reactor coolant system is pressurized above the 150 psig shutoff head of the normal residual heat removal pumps. For these sequences to be considered for the hydrogen threat to the containment, they are assumed to have been successfully depressurized manually with at least 2 of the 4 stage 4 automatic depressurization system valves opened. Manual depressurization is credited on the containment event tree if the operator is successful in opening the automatic depressurization system valves within 30 minutes of reaching ERG AFR.C-1 (see Chapter 36). Therefore, to maximize the time for potential for hydrogen

generation, it is assumed that the reactor coolant system is depressurized 30 minutes after the core-exit temperature reaches 1200°F. The extended time of core uncover provides heatup time for the uncovered cladding prior to reflood, which enhances hydrogen production. The automatic depressurization system valves are opened in sequence so that almost all the blowdown is through the in-containment refueling water storage tank.

The containment pressure is relatively low as the blowdown is quenched in the in-containment refueling water storage tank and does not result in a high-energy release to the containment atmosphere. The hydrogen release is above the operating deck through the in-containment refueling water storage tank vents, however, the operation of ADS stage 4 and the reflooding of the core creates mixing throughout the containment.

#### 41.4.7 Accident Class 1A

Accident class 1A represents non-loss-of-coolant-accident transient sequences that are not initially depressurized. The reactor coolant system is pressurized above the 1100 psia interlock pressure of the stage 4 automatic depressurization system valves. These sequences are assumed to be successfully depressurized manually. Manual depressurization is credited on the containment event tree if the operator is successful in opening the automatic depressurization system valves within 30 minutes of reaching ERG FR.C-1. Therefore, to maximize the time for hydrogen generation, it is assumed that the reactor coolant system is depressurized 30 minutes after the core-exit temperature reaches 1200°F. The valves are opened in sequence so that the blowdown is through the in-containment refueling water storage tank.

In accident class 1A cases, the core is recovered without significant hydrogen generation. The automatic depressurization system recovery success criteria are sufficiently conservative that, although the core is uncovered for an extended period of time, minimal core damage is predicted due to the cooling by natural circulation in the reactor coolant system at high pressure. For these cases, no hydrogen threat to the containment is considered.

#### 41.4.8 Accident Class 3A

Accident class 3A represents anticipated transient without scram (ATWS) sequences that are not recovered before core damage is assumed. For accident class 3A sequences to be considered for hydrogen analysis on the containment event tree, node DP is successful. Success at node DP indicates that the reactor coolant pumps are tripped, passive residual heat removal is successful, and the core makeup tank injects borated water. The reactor coolant system piping and steam generator tube remain intact throughout the pressure transient. Core damage is assumed due to departure from nucleate boiling. However, no significant hydrogen is generated and there is no significant release to the containment. For accident class 3A, no hydrogen threat to the containment is considered.

#### 41.4.9 Accident Class 6

Accident class 6 represents unisolated steam generator tube rupture sequences. For accident class 6 sequences to be considered for hydrogen analysis on the containment event tree, node DP is successful. Success at node DP indicates that operator action to actuate the automatic depressurization system has been successful to mitigate the accident. Accident

class 6 sequences are treated as accident class 3BL sequences on the containment event tree hydrogen nodes.

#### 41.4.10 Overall Mixing Insights

The containment mixing is mainly driven by the steam releases through ADS stage 4 or, in the event the core is not reflooded, boiling in the containment pool at the outer surface of the RCS vessel and piping. Steam and hydrogen rises from the loop compartments and is released as a plume from the top of the steam generator doghouses. The plume mixes with the upper compartment atmosphere as it rises 130 ft to the top of the upper compartment. The steam condenses on the passive containment cooling system shell, and the cooler air flows down the wall, through flow paths in the operating deck, and into the CMT room. The natural circulation mixing cycle is completed by the flow from the CMT room to the loop compartments through labyrinth doors at the 107'-2" elevation. Ninety-seven percent of the containment free volume participates in the mixing promoted by this natural circulation flow.

Hydrogen releases to the confined compartments (IRWST, PXS/CVS compartments) can create locally high hydrogen concentrations that are generally not flammable. However diffusion flames may be postulated at the exits from the confined compartments into the well-mixed volumes. The operation of ADS stage 4 significantly limits the magnitude and duration of hydrogen releases to the confined compartments, particularly the in-containment refueling water storage tank, which has a higher backpressure due to the static head of water above the spargers.

If stage 4 is failed (accident classes 3D and 1D), hydrogen is released above the operating deck elevation. There is no driving circulation to mix the hydrogen in the compartments below the operating deck until the containment pool in the floodable region begins to boil at the outer surface of the RCS vessel and piping during in-vessel retention of molten core debris (IVR). However the hydrogen plume is expected to mix in the upper compartment (85% of the containment volume), given the 150-ft rise height and cooling of the passive containment shell.

Reflooding the core results in periods of elevated containment pressure during the quenching of the core debris. Burns from elevated pressures can result in higher peak pressure, but the additional steam in the containment reduces the potential for detonation and can act to inert combustion. The containment pressure eventually subsides at an equilibrium pressure between 26 and 30 psia (1.8 and 2.0 bar).

The following parameters are considered to be particularly important to quantification of the hydrogen threat to the containment:

- Break location - steam generator rooms, PXS compartment
- In-containment refueling water storage tank water level during the hydrogen release
- PXS compartment flooding
- Damaged core reflooding and timing
- Containment pressure at the time of the burn

### 41.5 Hydrogen Burning at Igniters

MAAP4 analyses of AP600 cases demonstrated the effectiveness of the hydrogen igniter system as placed (Reference 41-2) in the passive containment geometry. The cases in the burning analysis were chosen for variation in hydrogen generation rate, release locations into containment, in-containment refueling water storage tank water level, and PXS compartment flooding. The cases considered 100 percent cladding reaction. The behavior of the AP1000 is essentially the same as the AP600 with respect to hydrogen release rates and locations.

Generally, the reactor coolant system is depressurized prior to hydrogen generation. Hydrogen is released to the containment through ADS stage 4 as it is generated in the core. Natural circulation in the containment provides oxygen for burning the hydrogen at the igniters in the loop compartments, close to the source. The loop compartments are shielded from the containment shell and most equipment and instrumentation that would be used to mitigate and monitor the accident.

Igniters located in the IRWST, PXS and CVS compartments, CMT room and at various elevations in the upper compartment provide coverage for hydrogen that may be released through the IRWST, PXS/CVS or in the CMT room.

The igniter system maintains the global uniform hydrogen concentration in the containment at or below lower flammability limits. In the most likely severe accidents, the hydrogen is burned primarily in a favorable location that protects the integrity of the containment and mitigative and monitoring equipment.

An AP1000-specific MAAP4 assessment of igniter effectiveness is presented in Chapter 41 Attachment B.

### 41.6 Early Hydrogen Combustion

Early hydrogen combustion is defined as burning that occurs as the hydrogen is released from the primary system to the containment. During this time, the hydrogen may not be well mixed in the containment and, depending on release locations, may be concentrated in the in-containment refueling water storage tank, PXS compartment or chemical and volume control system room, steam generator rooms, or core makeup tank room. If sufficient oxygen is available, the compartments may become locally detonable. If oxygen is not available in the compartment, the plume may travel to a location where oxygen is available and it can burn as a diffusion flame. The conditional probability of containment failure from diffusion flames and local detonation during the hydrogen release to containment is quantified in this section.

#### 41.6.1 Hydrogen Generation Rates

Qualitative hydrogen generation characteristics can be inferred from the availability of steam and the availability of overheated, unreacted zirconium in the reactor vessel. Based on the insights from the AP600 MAAP4 hydrogen generation and mixing analyses (Reference 41-2), the hydrogen generation can be classified into one of three categories: boiloff generation rate, early-reflood generation rate, and late-reflood generation rate. This

section briefly defines each type of hydrogen release in the AP1000 hydrogen analysis and the conditions under which they occur.

#### 41.6.1.1 Boiloff Hydrogen Generation

Boiloff hydrogen generation occurs as the water inventory in the reactor vessel is depleted by decay heat. The steam generation is limited to the decay heat boiloff in the covered fraction of the core and overheated, unreacted zirconium surface area is limited to the upper regions of the core, which have not relocated below the water line. Based on the AP600 MAAP4 analyses (Reference 41-2) and estimates from the initial core uncovering at Three Mile Island (TMI) Unit 2 (Reference 41-9), the boiloff release hydrogen generation is on the order of 10 kg/min. Core relocation to the lower head may produce a rapid steam generation that produces a brief period of rapid oxidation, but by this time, the core geometry is lost and very little unoxidized zirconium surface area is available for sustained hydrogen production.

Boiloff hydrogen generation occurs in AP1000 cases that are not reflooded. This can only occur in accident class 3BE cases in which the break is located in a PXS compartment that does not flood (direct vessel injection line break), in the accident class 3BL cases in which gravity recirculation fails or accident class 3D cases which are not sufficiently depressurized to allow gravity injection or recirculation.

#### 41.6.1.2 Early-Reflood Hydrogen Generation

Early-reflood hydrogen generation occurs in the event of the reflooding of an overheated, relatively intact core. Quenching of the core provides a large quantity of steam and a large, overheated, unreacted zirconium surface area for oxidation. Shattering of the cladding due to thermal stresses can enhance the oxidation rate. Based on the AP600 MAAP4 analyses (Reference 41-2) and on the first core reflood at TMI-2 (Reference 41-9), the early-reflood hydrogen generation rate is on the order of 100 kg/min. In the early-reflood case, the oxidation of the zirconium is limited only by the degree of core uncovering prior to the reflood. The rate and degree of zirconium oxidation is expected to be significantly greater than the no-reflood case.

Early-reflood hydrogen generation occurs in AP1000 accident class 3BE direct vessel injection line break cases in which the PXS compartment is flooded by in-containment refueling water storage tank water, as well as in all accident class 3BR, 3C, 3D/1D, and 1AP depressurization recovery cases.

#### 41.6.1.3 Late-Reflood Hydrogen Generation

Late-reflood hydrogen generation occurs in the event of a reflood after the core has degraded significantly and possibly after relocation to the lower head. Much of the core geometry is lost and little surface area is available for oxidation, even when steaming from quenching debris is available. Based on the AP600 MAAP4 analyses (Reference 41-2) and the second reflood at TMI-2, this release is very similar to the boiloff hydrogen generation rate.

Late hydrogen generation occurs in AP1000 accident class 3BE cases with steam generator compartment breaks. The reflooding cannot occur until after the water level in the

compartment reaches the elevation of the break. The earliest that late reflooding can occur is approximately 90 minutes after cavity flooding, which is initiated at the time rapid cladding oxidation begins.

#### 41.6.2 Hydrogen Release Locations

The hydrogen release locations in the containment determine the hydrogen mixing in the containment and regions of high hydrogen concentration in the event that the igniters fail. The flow paths from release points in confined compartments to the volumes where oxygen is available determine possible locations where diffusion flames may occur.

##### 41.6.2.1 Automatic Depressurization System Stages 1, 2, and 3

Stages 1, 2 and 3 of the automatic depressurization system relieve the reactor coolant system pressure from the top of the pressurizer to the in-containment refueling water storage tank. The water level in the in-containment refueling water storage tank at the time of the release determines the steam concentration in the tank. If the spargers are covered, the steam is quenched out of the gas flow and the hydrogen is released to the gas space of the tank. If the spargers are not covered, the steam concentration is high and will drive the air out of the tank. If the igniters are available, diffusion flames may be postulated at the in-containment refueling water storage tank vent exits for large sustained hydrogen releases. If igniters are not available, the possibility of hydrogen detonation must be evaluated.

##### 41.6.2.2 Automatic Depressurization System Stage 4

Stage 4 of the automatic depressurization system relieves steam and hydrogen from the hot leg of the reactor coolant system to the loop compartments in the containment. The loop compartments, along with the core makeup tank room and the upper compartment, form the major natural-circulation path in the containment. Oxygen starvation of any potential diffusion flames in the loop compartment is not expected for low-pressure hydrogen releases from automatic depressurization system stage 4. The containment shell is sheltered from flames in the loop compartments by the interior concrete walls and the steam generator doghouses, so diffusion flames at the igniters in the loop compartments are not considered to be a threat to the containment integrity. If igniters are not available, good mixing in the compartment mitigates the threat of detonation for the low-pressure releases. The threat of detonation in the lower compartments is examined for accident classes that are not fully depressurized.

##### 41.6.2.3 Break Location

The reactor coolant system break provides a pathway from the reactor coolant system to one of several compartments in the containment. A failure of a component in the reactor coolant system loop (hot leg or cold leg) will relieve hydrogen to the loop compartment. Hydrogen released from the break to the loop compartment will behave similarly to the hydrogen released from stage 4 automatic depressurization system as described in subsection 41.6.2.2.

A failure of the direct vessel injection line, a dominant severe accident sequence, or a break in the chemical and volume control system piping will relieve hydrogen to one of the small

compartments under the core makeup tank room, the chemical and volume control system room or one of the two PXS compartments. These compartments are dead-ended and communicate with the core makeup tank room through stairway or room vents. The initial blowdown through the break fills the compartment with steam and drives all of the air out of the compartment. After the blowdown and reactor coolant system depressurization, MAAP4 analyses show that countercurrent flow between the compartment and the core makeup tank room slowly replenishes the air.

Each of the dead-ended compartments has a one-way drain to the containment sump in the cavity. The break flow into a dead-ended compartment will not fill the compartment with water, as the flow and flashing from the break can be drained. However, a broken direct vessel injection line in a PXS compartment may allow the in-containment refueling water storage tank to drain into the PXS compartment if the injection valves open in the broken line. The draining of the in-containment refueling water storage tank water into the PXS compartment will fill the PXS compartment and spill water over the curb into the core makeup tank room.

If the igniters are available, hydrogen released to the dead-ended compartments during the core degradation may burn initially, but may become oxygen starved. The plume then rises through the stairway to the core makeup tank room, which is amply supplied with oxygen by the containment natural circulation. A diffusion flame can be postulated in the core makeup tank room at the exit of the compartment. The exterior wall of the core makeup tank room is the steel containment shell below the passive containment cooling system annulus, the lower-level equipment hatch, and the personnel hatch. Many electrical penetrations pass through the core makeup tank room wall to the auxiliary building.

#### 41.6.3 Early Hydrogen Combustion Ignition Sources

For a burn to be initiated, an ignition source is required. If the hydrogen igniters are successful, the probability of an ignition source is 1. In the analysis, all the igniters are assumed to be on and effective from the onset of the hydrogen release and burn the hydrogen as it is released and prevent the buildup of large flammable hydrogen concentrations. Therefore, igniters mitigate the threat to the containment integrity from global deflagration and detonation. If a hydrogen plume can produce a diffusion flame, the igniters provide the ignition source.

If the igniters are not available, a probability of 0.5 is assumed for the existence of a random ignition source during the hydrogen generation. Ignition is assumed to occur at the time that produces the most significant challenge to the containment integrity.

#### 41.7 Diffusion Flame Analysis – CET Node DF

Diffusion flames can be postulated to occur at vents or exits from compartments with a hydrogen source that are dead-ended or not well-mixed. Incombustible gas mixtures that include a high concentration of hydrogen may develop in the compartment. When the plume of hydrogen exits the compartment into a room containing oxygen and an ignition source, burning of the plume as a standing flame at the vent may produce locally high temperatures. If the

release of hydrogen is sustained, the heat load from the burning may threaten equipment, including the containment shell integrity.

The overall geometry of the AP1000 containment is relatively open. Ninety-seven percent of the containment free volume participates in containment natural circulation and is well-mixed. However, the IRWST, PXS and CVS compartments are small, confined rooms that may have a hydrogen source, and thus may be postulated to produce a diffusion flame at vents. This section discusses the conditions that may produce a standing diffusion flame in these locations, and presents the quantification of the containment failure probability given the presence of a sustained diffusion flame at a dead-ended compartment vent.

#### 41.7.1 AP1000 Diffusion Flame Mitigation Strategy

Hydrogen is a byproduct of a severe accident, and hydrogen pathways to the IRWST, PXS and CVS subcompartments cannot be completely ruled out, particularly in the IRWST, to which the effluent of the first stages of the reactor coolant system automatic depressurization system are directed. The other compartments can only have hydrogen releases in the event that a break occurs there, but some of the highest frequency severe accident sequences have breaks in a DVI line, which traverses a PXS compartment. Therefore, the potential for diffusion flames from these subcompartment locations cannot be excluded from the probabilistic risk assessment.

The AP1000 addresses diffusion flames by adopting a defense-in-depth philosophy in the design. In the highest frequency severe accidents, sustained hydrogen release is prevented from occurring in the dead-ended compartments. In sequences where diffusion flames at IRWST or PXS/CVS compartment vents may be postulated, design strategies are initiated to mitigate the threat to the containment integrity by locating hydrogen plumes away from the containment shell.

The first level of defense against the threat to containment integrity from diffusion flames is the prevention of sustained hydrogen releases to dead-ended compartments. The highest frequency severe accident sequences have full reactor coolant system depressurization prior to core damage. Hydrogen is released at low pressure to the containment as it is produced in the core. Stage four of the automatic depressurization system provides a pathway of substantially lower resistance (by approximately one order of magnitude) compared to the maximum break size in the DVI line that relieves to the PXS compartment and to the other three ADS stages that relieve to the IRWST. Additionally, the ADS spargers in the IRWST generally have a 10-ft static head of water above them, which further increases the resistance to flow of hydrogen to the IRWST.

Hydrogen released from ADS stage 4 is relieved to the loop compartments, which are supplied with oxygen by the containment natural circulation and shielded from the containment shell by high concrete walls. Hydrogen is able to burn in the loop compartments without threatening the containment integrity. Therefore, ADS stage 4 provides the first level of defense against diffusion flames.

In the event that ADS stage 4 fails to adequately direct hydrogen away from confined compartments, the compartment vents are designed to preferentially release the hydrogen at locations where it burns away from the containment shell.

The IRWST has four types of vents. Two hooded vacuum breaker vents are located along the containment wall but only allow flow into the IRWST. The vacuum breaker vents are not considered to be potential diffusion flame locations. There are 21 hooded IRWST vents, which are located along the containment wall, 5 pipe vents, which are located along the steam generator doghouse wall, and 6 overflow vents to the refueling canal. The IRWST vents are pictured in Figure 41-1.

The five 1'-10" inner diameter pipe vents are normally closed, and are designed to open at a low pressure differential. After opening, these dampers do not automatically re-close. The flow area of the pipe vents is sufficient to relieve early reflood hydrogen releases of 100 kg/min with a low pressure drop from the IRWST to the upper compartment. The hooded IRWST vents have louvers that are normally closed and open with a sufficiently higher differential pressure than the pipe vents. Once opened, the louvers close again under their own weight when the differential pressure is reduced. The IRWST overflows operate in the same way and with the same differential pressures (DPs) as the hooded vents.

During hydrogen release to the IRWST in which the steam is quenched in the IRWST water, only the pipe vents will open, preferentially releasing the hydrogen through the pipe vents, which are located a minimum of 18-ft away from the containment shell.

ADS steam and hydrogen releases into a saturated IRWST could be sufficient to open all the vents simultaneously. This situation would only occur for very small LOCAs, in which the PRHR HX operates for several hours before ADS is actuated. However, such releases would produce a copious amount of steam that would be released through the vents along with the hydrogen, which would inert the burning at the vents.

Vents from the PXS and CVS compartments to the CMT room are located well away from the containment shell and containment penetrations. Access hatches to the subcompartments that are near the containment shell are covered and secured closed such that they will not open as a result of a pipe break inside the compartment. Therefore, hydrogen releases to the CMT room from the subcompartments are not considered as a threat to the containment integrity.

#### 41.7.2 Node DF Containment Failure Probability Assignment

The question posed at node DF of the containment event tree is "Does the containment not fail from elevated temperature due to diffusion flame in the CMT room and at the IRWST vent?"

Success Criteria: 2 of 4 ADS stage 4 lines open OR all the hooded IRWST vents closed.

Success of ADS stage 4 can be determined from the accident class. Only accident classes 3D/1D and 1AP may have hydrogen generation prior to full RCS depressurization. Therefore, success at node DF is guaranteed for accident classes 3BE, 3BL, 3BR, 3C, and 6. A failure probability of zero is assigned at node DF for these accident classes.

Failures that are considered to result in the hooded vents opening include either of the following:

- Failure of more than one of the 5 pipe vents to open
- Failure of all of the hooded vents to re-close once open

The hooded IRWST vents would only open during a blowdown of the ADS into a saturated IRWST, which should only occur during very small LOCAs. Blowdown into a subcooled IRWST is quenched without significant pressurization of the tank and any steaming could be handled by the pipe vents. Decay heat steaming with the pipe vents open is not sufficient to open the hooded vents.

For the quantification of the failure probability of a vent for accident classes 3D/1D and 1AP, it is assumed that the IRWST hooded vents and overflow vents cycle through one opening and closing. The pressure transient that opens the vents is assumed to occur from either a steam release or hydrogen burning at the igniter at the upward flammability limit until the oxygen is depleted. The failure probability of the IRWST vents closing is estimated based on the  $7 \times 10^{-4}$  probability of gravity damper to fail to operate. For the 21 hooded vents and the first two overflow vents near the containment wall to fail to close, the overall failure probability is  $1.6 \times 10^{-2}$  assuming that all of these vents need to close.

The probability of 2 of the 5 pipe vents not opening is calculated to be  $1.4 \times 10^{-3}$  based on the failure probability of the gravity dampers. The sum of the two probabilities,  $1.7 \times 10^{-2}$ , is the total probability of failure at node DF for accident classes 3D/1D and 1AP.

The failure probabilities at containment event tree node DF are summarized in Table 41-2.

#### 41.8 Early Hydrogen Detonation – Containment Event Tree Node DTE

The likelihood of containment failure due to detonation during the hydrogen release to the containment is evaluated at node DTE on the containment event tree. Hydrogen igniter failure is an initial condition of this analysis.

Hydrogen detonation can be initiated from a high-energy ignition source or by deflagration-to-detonation transition during flame acceleration. Potential ignition sources in containment are too small to directly initiate a detonation. Therefore, the occurrence of detonation is related to the potential for deflagration-to-detonation transition in the AP600 containment analysis.

An analysis of the potential for early deflagration-to-detonation transition is presented in this section. The results are presented as a probability that is assigned to node DTE on the containment event tree for each of the accident classes. The methodology of Sherman and Berman (Reference 41-6) is used to evaluate the likelihood of deflagration-to-detonation transition. The analysis considers the hydrogen release rates to the containment, core reflooding, the containment release locations, and in-containment refueling water storage tank and PXS compartment water levels to determine the probabilities. The probabilities of detonation as calculated for AP600 are used to quantify detonation probability for AP1000 decomposition event trees (Figures 41-2 through 41-7).

##### 41.8.1 Containment Success Criteria at Node DTE

Detonation produces sonic to supersonic pressure fronts that result in impulsive loading on containment structural members. The loading is not spatially uniform and the peak can be higher than the adiabatic, isochoric, complete combustion pressure. No specific impulsive

loading analysis is presented for the AP1000 containment shell or internal structures other than the reactor cavity wall, which is under water and not subjected to hydrogen burning.

Containment failure is assumed in the event of a detonation in the containment.

#### **41.8.2 Early Hydrogen Detonation Decomposition Event Tree**

To quantify the probability of detonation for each accident class, a decomposition event tree is used to identify the initial conditions for the detonation in each accident class. The decomposition event tree structure and quantification for each accident class is presented in Figures 41-2 through 41-7. The nodal questions on the decomposition event tree are presented and discussed below.

##### **41.8.2.1 Node N1 – Is the hydrogen not ignited?**

Success is credited if the hydrogen is not ignited. The probability of random hydrogen ignition at the worst possible time to create DDT in the early time frame is assumed to be 0.5 for all cases without igniters.

##### **41.8.2.2 Node N2 – What is the location of the break?**

Success is credited at node N2 if the reactor coolant system break occurs outside the dead-ended compartments or if there is no break. The dominant sequences in each accident class (see Chapter 43) determine the split fractions at this node. Only direct vessel injection line breaks (safety injection line breaks) can occur in the PXS compartments, and direct vessel injection line breaks are always pessimistically assumed to be in the PXS compartment for this analysis. Chemical and volume control system breaks make up approximately 7 percent of the intermediate break initiating event. Therefore, the split fraction at the second branch of node N2 is the sum of the probabilities of the sequences initiated by direct vessel injection line break in each accident class. The split fraction at the third branch of node N2 is 7 percent of the sum of intermediate loss-of-coolant accident probability in each accident class.

##### **41.8.2.3 Node N3 – Does containment remain intact?**

Success is defined as the mixture not being flammable, detonable, or if deflagration-to-detonation transition does not occur during the hydrogen relocation. Success is credited at node N3 if one or more of the following conditions is true: the hydrogen concentration is less than 10 percent, the oxygen concentration is less than 5 percent, or detonation does not occur as assessed using the Sherman-Berman (S-B) methodology (Reference 41-6) as described in the AP600 PRA (Reference 41-2) The conditional probabilities of DDT as calculated in the AP600 PRA (Reference 41-2) are used at Node N3.

##### **41.8.2.4 Early Detonation Containment Event Tree Probability Assignment**

The failure probabilities for containment event tree node DTE are calculated in Figures 41-2 through 41-7 for each accident class and are summarized in Table 41-2.

### 41.9 Deflagration in Time Frame 3

The purpose of this section is to document the conditional probability of containment failure for top event DFG on the containment event tree. Node DFG is in time frame 3 on the AP600 containment event tree when the hydrogen release to containment is mixed with the atmosphere. Operation of the hydrogen igniters burns the hydrogen as it is released to the containment, so success of the igniters guarantees success at node DFG.

#### 41.9.1 Containment Success Criterion at Node DFL

In a hydrogen deflagration, the combustion is relatively slow (on the order of several seconds), the containment pressure is spatially uniform and bounded by the adiabatic, isochoric (constant volume), complete combustion pressure. The loading on the containment is quasi-static or equal to the loading from a constant pressure of equal magnitude. For each accident class, probability distributions of the fraction of cladding reacted (which dictates the in-vessel hydrogen generation) and the containment pressure prior to a burn are developed. The probability distributions are combined to calculate a probability distribution of the peak adiabatic, isochoric, complete combustion pressure and temperature. The peak adiabatic, isochoric, complete combustion pressure and temperature distributions are compared to a containment failure criterion to determine the conditional probability of containment failure for each accident class.

The development of a conditional containment failure probability distribution as a function of pressure, often referred to as a containment fragility curve, for the AP1000 containment is presented in Chapter 42. This probability distribution is used as the containment failure criterion for the deflagration analysis. The curve is calculated assuming an upper-bound containment shell temperature of 400°F (480K).

The containment shell temperature during the burn should not exceed 400°F to properly apply the conditional failure distribution. The following calculation presents the bounding containment shell temperature as a function of the mass of hydrogen burned assuming:

- All of the heat from the hydrogen burning is adiabatically transferred to the containment shell above the operating deck.
- The initial temperature of the containment shell is 212°F (373K).

The maximum containment temperature is found with equation 41-1.

$$\Delta T = \frac{M_{H2} q_{H2}}{M_{st} C_{vst}} \quad (41-1)$$

where:

- $\Delta T$  = temperature rise in steel shell
- $M_{st}$  = mass of steel shell above operating deck = 2,303,020 kg (5,077,200 lbm)
- $C_{vst}$  = specific heat of steel = 448 J/kg/K (0.107 btu/lbm/F)

$$m_{H_2} = \text{maximum hydrogen mass} = 930 \text{ kg (118\% of active cladding)}$$

$$q_{H_2} = \text{heat of combustion} = 121. \text{ MJ/kg-H}_2 \text{ (52,000 btu/lbm-H}_2\text{)}$$

The bounding peak temperature of 408°F is approximately 400°F. Given that the heatup is calculated very conservatively, the containment failure probability can be based on the conditional containment failure probability distribution for hydrogen analyses.

#### 41.9.2 AICC Peak Pressure

To calculate the adiabatic, isochoric, complete combustion peak pressure, first the initial conditions in the containment prior to the accident need to be established to find the initial moles of dry air and steam in the containment. The dry-air moles are found by the ideal gas law. The initial containment temperature is assumed to be 70°F (295K).

$$n_{\text{air}} = \frac{PV}{RT} \quad (41-2)$$

where:

$$n_{\text{air}} = \text{kg-moles of air}$$

$$P = \text{initial containment pressure} = 1.01\text{E}5 \text{ Pa} = 14.7 \text{ psia}$$

$$T = \text{initial containment temperature (assumed to be } 295\text{K} = 70^\circ\text{F)}$$

$$V = \text{containment volume} = 58,622.4 \text{ m}^3 = 2.07 \times 10^6 \text{ ft}^3$$

$$R = \text{universal gas constant} = 8314 \text{ J/kg-mole/K}$$

The mass of hydrogen is an input value that provides the moles of hydrogen ( $n_{H_2}$ ), and the dry-air hydrogen mole fraction ( $N_{F_{H_2}}$ ) is found by the equation:

$$N_{F_{H_2}} = \frac{n_{H_2}}{n_{\text{air}} + n_{H_2}} \quad (41-3)$$

The total pre-burn pressure ( $P_0$ ) and the relative humidity ( $N$ ) are input values that provide the partial pressure of steam. A guess at the steam partial pressure ( $PP_{st}$ ) is made and the saturation temperature ( $T_{sat}$ ) is found from the saturation pressure ( $P_{sat}$ ):

$$P_{sat} = \frac{PP_{st}}{\phi} \quad (41-4)$$

The non-condensable gas partial pressure ( $PP_{NC}$ ) is found by the ideal gas law:

$$PP_{NC} = \frac{(n_{\text{air}} + n_{H_2})R T_{sat}}{V} \quad (41-5)$$

The total pressure ( $PP_{st} + PP_{nc}$ ) is compared to  $P_0$  and iterated to find the initial partial pressure of the steam.

Once the initial conditions are known, the adiabatic, isochoric, complete combustion temperature is found by the energy balance before and after the burn (assuming the burn is instantaneous):

$$\sum_{i=1}^4 (m_i C_{vi})_0 * T_0 + Q_b = \sum_{i=1}^4 (m_i C_{vi})_f * T_f \quad (41-6)$$

where:

- i = N<sub>2</sub>, O<sub>2</sub>, H<sub>2</sub>, H<sub>2</sub>O
- m<sub>i</sub> = mass of i<sup>th</sup> component
- C<sub>vi</sub> = constant volume specific heat of i<sup>th</sup> component
- Q<sub>b</sub> = heat of combustion = m<sub>H2</sub> \* 121 MJ/kg
- T<sub>0</sub> = initial temperature
- T<sub>f</sub> = AICC temperature

The adiabatic, isochoric, complete combustion pressure is found from the adiabatic, isochoric, complete combustion temperature (T<sub>f</sub>) and the post-burn number of moles in the containment (n<sub>f</sub>) using the ideal gas law:

$$P_f = \frac{n_f R T_f}{V} \quad (41-7)$$

For base analyses, the relative humidity is assumed to be 100 percent. The sensitivity to this assumption is explored in the deflagration analyses results.

### 41.9.3 Conditional Containment Failure Probability from Deflagration

This section describes the calculation of the failure probabilities assigned to node DFL of the containment event tree for each accident class. The probabilities of node DFL may be contingent on damaged core reflooding, which is the upstream outcome of node RFL. Therefore, for appropriate accident classes, two failure probabilities for node DFL will be calculated, one for success at node RFL and one for failure at node RFL.

Global deflagration can occur only if the containment hydrogen igniters are failed (containment event tree node IG). Global deflagration is assumed to occur after core damage and hydrogen generation are completed and the gases are mixed (intermediate time frame). It is conservatively assumed that the conditional probability of random ignition and containment threat from global combustion prior to 24 hours (intermediate time frame) is 1. Subsequent combustion is not considered since there is no additional hydrogen generation. In base-case analyses, the lower flammability limit for global combustion is assumed to be 6 percent hydrogen concentration with a steam-inerting limit of 55 percent.

The hydrogen generation probability distribution and the pre-burn pressure distribution are combined to calculate a probability distribution of the peak adiabatic, isochoric, complete combustion pressure. This final pressure distribution is combined with the conditional containment failure probability distribution (see Chapter 42) to calculate the probability of containment failure at node DFL.

The failure probabilities assigned to node DFL on the AP1000 containment event tree are summarized in Table 41-2. In each case, as described below, the containment failure probability from deflagration is negligible and assigned a value of zero.

#### 41.9.3.1 No-Reflood Case

The probability of containment failure from deflagration in the no-reflood cases is quantified in this section. The no-reflood cases are accident class 3BE direct vessel injection line break with no PXS compartment flooding, all accident class 3BL, 3D/1D, and 6 cases.

##### 41.9.3.1.1 Hydrogen Generation Probability Distribution

The hydrogen generation probability distributions are based on insights of hydrogen generation from the AP600 MAAP4 analyses (Reference 41-2) and engineering judgment based on the accident sequence progression and comparisons to expert opinion (Reference 41-11), as applicable.

The AP600 no-reflood MAAP4 3BE results (Reference 41-2) show zirconium oxidation fractions between approximately 50 and 60 percent of the active cladding. Because most of the oxidation occurs in a relatively intact core geometry, this is considered to be an upper bound of the best-estimate range for the cladding oxidation with no reflood. Fractions up to 75-percent cladding reaction are considered to be possible, but not likely, so 60 to 75 percent is assigned a probability of 0.1. Above 75 percent is considered highly unlikely and is assigned a probability of 0.01 up to 100-percent oxidation fraction. The hydrogen generation probability distribution is presented in Figure 41-8.

##### 41.9.3.1.2 Pre-Burn Containment Pressure Probability Distribution

The pre-burn containment pressure probability distributions are based on insights regarding containment pressure from the AP600 MAAP4 analyses (Reference 41-2) and engineering judgment. By assumption, all of the cases have passive containment cooling system water cooling the containment shell. MAAP4 analyses reach equilibrium pressures of approximately 26 to 30 psia (1.8 to 2.0 bar), while WGOTHIC design basis analysis with conservative thermal-hydraulic assumptions predicts an equilibrium pressure of approximately 30 psia (2 bar). The pre-burn pressure distribution captures the containment pressure fluctuations after the hydrogen generation is completed.

The MAAP4 non-reflooded cases have a post-hydrogen-generation (intermediate time frame) equilibrium pressure ranging from 26 psia to 30 psia (1.8 bar to 2.0 bar). These pressures are considered to be the lower and upper bounds of the pre-burn pressure best-estimate range. Following the core melt and hydrogen generation, there is a limited period with pressures as low as 22 psia (1.5 bar). The range from this minimum pressure to the best-estimate lower bound is assigned a probability of 0.4. In time frame 3 with no reflood, there are no rapid steaming events to pressurize the containment above the equilibrium pressure. A small probability of 0.01 is assigned from the upper bound of the best-estimate range to the steam-inerting pressure (3.0 bar) to account for possible degradation of the passive containment cooling system heat removal and other uncertainties. The non-reflooded, pre-burn containment pressure probability distribution is presented in Figure 41-9.

#### 41.9.3.1.3 No-Reflood Case Deflagration Containment Failure Probability

The node DFL containment failure probability calculation results for accident class 3BE, non-reflooded case, are presented in Figure 41-10. The “double-hump” in the probability distribution occurs because cases that are not flammable are assigned a peak pressure equal to the initial pressure. Therefore, the area under the “hump” at the lower pressures estimates the probability that the containment is not globally flammable (0.80), while the area under the “hump” at the higher pressures estimates the probability that the containment is globally flammable (0.20). The containment failure probability calculated from the containment fragility curve is less than  $1 \times 10^{-4}$ . This is considered to be negligible and a containment failure probability of zero is assigned to containment failure from deflagration for non-reflooded cases.

#### 41.9.3.2 Early-Reflood Case

The probability of containment failure from deflagration in the early-reflood cases is quantified in this section. Early-reflood cases comprise accident class 3BE direct vessel injection line breaks with PXS compartment flooding, and all accident class 3BR, 3C, and 1AP cases.

##### 41.9.3.2.1 Hydrogen Generation Probability Distribution

The hydrogen generation probability distributions are based on sequence progression and hydrogen generation insights from AP600 MAAP4 analyses and engineering judgment based on the accident sequence progression, comparisons to Reference 41-11, and expert opinion, as applicable.

Early reflooding is defined as the reflooding of an overheated, relatively intact core. Significant quantities of unreacted zirconium surface area and steam are available for oxidation. The overheated area may be limited by the degree of core uncover at the time of the reflooding. Since early-reflood cases reflood the core at approximately the same time that hydrogen generation is beginning, the boiloff hydrogen generation before the reflood is considered insignificant compared to the reflood hydrogen generation. The early-reflood AP600 MAAP4 3BE results show active cladding oxidation fractions between approximately 60 and 100 percent of the active cladding. Because of the considerable uncertainty in predicting oxidation for this reflood event, the hydrogen generation probability distribution is estimated conservatively higher. The best-estimate range is assigned from a lower bound of 75-percent reaction to 100 percent. Fractions up to 113-percent cladding reaction (all the zirconium in the core) are considered possible, but not likely, so 100 to 113 percent is assigned a probability of 0.1. Below 75 percent is considered to be highly unlikely and is assigned a probability of 0.01. The hydrogen generation probability distribution developed for the early-reflood case is presented in Figure 41-11.

##### 41.9.3.2.2 Pre-Burn Containment Pressure Probability Distribution

The pre-burn containment pressure probability distributions are based on accident progression insights from the AP600 MAAP4 analyses. By assumption, all of the cases have passive containment cooling system water cooling the containment shell. For the

early-reflood cases, containment pressure is elevated at the time of the rapid oxidation due to the quenching of the core by the reflood. The containment pressures reach a peak of 35 psia (2.4 bar) during the hydrogen generation before falling to the equilibrium pressures of approximately 26 to 30 psia (1.8 to 2.0 bar). The pre-burn pressure distribution captures the containment pressure fluctuations after the hydrogen generation is completed.

The equilibrium pressures are considered to be the lower and upper bounds of the pre-burn pressure best-estimate range. During the reflood and hydrogen generation, there is a limited period with pressures as high as 35 psia (2.4 bar). The range from the best-estimate upper bound to a peak pressure of 2.5 bar is assigned a probability of 0.4. The range from the peak pressure to the steam-inerting limit of 3.0 bar is assigned a probability of 0.1 to account for passive containment cooling system degradation and other uncertainties. The pre-burn containment pressure probability distribution developed for the early-reflood case is presented in Figure 41-12.

#### 41.9.3.2.3 Early-Reflood Case Deflagration Containment Failure Probability

The node DFL containment failure probability calculation results for the early-reflood case are presented in Figure 41-13. The reflood cases are 95 percent flammable as almost all of the peak pressure probability is distributed around elevated pressures. The containment failure probability calculated from the containment fragility curve is negligible and a containment failure probability of zero is assigned for early-reflood deflagration.

#### 41.9.3.3 Late-Reflood Case

The probability of containment failure from deflagration in the late-reflood cases is quantified in this section. Late-reflood cases are accident class 3BE loop compartment breaks.

##### 41.9.3.3.1 Hydrogen Generation Probability Distribution

The hydrogen generation probability distribution is based on accident progression and hydrogen generation insights from the MAAP4 analyses and engineering judgment based on the accident sequence progression, comparisons to Reference 41-11, and expert opinion, as applicable.

Late reflooding is defined as the reflooding of a highly degraded core that has none of its intact geometry remaining. As there is little remaining unreacted cladding surface area, insignificant additional oxidation is expected over the boiloff hydrogen generation, which occurs prior to the reflood. The no-reflood hydrogen probability distribution is the same as that used for the late-reflood case (Figure 41-14).

##### 41.9.3.3.2 Pre-Burn Containment Pressure Probability Distribution

The pre-burn containment pressure probability distributions are based on insights from the AP600 MAAP4 analyses (Reference 41-2). By assumption, all of the MAAP4 cases have passive containment cooling system water cooling the containment shell. Analyses show that for the late-reflood cases, containment pressure is low, similar to the no-reflood case pressure, at the time of the oxidation. When the late reflood occurs, molten core debris is

quenched and the containment pressures reach a peak of 35 psia (2.4 bar) before falling to the equilibrium pressure of approximately 26 to 30 psia (1.8 to 2.0 bar). The pre-burn pressure distribution captures the containment pressure fluctuations after the hydrogen generation is completed.

The equilibrium pressures are considered to be the lower and upper bounds of the pre-burn pressure best-estimate range. After the hydrogen generation and before reflood, the pressure is below the equilibrium pressure. During the reflood, there is a limited period with pressures as high as 35 psia (2.4 bar). The range below equilibrium from 22 to 26 psia (1.5 to 1.8 bar) is assigned a probability of 0.1. The range from the best-estimate upper bound to a peak pressure of 37 psia (2.5 bar) is assigned a probability of 0.3. The range from the peak pressure to the steam-inerting pressure of 3.0 bar is assigned probability of 0.1 to account for passive containment cooling system degradation and other uncertainties. The pre-burn containment pressure probability distribution developed for the late-reflood case is presented in Figure 41-15.

#### 41.9.3.3.3 Late-Reflood Case Deflagration Containment Failure Probability

The containment failure probability calculation results for the late-reflood case are presented in Figure 41-16. The probability that the containment is globally flammable is approximately 0.2 based on the “double-hump” peak pressure distribution. The containment failure probability calculated from the containment fragility curve is less than  $1 \times 10^{-4}$ . This is negligible and a containment failure probability of zero is assigned for deflagration in the late-reflood cases.

### 41.10 Detonation in Intermediate Time Frame

This section documents the calculation of the failure probability split fractions assigned to node DTI on the containment event tree. Node DTI is in the intermediate time frame (prior to 24 hours after core damage) when the hydrogen is mixed in the containment atmosphere. The analysis assumes the failure of the igniter system.

#### 41.10.1 Containment Success Criterion at Node DTI

Detonation produces sonic to supersonic pressure fronts that result in impulsive loading on containment structural members. The loading is not spatially uniform and the peak can be higher than the adiabatic, isochoric, complete combustion pressure. No specific impulsive loading analysis is presented for the AP600 containment shell or internal structures other than the reactor cavity wall, which is under water in this case and not subjected to hydrogen burning. The probability values calculated for AP600 (Reference 41-2) are used to quantify the AP1000 decomposition event tree Node N3.

#### 41.10.2 Mixing and Stratification

Based on the large-scale passive containment cooling system tests (Reference 41-12) and HDR test E11.4 (Reference 41-13) for hydrogen releases at the bottom of the containment, the containment hydrogen and air are expected to be well mixed (within several percent) above and below the operating deck after the hydrogen release to the containment is

completed and the containment reaches steady-state conditions. However, the results of the large-scale passive containment cooling system test suggest that the steam concentration in compartments below the operating deck that do not have a steam source may be significantly lower than the steam concentration in the upper compartment. To conservatively bound this situation, the mixture reactivity in the lower compartments that do not have a steam source is estimated assuming dry air (Reference 41-2). Compartments that contain a steam source or are above the operating deck are assumed to have the well mixed concentrations including the steam.

The assumption of dry air below the operating deck assumes a conservative natural-circulation pattern in the containment that maximizes the potential for deflagration-to-detonation transition. Steam from the removal of decay heat through the break or through the reactor vessel wall rises through the steam generator rooms mixing with the dry air and hydrogen, past the steam generators to the upper compartment. The cool, dense air flowing from the passive containment cooling system shell in the upper compartment falls along the wall to the core makeup tank rooms, through the tunnel to the steam generator compartments where it mixes with the steam to complete the cycle. This natural-circulation pattern is conservative since it provides a more reactive dry air/hydrogen mixture in a compartment that has a geometry that promotes flame acceleration (the core makeup tank room).

#### 41.10.3 Quantification of DTI Failure Probabilities

The DTT analysis uses the same decomposition event tree structure as the early deflagration-to-detonation analysis, but the probability of a random ignition source is assumed to be 1. The conditional probabilities of DDT applied at Node N3 are taken from the AP600 PRA (Reference 41-2). The decomposition event tree quantification for each accident class is presented in Figures 41-17 through 41-22. The probabilities applied to node DTI of the containment event tree are summarized in Table 41-2.

#### 41.11 Safety Margin Basis Containment Performance Requirement

An analysis is performed to quantify the margin in the containment design to withstand the peak pressure from a hydrogen burn. This analysis investigates the ability of the containment to satisfy the structural requirements of 10 CFR 50.34(f) when subjected to the pressure and temperature loading from a loss-of-coolant accident, 100-percent active cladding reaction, and complete combustion of the hydrogen.

A conservative adiabatic, isochoric, complete combustion hydrogen burn analysis with the defined boundary conditions is presented in Table 41-4. The analysis is performed with an initial hydrogen mass of 788 kg (100-percent active cladding reaction) at an initial pressure of 46 psia (3.2 bar). The steam concentration in the containment is 55 percent and the hydrogen concentration is 6.8 percent. Adiabatic, isochoric, complete combustion is assumed. The peak containment pressure is 90 psig (7.2 bar).

As stated in subsection 3.8.2.4.2.7 of the AP1000 DCD, the American Society of Mechanical Engineers (ASME) service level C stress intensity limits is 91 psig. Therefore, AP1000 meets the requirement.

### 41.12 Summary

The conditional failure probability of the containment from hydrogen combustion is quantified. The failure probabilities assigned to the containment event tree node DF, DTE, DFL, and DTE are summarized in Table 41-2. The major insights of the analysis are as follows:

- No containment failure from hydrogen is predicted if the hydrogen igniters are operational.
- Operation of the stage 4 automatic depressurization system valves releases much of the hydrogen generated in the reactor coolant system to the steam generator rooms where it can be well mixed in the containment to mitigate the threat of diffusion flames from hydrogen released through the in-containment refueling water storage tank.
- The threat of detonation is predominantly due to hydrogen releases to the PXS compartments below the 107' 2" containment elevation (direct vessel injection line breaks). The compartment is a confined region with little mixing. Equipment and grating are present to promote turbulence. A break in the compartment induces a high-temperature environment creating good conditions for potential deflagration-to-detonation transition.
- The probability of containment failure due to diffusion flames is very small.
- No containment failure is predicted from deflagration.

Analyses are performed to meet the requirements of 10 CFR 50.34(f). The igniter system maintains the global uniform hydrogen concentration in the containment at or below lower flammability limits. If the stage 4 automatic depressurization system is available, the hydrogen is well mixed in the containment and no excessive concentrations are predicted in the in-containment refueling water storage tank or PXS compartments. If the stage 4 automatic depressurization system is failed, hydrogen in the in-containment refueling water storage tank and possibly the PXS compartments can reach high concentrations. However, the mixtures are oxygen starved and are not flammable or detonable. The safety margin basis containment performance requirement is met as the loss-of-coolant accident plus 100-percent active cladding reaction hydrogen burn peak pressure is 74 psig, providing greater than 15 psi margin to service level C at 400°F.

### 41.13 References

- 41-1 Tieszen, S. R., et al., "Hydrogen Distribution and Combustion," in *Ex-Vessel Severe Accident Review for the Heavy Water New Production Reactor* (ed. by K. D. Bergeron), NPRW-SA90-3, Sandia National Laboratories, 1993.
- 41-2 AP600 PRA Report, GW-GL-022, August 1998.
- 41-3 Ratzel, A. C., "Data Analysis for the Nevada Test Site (NTS) Premixed Combustion Tests," NUREG/CR-4138, SAND85-0135, Sandia National Laboratories, 1985.

- 41-4 Hertzber, Martin, "Flammability Limits and Pressure Development in Hydrogen-Air Mixtures," *Proc. Workshop on the Impact of Hydrogen on Water Reactor Safety*, Volume III, NUREG/CR-2017, SAND81-0661, Sandia National Laboratories, 1981.
- 41-5 Sherman, M. P., et al., "Deliberate Ignition and Water Fogs as H<sub>2</sub> Control Measures for Sequoyah," *Proc. Workshop on the Impact of Hydrogen on Water Reactor Safety*, Volume IV, NUREG/CR-2017, SAND81-0661, Sandia National Laboratories, 1981.
- 41-6 Sherman, M. P., and Berman, M., "The Possibility of Local Detonation During Degraded Core Accidents in the Bellefonte Nuclear Plant," NUREG/CR-4803, SAND86-1180, Sandia National Laboratories, 1987.
- 41-7 Sherman, M. P., et al., "FLAME Facility," NUREG/CR-5275, SAND85-1264, Sandia National Laboratories, 1989.
- 41-8 MAAP4 User's Manual, EPRI, 1994.
- 41-9 Henrie, J. O., "Timing of the TMI-2 Core Degradation as Determined by Forensic Engineering," *Nuclear Technology*, Vol. 87, p. 857, 1989.
- 41-10 "Assessment of the Potential Impact of Diffusion Flames on the AP600 Containment Wall and Penetrations," FAI/96-31, Fauske and Associates, Inc., July 1996.
- 41-11 "Evaluation of Severe Accident Risks: Quantification of Major Input Parameters, Expert Opinion Elicitation on In-Vessel Issues," NUREG/CR-4551, Volume 2, Part 1, December 1990.
- 41-12 "Final Data Report for PCS Large-Scale Tests, Phase 2 and Phase 3," WCAP-14135, Rev. 0, July 1994.
- 41-13 Wolf, L., Cron, T., "Detailed Assessment of the HDR-Hydrogen Mixing Experiments E11," International Conference on New Trends in Nuclear Systems Thermodynamics, Pisa, Italy, May 30-June 2, 1994.

Table 41-1

<b>CONTAINMENT EVENT TREE IG NODAL FAILURE PROBABILITY</b>	
<b>Accident Class</b>	<b>Failure Probability</b>
All	VLH

Table 41-2

<b>CONTAINMENT EVENT TREE NODAL FAILURE PROBABILITIES</b>				
<b>Accident Class</b>	<b>Node DF</b>	<b>Node DTE</b>	<b>Node DFL</b>	<b>Node DTI</b>
3BE RFL Success	0.0	.254	0.0	0.124
3BE RFL Failure	0.0	.117	0.0	1.3E-3
3BL	0.0	.005	0.0	1.3E-3
3BR	0.0	.19	0.0	1.30E-01
3C	0.0	1.90E-01	0.0	1.30E-01
3D/1D	1.7E-2	.115	0.0	1.30E-03
1AP	1.7E-2	.054	0.0	1.30E-01
1A	0.0	0.0	0.0	0.0
3A	0.0	0.0	0.0	0.0
6	0.0	.005	0.0	1.30E-03

Accident Class	Break Location	PXS Compartment Flood	Core Reflood	Stage 4 ADS	ADS 1-3 IRWST Sparger Covered
3BE	PXS Compartment	No	None	Yes	Yes
	PXS Compartment	Yes	Early		
	SG Room	–	Late		
3BL	SG Room	–	None	Yes	No
3BR	SG Room	–	Early	Yes	Yes
3C	SG Room	–	Early	Yes	Yes
3D/1D	PXS Compartment	Yes	Early	No	Yes
1AP (Manual ADS)	None	–	Early	No	Yes
1A (Manual ADS)	None	–	Before H <sub>2</sub> Generation	No H <sub>2</sub> Released	No H <sub>2</sub> Release
3A	None	–	Never Uncovered	No ADS	No ADS
6	SG Tube	–	Early	Yes	Yes

Table 41-4

**SAFETY MARGIN BASIS CONTAINMENT PERFORMANCE REQUIREMENT**

ADIABATIC HYDROGEN BURN CALCULATION  
USING TEMP-DEPEND NC GAS PROPERTIES

CONTAINMENT VOLUME= 5.8622E+04 M3  
HYDROGEN MASS= 7.8800E+02 KG (100% Active Clad Oxidation)

AICC HYDROGEN BURN CALCULATION WITH INITIAL CONTAINMENT PRESSURE  
CONTAINMENT INITIAL CONDITIONS :

AIR PRESSURE : 1.2188E+05 PA  
STEAM PRESSURE : 1.7137E+05 PA  
HYDROGEN PRESSURE : 2.1712E+04 PA

PREBURN PRESSURE : 3.1496E+05 PA  
PREBURN TEMPERATURE : 3.8856E+02 K

STEAM MOLE FRACTION : 0.5498  
HYDROGEN MOLE FRACTION : 0.0681  
OXYGEN MOLE FRACTION : 0.0764

PRE AND POST BURN GAS COMPOSITION

		MASS (KG)	SPEC HT (J/KG-K)
NITROGEN	INITIAL	: 4.7064E+04	7.4503E+02
	FINAL	: 4.7064E+04	8.5140E+02
CARBON DIOXIDE	INITIAL	: 3.8925E+03	7.3981E+02
	FINAL	: 3.8925E+03	1.0112E+03
STEAM	INITIAL	: 5.7279E+04	1.4329E+03
	FINAL	: 6.4371E+04	1.7628E+03
OXYGEN	INITIAL	: 1.4155E+04	6.7648E+02
	FINAL	: 7.8506E+03	8.1068E+02
HYDROGEN	INITIAL	: 7.8800E+02	1.0444E+04
	FINAL	: 0.0000E+00	

HYDROGEN BURN AT INITIAL PRESSURE= 3.15 BAR

H2 V/O CONCENTRATION 6.8%

CONTAINMENT PEAK PRESSURE 7.24 BAR (90.3 psig)  
CONTAINMENT PEAK TEMPERATURE 913.6 K

PRESSURE RISE 4.09 BAR

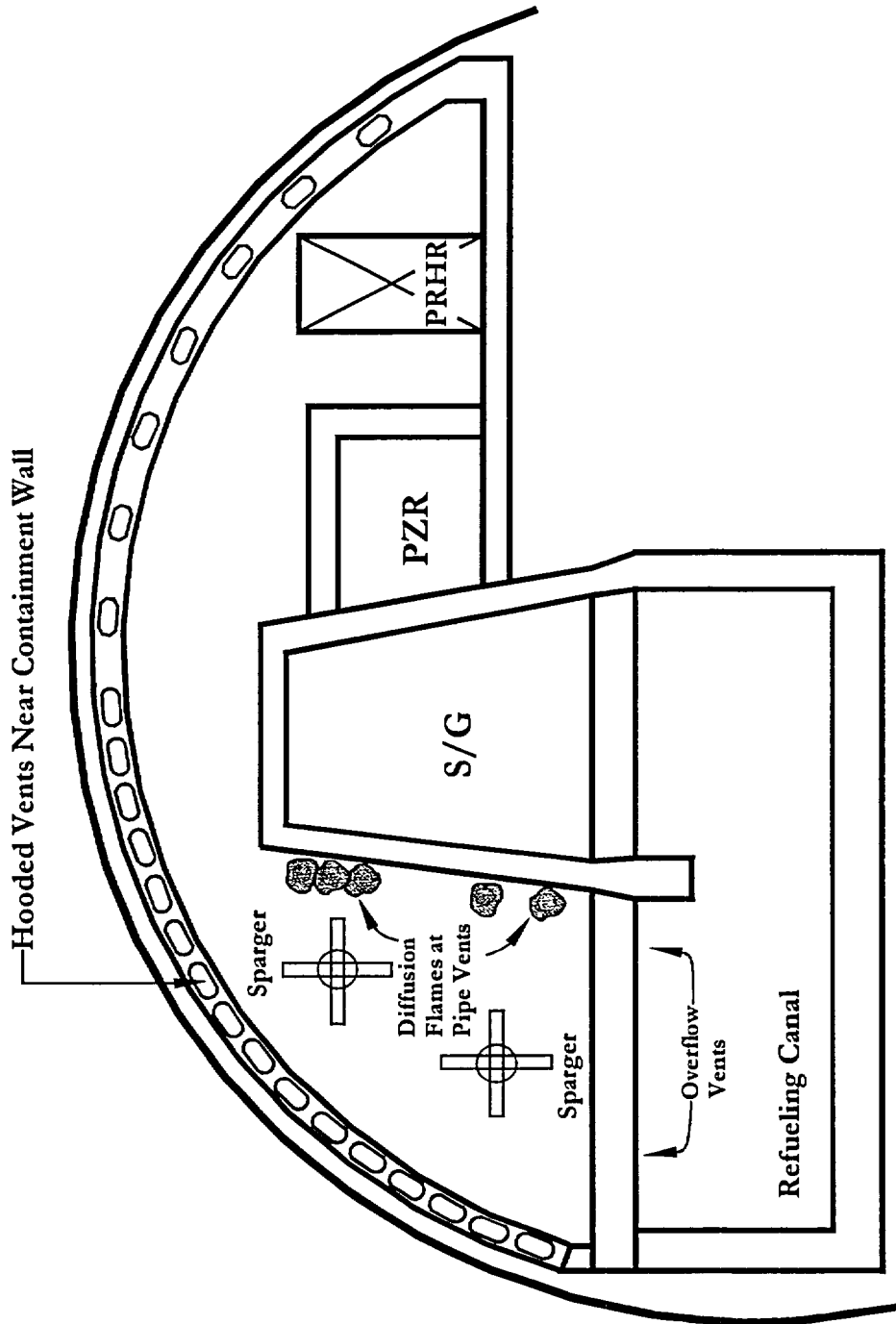


Figure 41-1

IRWST Hydrogen Venting

Node N1 Ignition Source		Node N2 Break Compartment		Node N3 DDT				
0.500	No Ignition					1	No ign	0.500
0.500	Ignition	0.047	Loop Compt	0.692	No DDT	2	No DDT	0.016
				0.308	DDT	3	DDT	0.007
		0.953	PXS	0.482	No DDT	4	No DDT	0.230
				0.518	DDT	5	DDT	0.247
		0.000	CVS	0.457	No DDT	6	No DDT	0.000
				0.543	DDT	7	DDT	0.000
							Total	1.000

	End State	Probability
	No Ign	0.500
	No DDT	0.246
CET Node DTE Failure Probability =	DDT	0.254

Figure 41-2

Accident Class 3BE Early Detonation Decomposition Event Tree – Given RFL Success

Node N1 Ignition Source		Node N2 Break Compartment		Node N3 DDT							
0.500	No Ignition					1	No ign	0.500			
0.500	Ignition	0.342	Loop Compt	0.998	No DDT	2	No DDT	0.171			
					DDT	3	DDT	0.000			
					0.649	PXS	0.648	No DDT	4	No DDT	0.210
					0.352	DDT	5	DDT	0.114		
					0.009	CVS	0.457	No DDT	6	No DDT	0.002
								DDT	7	DDT	0.002

	End State	Probability
	No Ign	0.500
	No DDT	0.383
CET Node DTE Failure Probability =	DDT	0.117

Figure 41-3

Accident Class 3BE Early Detonation Decomposition Event Tree – Given RFL Failure

Node N1 Ignition Source		Node N2 Break Compartment		Node N3 DDT				
0.500	No Ignition					1	No ign	0.500
0.500	Ignition	0.827	Loop Compt	0.998	No DDT	2	No DDT	0.413
				0.002	DDT	3	DDT	0.001
		0.149	PXS	0.998	No DDT	4	No DDT	0.074
				0.002	DDT	5	DDT	0.000
		0.024	CVS	0.659	No DDT	6	No DDT	0.008
				0.341	DDT	7	DDT	0.004
							Total	1.000

	End State	Probability
	No Ign	0.500
	No DDT	0.495
CET Node DTE Failure Probability =	DDT	0.005

Figure 41-4

Accident Class 3BL Early Detonation Decomposition Event Tree

Node N1 Ignition Source		Node N2 Break Compartment		Node N3 DDT				
0.500	No Ignition					1	No ign	0.500
0.500	Ignition	1.000	Loop Compt	0.620	No DDT	2	No DDT	0.310
				0.380	DDT	3	DDT	0.190
		0.000	PXS	0.000	No DDT	4	No DDT	0.000
				1.000	DDT	5	DDT	0.000
		0.000	CVS	0.000	No DDT	6	No DDT	0.000
				1.000	DDT	7	DDT	0.000
							Total	1.000

End State	Probability
No Ign	0.500
No DDT	0.310
CET Node DTE Failure Probability = DDT	0.190

Figure 41-5

Accident Class 3C/3BR Early Detonation Decomposition Event Tree

Node N1 Ignition Source		Node N2 Break Compartment		Node N3 DDT				
0.500	No Ignition					1	No ign	0.500
0.500	Ignition	0.610	Loop Compt	0.748	No DDT	2	No DDT	0.228
				0.252	DDT	3	DDT	0.077
		0.384	PXS	0.806	No DDT	4	No DDT	0.155
				0.194	DDT	5	DDT	0.037
		0.006	CVS	0.806	No DDT	6	No DDT	0.002
				0.194	DDT	7	DDT	0.001
							Total	1.000

	End State	Probability
	No Ign	0.500
	No DDT	0.385
CET Node DTE Failure Probability =	DDT	0.115

Figure 41-6

Accident Class 3D/1D Early Detonation Decomposition Event Tree

Node N1 Ignition Source		Node N2 Break Compartment		Node N3 DDT				
0.500	No Ignition					1	No ign	0.500
0.500	Ignition	0.968	Loop Compt	0.922	No DDT	2	No DDT	0.446
				0.078	DDT	3	DDT	0.038
		0.000	PXS	0.000	No DDT	4	No DDT	0.000
				1.000	DDT	5	DDT	0.000
				0.032	CVS	0.000	No DDT	6
				1.000	DDT	7	DDT	0.016

End State	Probability
No Ign	0.500
No DDT	0.446
CET Node DTE Failure Probability = DDT	0.054

Figure 41-7

Accident Class 1AP Early Detonation Decomposition Event Tree

AP1000 Hydrogen Deflagration Analysis – Non-Reflooded Case  
Hydrogen Generation Probability Distribution

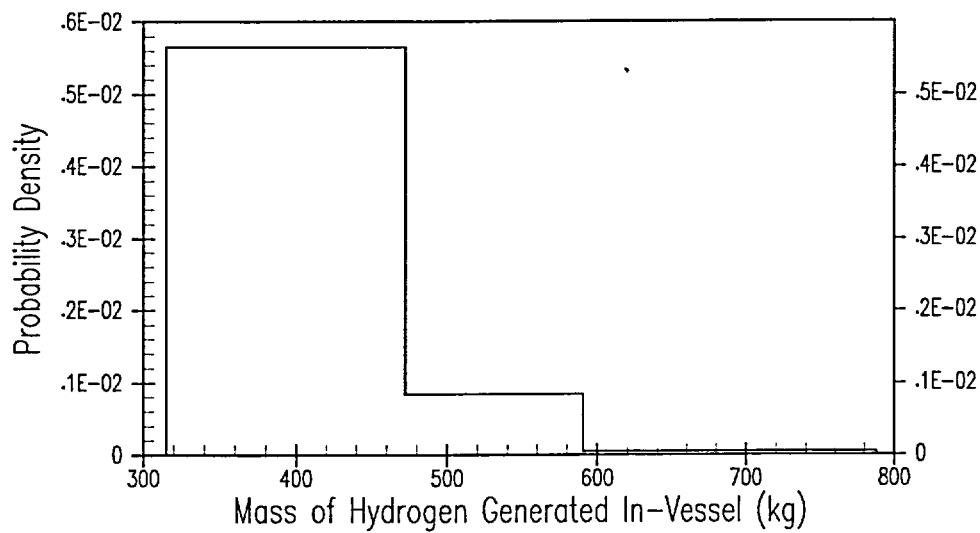


Figure 41-8

**Boil-Off Hydrogen Generation Probability Density Function**

AP1000 Hydrogen Deflagration Analysis – Non-Reflooded Case  
Pre-Burn Pressure Probability Distribution

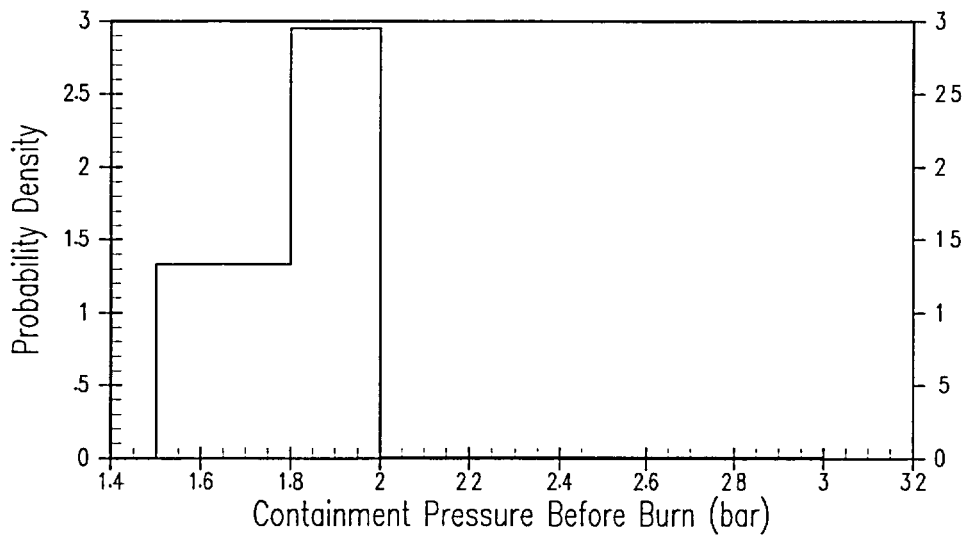


Figure 41-9

No Reflood Pre-Burn Containment Pressure Probability Density Function

AP1000 Hydrogen Deflagration Analysis – Non-Reflooded Case  
Probability Distribution of AICC Peak Pressure

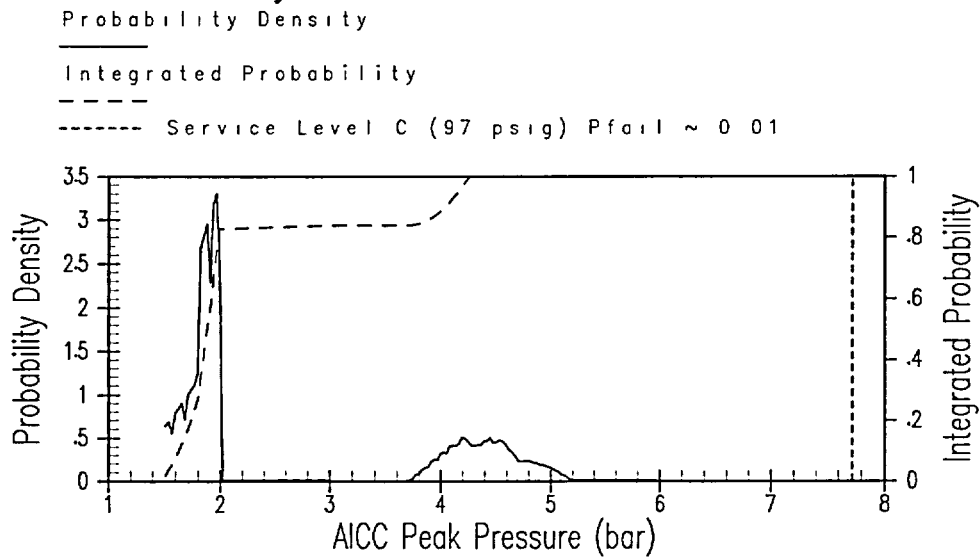


Figure 41-10

No-Reflood Hydrogen Deflagration Peak Pressure Probability

AP1000 Hydrogen Deflagration Analysis – Early–Reflooded Case  
Hydrogen Generation Probability Distribution

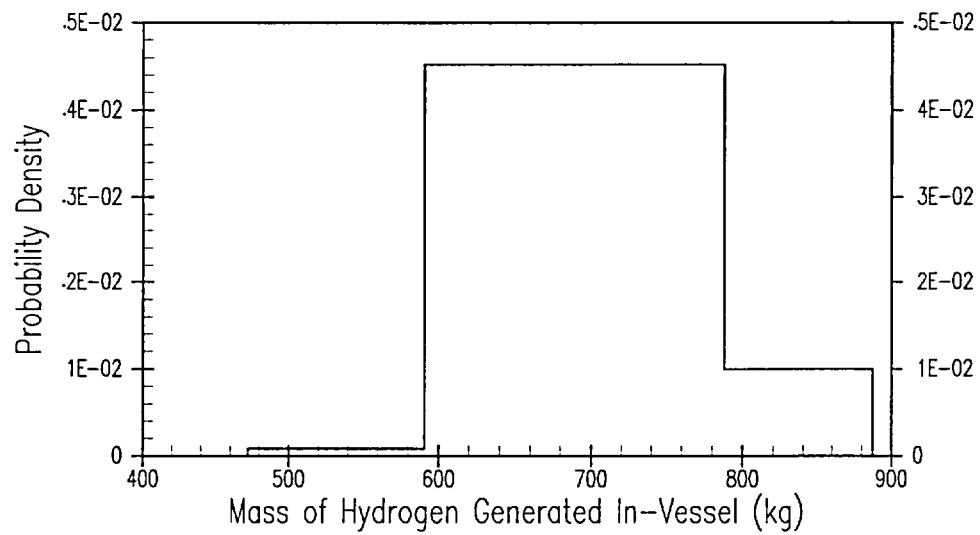


Figure 41-11

Early Reflood Hydrogen Generation Probability Density Function

AP1000 Hydrogen Deflagration Analysis – Early-Reflooded Case  
Pre-Burn Pressure Probability Distribution

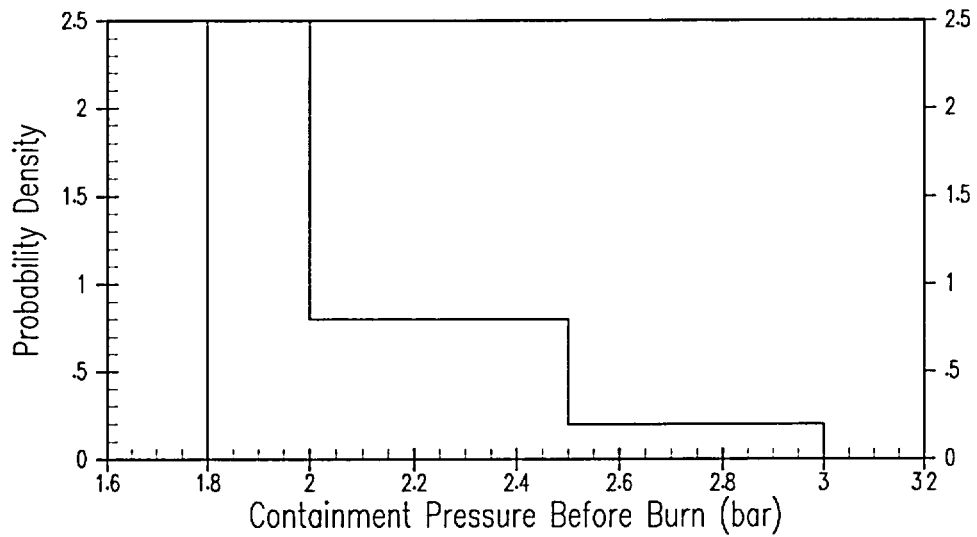


Figure 41-12

Early Reflood Pre-Burn Containment Pressure Probability Density Function

AP1000 Hydrogen Deflagration Analysis – Early-Reflooded Case  
 Probability Distribution of AICC Peak Pressure

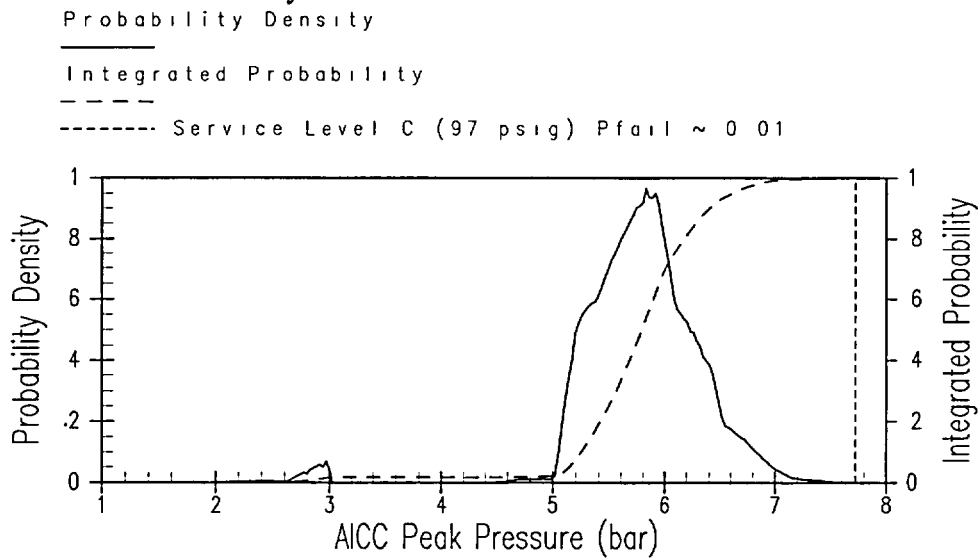


Figure 41-13

Early Reflood Hydrogen Deflagration Peak Pressure Probability

AP1000 Hydrogen Deflagration Analysis – Late-Reflooded Case  
Hydrogen Generation Probability Distribution

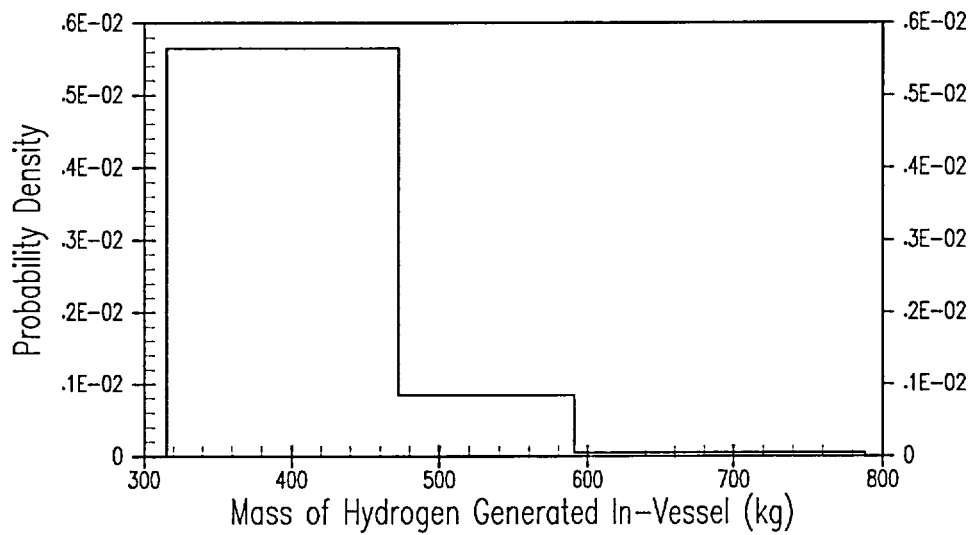


Figure 41-14

Late Reflood Hydrogen Generation Probability Density Function

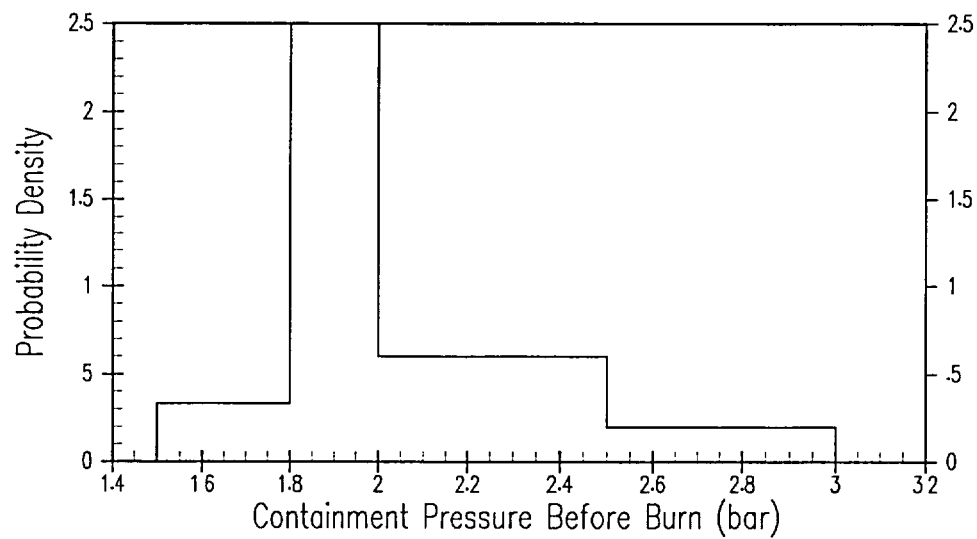
AP1000 Hydrogen Deflagration Analysis – Late-Reflooded Case  
Pre-Burn Pressure Probability Distribution

Figure 41-15

Late Reflood Pre-Burn Containment Pressure Probability Density Function

AP1000 Hydrogen Deflagration Analysis – Late-Reflooded Case  
 Probability Distribution of AICC Peak Pressure

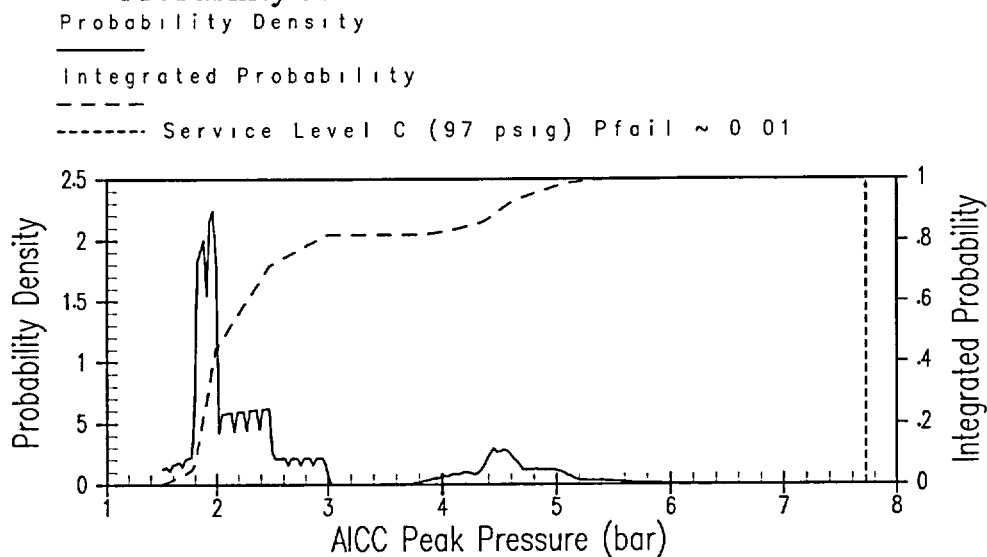


Figure 41-16

Late Reflood Hydrogen Deflagration Peak Pressure Probability

Node N1 Ignition Source		Node N2 Break Compartment		Node N3 DDT				
0.000	No Ignition					1	No ign	0.00E+00
1.000	Ignition	0.047	Loop Compt	0.999	No DDT	2	No DDT	4.69E-02
				0.001	DDT	3	DDT	6.11E-05
		0.953	PXS	0.870	No DDT	4	No DDT	8.29E-01
				0.130	DDT	5	DDT	1.24E-01
		0.000	CVS	0.999	No DDT	6	No DDT	0.00E+00
				0.001	DDT	7	DDT	0.00E+00

	End State	Probability
	No Ign	0.00E+00
	No DDT	8.76E-01
CET Node DTI Failure Probability =	DDT	1.24E-01

Figure 41-17

Accident Class 3BE Intermediate Detonation Decomposition Event Tree – Given RFL Success

Node N1 Ignition Source		Node N2 Break Compartment		Node N3 DDT				
0.000	No Ignition					1	No ign	0.00E+00
1.000	Ignition	0.342	Loop Compt	0.999	No DDT	2	No DDT	3.42E-01
				0.001	DDT	3	DDT	4.45E-04
		0.649	PXS	0.999	No DDT	4	No DDT	6.48E-01
				0.001	DDT	5	DDT	8.44E-04
		0.009	CVS	0.999	No DDT	6	No DDT	8.99E-03
				0.001	DDT	7	DDT	1.17E-05

	End State	Probability
	No Ign	0.00E+00
	No DDT	9.99E-01
CET Node DTI Failure Probability =	DDT	1.30E-03

Figure 41-18

Accident Class 3BE Intermediate Detonation Decomposition Event Tree – Given RFL Failure

Node N1 Ignition Source		Node N2 Break Compartment		Node N3 DDT				
0.000	No Ignition					1	No ign	0.00E+00
1.000	Ignition	0.827	Loop Compt	0.999	No DDT	2	No DDT	8.26E-01
				0.001	DDT	3	DDT	1.08E-03
		0.149	PXS	0.999	No DDT	4	No DDT	1.49E-01
				0.001	DDT	5	DDT	1.94E-04
		0.024	CVS	0.999	No DDT	6	No DDT	2.36E-02
				0.001	DDT	7	DDT	3.07E-05

	End State	Probability
	No Ign	0.00E+00
	No DDT	9.99E-01
CET Node DTI Failure Probability =	DDT	1.30E-03

Figure 41-19

Accident Class 3BL Intermediate Detonation Decomposition Event Tree

Node N1 Ignition Source		Node N2 Break Compartment		Node N3 DDT				
0.000	No Ignition					1	No ign	0.00E+00
1.000	Ignition	1.000	Loop Compt	0.870	No DDT	2	No DDT	8.70E-01
				0.130	DDT	3	DDT	1.30E-01
		0.000	PXS	0.000	No DDT	4	No DDT	0.00E+00
				1.000	DDT	5	DDT	0.00E+00
		0.000	CVS	0.000	No DDT	6	No DDT	0.00E+00
				1.000	DDT	7	DDT	0.00E+00
							Total	1.000

End State	Probability
No Ign	0.00E+00
No DDT	8.70E-01
CET Node DTI Failure Probability = DDT	1.30E-01

Figure 41-20

Accident Class 3C/3BR Intermediate Detonation Decomposition Event Tree

Node N1 Ignition Source		Node N2 Break Compartment		Node N3 DDT				
0.000	No Ignition					1	No ign	0.00E+00
1.000	Ignition	0.610	Loop Compt	0.999	No DDT	2	No DDT	6.09E-01
				0.001	DDT	3	DDT	7.93E-04
		0.384	PXS	0.999	No DDT	4	No DDT	3.84E-01
				0.001	DDT	5	DDT	4.99E-04
		0.006	CVS	0.999	No DDT	6	No DDT	5.99E-03
				0.001	DDT	7	DDT	7.80E-06

	End State	Probability
	No Ign	0.00E+00
	No DDT	9.99E-01
CET Node DTI Failure Probability =	DDT	1.30E-03

Figure 41-21

Accident Class 3D/1D Intermediate Detonation Decomposition Event Tree

Node N1 Ignition Source		Node N2 Break Compartment		Node N3 DDT				
0.000	No Ignition					1	No ign	0.00E+00
1.000	Ignition	0.968	Loop Compt	0.870	No DDT	2	No DDT	8.42E-01
				0.130	DDT	3	DDT	1.26E-01
		0.000	PXS	0.000	No DDT	4	No DDT	0.00E+00
					DDT	5	DDT	0.00E+00
					0.870	No DDT	6	No DDT
		0.032	CVS	0.870	No DDT	6	No DDT	2.82E-02
					0.130	DDT	7	DDT
							Total	1.000

End State	Probability
No Ign	0.00E+00
No DDT	8.70E-01
CET Node DTI Failure Probability = DDT	1.30E-01

Figure 41-22

Accident Class 1AP Intermediate Detonation Decomposition Event Tree